REVIEW

of the

ECTRICAL COMMUNICATION LABORATORY

PPON TELEGRAPH AND TELEPHONE PUBLIC CORPORATION

Former, Reports of the Electrical Communication Laboratory
Nippon Telegraph and Telephone Public Corporation
from Vol.1, No.1, Sept. 1953 to Vol.7, No.12, Dec. 1959

VOLUME 9
NUMBERS 9-10

Published Bimonthly by

HE ELECTRICAL COMMUNICATION LABORATORY
NIPPON TELEGRAPH AND TELEPHONE PUBLIC CORPORATION
1551, Kitizyôzi, Musasino-si, Tôkyô, Japan

September - October
1961

Review of the Electrical Communication Laboratory

The Review of the Electrical Communication Laboratory is published six times a year (bi-monthly) by the Electrical Communication Laboratory, Nippon Telegraph and Telephone Public Corporation, 1551, Kitizyôzi, Musasino-si, Tôkyô, Japan. Telephone: Tôkyô (391) 2261 and 2271.

Subscriptions are accepted at ¥1,200 per year. Single copy ¥300 each. Foreign postage is ¥400 per year or ¥65 per copy. Remittance should be made in check payable to the Electrical Communication Laboratory and sent to the Director.

Printed by Aoyama Printing Co., Tokyo, Japan

REVIEW
of the
ELECTRICAL COMMUNICATION LABORATORY

NIPPON TELEGRAPH AND TELEPHONE PUBLIC CORPORATION

Volume 9, Numbers 9-10 September-October, 1961

U.D.C. 621.318.57:[621.382.2:621.314.63

Compound pnpnp Switches for Bidirectional-bistable Electronic Switches*

Kingo YAMAGISHI†

In the usual bistable electronic switches, the current direction in the conducting state is generally limited in only one direction. Therefore, the field of application of the electronic switches will be extended by the realization of bidirectional-bistable electronic switches.

In this paper, the fundamental characteristics of the compound pnpnp diode and its variations which are made by combination of one npn transistor and two pnp transistors are examined from the point of view of developing the bidirectional-bistable electronic switch. The results of this study show that the compound pnpnp diode (or compound npnpn diode) can be used as a bidirectional-bistable switch. The multiterminal compound pnpnp devices exhibit some interesting characteristics which are usable in controlling these devices. It is also possible to foresee the development of single-element bidirectional-bistable switches.

1. Introduction

In the usual electronic switches using the thermionic vacuum tube, semi-conductor element, etc., the current flows only in one direction. This limitation in the direction of current has narrowed their field of application. Consequently, if we can develop bidirectional-bistable electronic switches, their field of application could be expanded.

Fig. 1 shows the typical input voltage-current characteristics of such bidirectional-bistable electronic switches. It is of course possible to build an electronic switch having the voltage-current characteristics shown in Fig. 1 by using two unidirectional-bistable electronic switches. For instance, by putting two pnpn diodes with their polarity opposite to each other in parallel connection. In this case, however, two unidirectional-bistable electronic switches have to be used.

Thus, in trying to build a bidirectional bistable electronic switch possessing the voltage-current characteristics shown in Fig. 1 by using a single element, a basic examination has been attempted on the characteristics of the compound pnpnp diode. The results of

* MS received by the Electrical Communication Laboratory on February 18, 1961. Originally published in the *Kenkyû Zituyôka Hôkoku* (*Electrical Communication Laboratory, Technical Journal*), N.T.T., Vol. 10, Nos. 6, pp. 1173-1180, 1961.

† Switching Research Section.

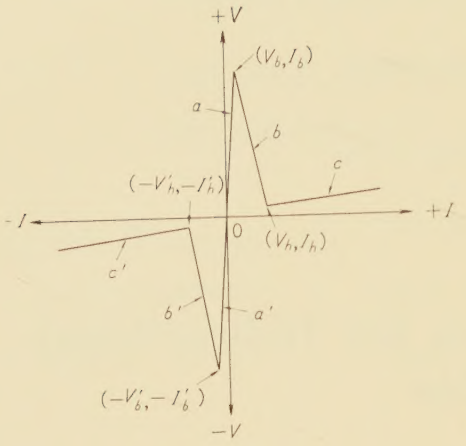

Fig. 1—A typical voltage-current characteristics of bidirectional-bistable electronic switch.

this examination have indicated that it is possible to use the compound pnpnp diode as a bidirectional-bistable electronic switch possessing the voltage-current characteristics shown in Fig. 1.[1]

This paper examines the basic characteristics of the compound pnpnp diode and its variations from the point of view of developing the bidirectional-bistable electronic switch. The results of this examination have indicated that it is possible to develop a bidirectional-bistable electronic switch of a single element of the pnpnp or mpnpm structure.

2. The Structure of the Compound pnpnp Diode and Its Characteristics

The pnpn diode is equivalent to the compound pnpn diode, as pointed out by Shockley.[2] The characteristics of the compound pnpnp diode which is a combination of two pnp transistors and one npn transistor connected as in Fig. 2 (a) are examined, and the results of this examination are described below.

In Fig. 2(a), T_1 and T_3 are pnp transistors of approximately the same characteristics, and T_2 is a symmetrical npn transistor. For T_2,

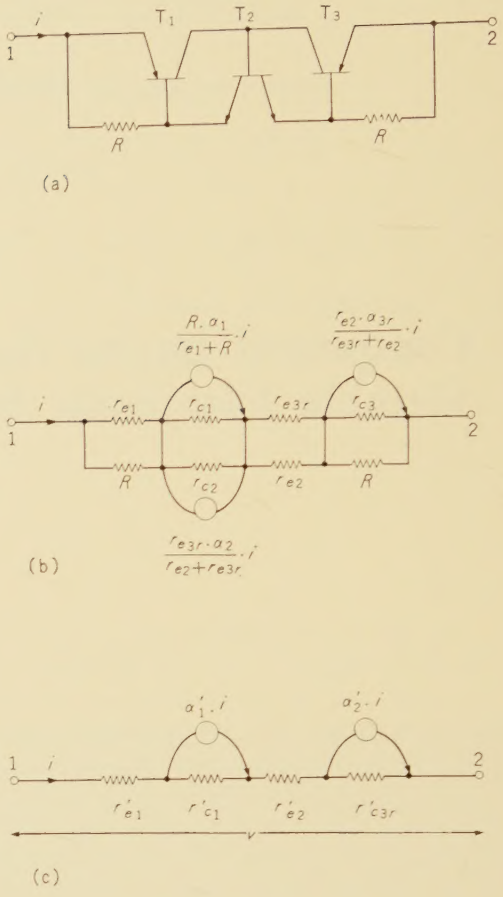

Fig. 2—A compound pnpnp diode and its equivalent circuits.

however, an ordinary npn transistor instead of a symmetrical npn transistor may be used. There is no rigid rule for the polarity of the pnp transistors T_1 and T_3 in their connection. It is nevertheless preferable to make the symmetrical connection to the symmetrical npn transistor, and as shown in the figure, to place the emitters (e) of the pnp transistors T_1 and T_3 at both ends, and to connect their collector (c) with the base (b) of the npn transistor T_2. Furthermore, it is also preferable to use the symmetrical pnp transistor for T_1 and T_3 as well as T_2. R is the bypassing resistor.

Next, let us seek the voltage-current characteristics of the compound pnpnp diode shown

in Fig. 2 (a). The equivalent circuit of this compound pnpnp diode may be drawn as Fig. 2 (b), disregarding the base resistance of T_1, T_2, T_3. Here r_{e1}, r_{c1}, α_1 are respectively the emitter resistance, the collector resistance, and the current amplification factor of T_1; r_{e2}, r_{c2}, α_2 are respectively the emitter resistance, the collector resistance, and the current amplification factor of T_2; r_{e3r}, r_{c3r}, α_{3r} are respectively the inverted emitter resistance, the inverted collector resistance, and the inverted current amplification factor of T_3.

The circuit of Fig. 2 (b) can be represnted by the simplified equivalent circuit as indicated in Fig. 2 (c), where

$$\left.\begin{aligned} r_{e1}' &= \frac{r_{e1}\cdot R}{(r_{e1}+R)}, \quad r_{c1}' = \frac{r_{c1}\cdot r_{c2}}{(r_{c1}+r_{c2})} \\ r_{e2}' &= \frac{r_{e2}\cdot r_{e3r}}{(r_{e2}+r_{e3r})}, \quad r_{c3r}' = \frac{R\cdot r_{c3r}}{(R+r_{c3r})} \\ \alpha_1' &= \frac{R\cdot\alpha_1}{(r_{e1}+R)} + \frac{r_{e3r}\cdot\alpha_2}{(r_{e2}+r_{e3r})} \\ \alpha_2' &= \frac{r_{e2}\cdot\alpha_{3r}}{(r_{e2}+r_{e3r})} \end{aligned}\right\} \quad (1)$$

In Fig. 2 (c), the voltage-current characteristics between terminals 1 and 2 are represented by the following equation:

$$v = i\{r_{e1}'+r_{e2}'+r_{c1}'(1-\alpha_1')+r_{c3r}'(1-\alpha_2')\} \quad (2)$$

Therefore, r, the internal resistance of this compound pnpnp diode can be represented by the following equation:

$$r = \frac{v}{i} = \{r_{e1}'+r_{e2}'+r_{c1}'(1-\alpha_1')+r_{c3r}'(1-\alpha_2')\} \quad (3)$$

Now, α_1', as indicated by the equation (1), can be made larger than unity, so r can be negative. Then, the conditions for r to be negative are represented in the following equation:

$$\alpha_1' > \frac{\{r_{e1}'+r_{e2}'+r_{c1}'+r_{c3r}'(1-\alpha_2')\}}{r_{c1}'} \quad (4)$$

And when R is small, and $r_{c1}' \gg r_{e1}'$, r_{e2}', r_{c3r}', the equation (4) can be represented as follows:

$$\alpha_1' > 1 \quad (5)$$

In other words, when R is small and α_1' is more than unity, this compound pnpnp diode presents a negative resistance. And, in this case, the value of the negative resistance, $\bar{r}$ is represented roughly as follows:

$$\bar{r} \fallingdotseq r_{c1}'(\alpha_1'-1) \quad (6)$$

Namely, $\bar{r}$ is in proportion to r_{c1}'. Consequently, it will be possible to obtain $\bar{r}$ at any value by connecting the resistor R_c as shown in Fig. 3 (a). In this case, $\bar{r}$ may be represented as the following equation:

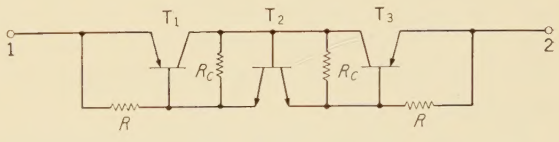

(a)

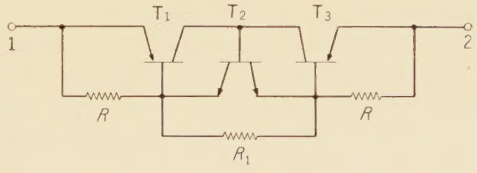

(b)

Fig. 3—Methods for varying the negative resistance $\bar{r}$.

$$\bar{r} \fallingdotseq \frac{r_{e1} \cdot r_{e2} \cdot R_e(\alpha_1' - 1)}{\{r_{e1} \cdot r_{e2} + R_e(r_{e1} + r_{e2})\}} \qquad (7)$$

It is of course possible to obtain any value of $\bar{r}$ by connecting resistor R_1 as shown in Fig. 3 (b).

In Fig. 2 (a), a negative resistance appears when the equation (3) become negative. In this case, if we assume that $r_{e1}=r_{e2}=r_{e3r}=r_e$, $R \ll r_{e3r}$, $\alpha_1=\alpha_{3r} \fallingdotseq 1$, r_e, $R \ll r_c'$, we obtain the following equation:

$$r_e < R \qquad (8)$$

Namely, when $r_e<R$, a negative resistance appears. Now, r_e generally decreases as the emitter current increases. So taking this into consideration, as we increase the value of R, the quantity of current at the point where a negative resistance appears decreases. However, if we make R too large, r_{e3r}' becomes large, and as the equation (4) shows, a negative resistance hardly appears.

The foregoing discusses the voltage-current characteristics in Fig. 2 (a) when the voltage V is applied in the direction where the terminal 1 is positive as compared with the terminal 2. The voltage-current characteristics when the voltage V is applied inversely can be sought similarly.

If we use pnp transistors of the same characteristics for T_1 and T_3, and a symmetrical npn transistor for T_3, we can realize a symmetrical compound pnpnp diode. For the by-passing resistor R, a non-linear resistor or other impedance element may be used according to its use. For example, a diode may be used for R to reduce the conducting resistance of the pnpnp diode.

Next, when it is necessary to fix the values of the breakdown voltage $|Vb|$ and $|Vb'|$ at certain quantities, we can meet this requirement by the circuit configurations as indicated in Fig. 4 (a), (b), (c). Namely, the breakdown voltage of the compound pnpnp diode can be fixed to the value of the Zener voltage E_z by using two Zener diodes D_{zr}, $|Vb'|$. Furthermore, it is possible to obtain asymmetrical charactristics by using two Zener diodes of different Zener voltage. Also, it is possible to make the asymmetrical characteristics by using two by-passing resistors R_r of different value.

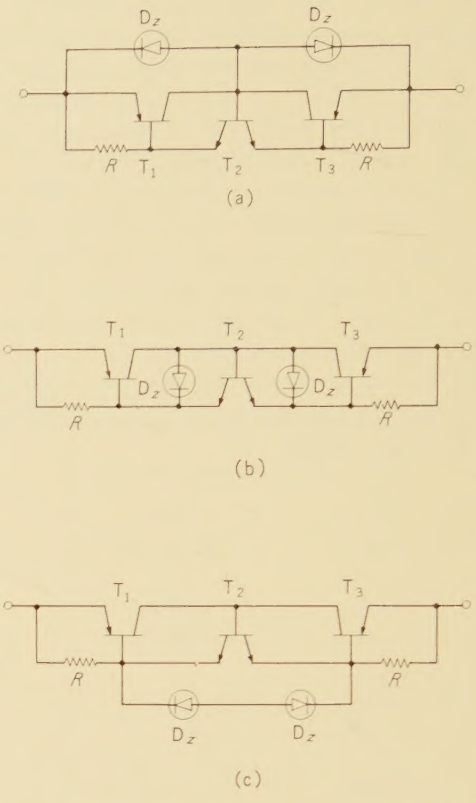

Fig. 4—Methods for setting the breakdown voltage by using Zener diodes.

In the foregoing description, the compound pnpnp diode is treated. It is of course possible to develop a compound npnpn diode which is complementary to the compound pnpnp diode.

3. Experimental Results

Fig. 5 shows an example of the voltage-current characteristics of the compound pnpnp diode connected as shown in Fig. 2 (a), where 2T14 is used for the pnp transistor, and 2T64 for the npn transistor. In Fig. 5, Vb, Ib, etc. when $R=500$ ohms are smaller than those when $R=200$ ohms. This fact matches that

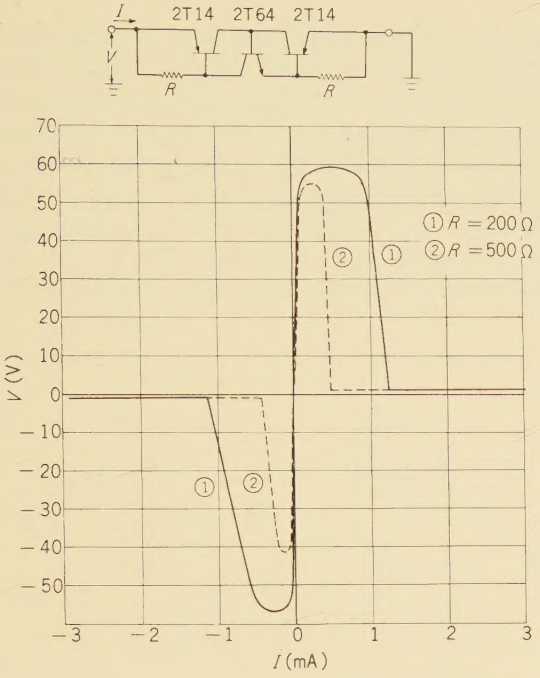

Fig. 5—Experimental voltage-current characteristics of a compound pnpnp diode.

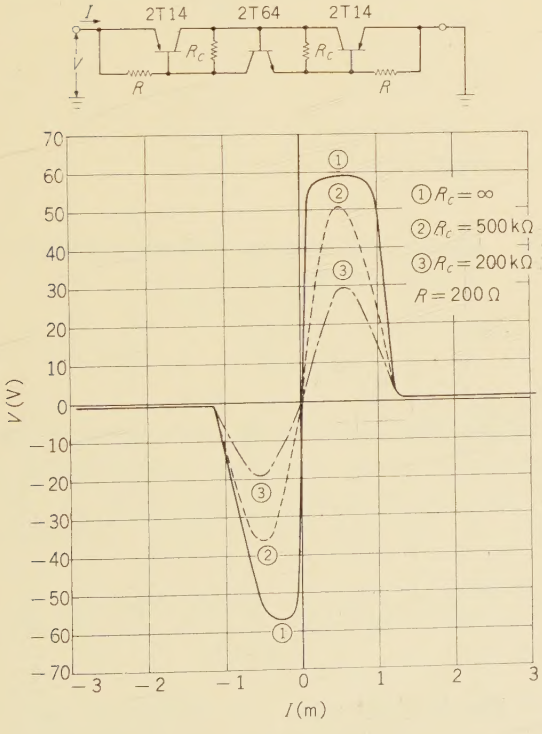

Fig. 6—Variations of voltage-current characteristics for the value of R_c.

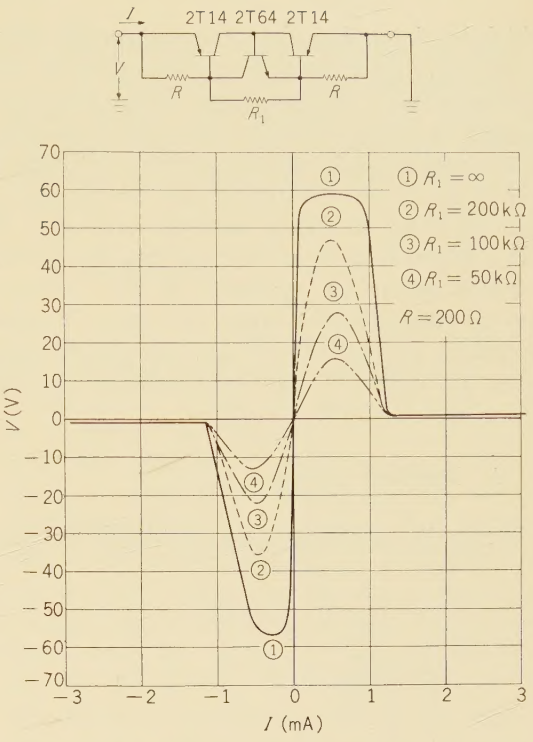

Fig. 7—Variations of voltage-current characteristics for the value of R_1.

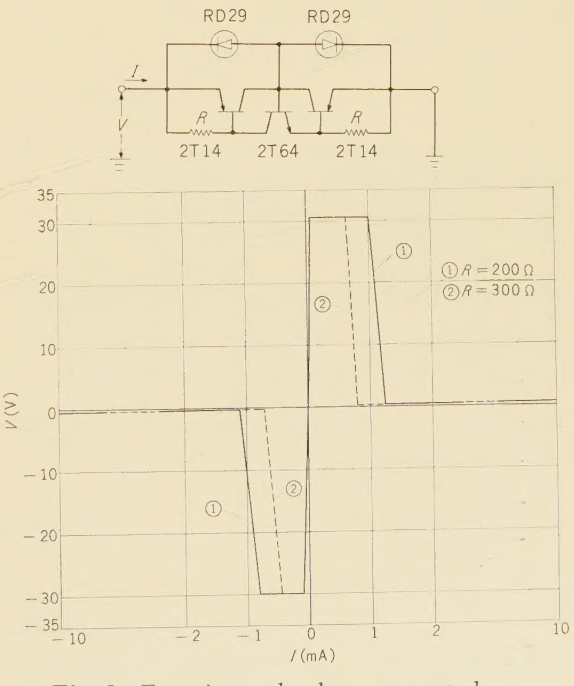

Fig. 8—Experimental voltage-current characteristics of a compound pnpnp diode with two Zener diodes.

which has been described in equation (8). Fig. 6 and Fig. 7 show respectively examples of the voltage-current characteristics when the connection is made as in Fig. 3 (a) and Fig. 3 (b). The asymmetrical characteristics in Figs. 5 to 7 seems to be due to the uneven characteristics of the two 2T14s used and the use of 2T64 which is an asymmetrical npn transistor.

Fig. 8 shows an example of the voltage-current characteristics when the circuit is connected as in Fig. 4 (a). As the figure indicates, *Vb* and *Vb'* are well regulated by the Zener diode RD29.

4. Modified Circuits

When the compound pnpnp element is used as the multi-terminal element, we can obtain some interesting characteristics. Fig. 9 shows the change in the voltage-current characteristics, when the value of the current I_3 flowing into the intermediate *p* layer of the compound pnpnp element from a positive bias voltage source $(+E_3)$ through the resistor R_3 is changed. In this case, as I_3 increases, *Vb*, *Ib*, *Ih*, etc. decrease. Fig. 10 shows the change in the

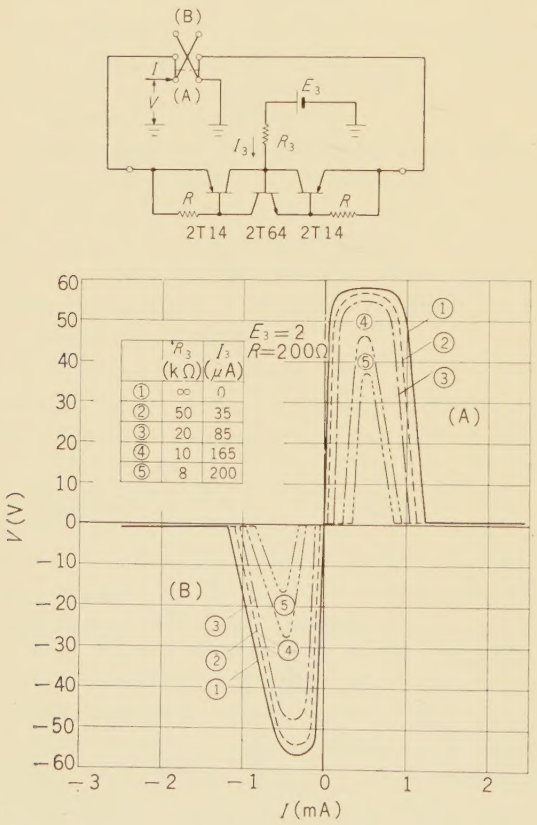

Fig. 9—Variations of voltage-current characteristics of a multi-terminal compound pnpnp switch with a positive bias voltage $+E_3$.

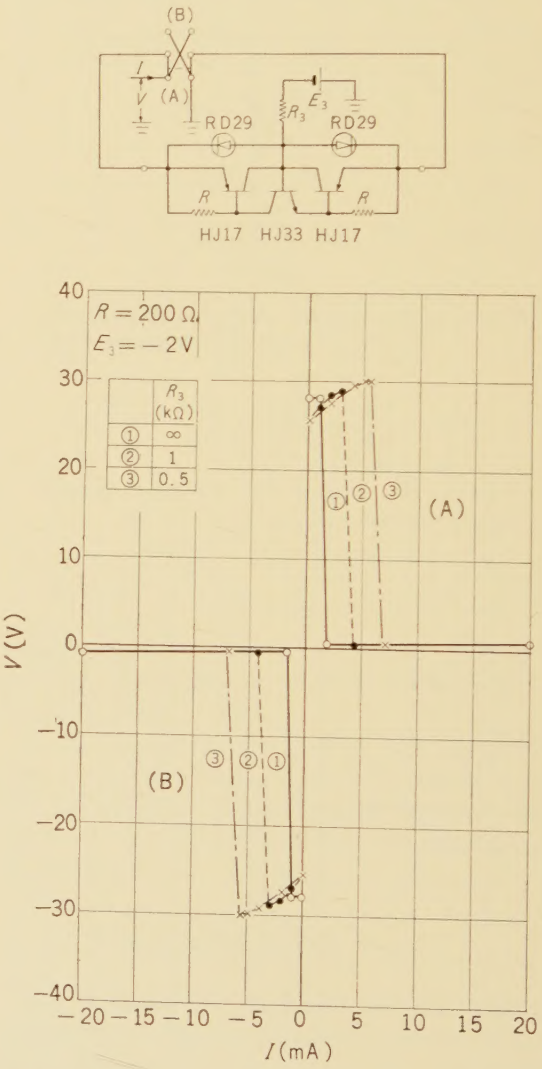

Fig. 10—Variations of voltage-current characteristics of a multi-terminal compound pnpnp switch with a negative bias voltage $-E_3$.

voltage-current characteristics when a negative bias voltage ($-E_3$) is applied to the p layer through the resistor R_3. In this case, I_b increases by about E_3/R_3. The characteristics as shown in Fig. 9 and Fig. 10 can be utilized for controlling this multi-terminal compound pnpnp element.

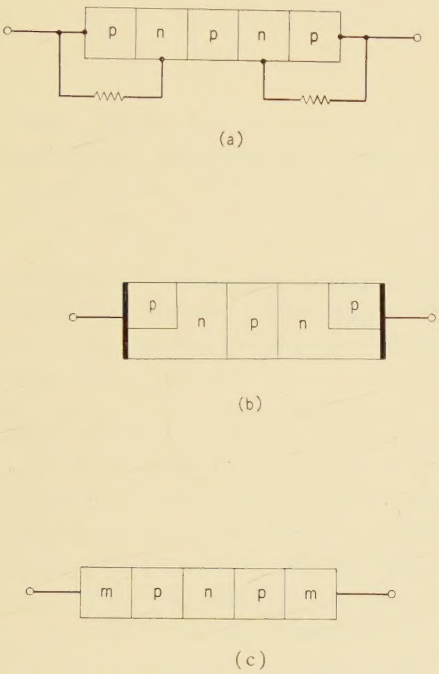

Fig. 11—Devised structures of single-element bidirectional-bistable electronic switches.

Also, in a similar way to the development of the single-elements of pnpn and pnpm[3], a single-element possessing similar characteristics to the compound pnpnp switch may be developed. Some devised structures of such a single element are indicated in Fig. 11 (a), (b), and (c). In this connection, the author would like to point out that the one shown in Fig. 11 (b) has been reported independently from the author by Aldrich et al.[4]

5. Conclusion

The results of this study have indicated that the compound pnpnp switch or the compound npnpn switch can be adequately used as a bidirectional-bistable electronic switch. They have also shown that when these devices are used as the multi-terminal element, we can obtain interesting characteristics that are convenient for controlling them. And from the results of this study, we can also foresee that a single-element bidirectional-bistable electronic switch with the pnpnp or mpnpm structure can be developed. The application of the bidirectional-bistable electronic switch may be extensive for electric power supply, communications, automatic control, etc. The author believes that the development of the electronic switch of this sort will expand the fleld of application of the electronic switch.

Reference

(1) K. Yamagishi: Bidirectional bistable electronic switches,—Compound pnpnp switches, *Transaction of the 1960 Joint Convention of the Four Electrical Institutes of Japan*, p. 1613. 1960, (in Japan).
(2) W. Shockley: The four-loyer diode, *Electr, Ind.*, **16,** 8, p. 58, 1957.
(3) J. Philips, H. C. Chang: Germanium power switching devices, *Trans. I. R. E., ED-5* 1, p. 13, 1958.
(4) R. W. Aldrich, N. Holonyak, Jr. Two-terminal Asymmetrical silicon negative resistance switches, *J. appl. Phys.*, **30,** 11, p. 1819 1959.

* * * *

REVIEW OF THE ELECTRICAL COMMUNICATION LABORATORY
VOLUME 9, NUMBERS 9-10, SEPTEMBER-OCTOBER, 1961

U.D.C. 621.394.1 : [621.391.883
: 621.317.799.087.6

Circuit Interruption and Circuit Interruption Measuring Set*

Toshi MINAMI† and *Masamichi ONO*†

First, circuit interruption is defined as a phenomenon which nullifies the channel capacity of a communication system, and includes the signal detector characteristic. A method of detecting thus defined interruption is given. Then it is illustrated that an automatic record is required to analyze circuit interruption, various kinds of recording systems are compared, and it is concluded that a magnetic tape recorder with delay apparatus is best. According to this conclusion a new circuit interruption measuring set is developed which is able to record the date and time when circuit interruption occurs and to record its duration. Finally, data measured by this set is analyzed from various viewpoints.

1. Introduction

Together with the development of economic activities, the volume of business communication is increasing enormously. This communication requires very low rates of transmitted data error, therefore circuit interruption and impulsive noise deteriorate the quality of a data transmission system. To find the effect of interruption on the quality of data transmission, it is necessary to collect data on interruptions: that is, time of occurence of interruption, duration of interruption, and length of interval between successive interruptions. However, the frequency of occurrence of circuit interruption is comparatively low and it is very difficult to find the cause of circuit interruption. Therefore, systematic research on circuit interruption has not yet been performed.

To overcome these difficulties, the authors developed a new circuit interruption measuring set, which consists of a delay apparatus and a magnetic tape recorder; and analyzed circuit interruption. In this paper, a method of analyzing interruption, details of the measuring set, and data on circuit interruption of Japanese telephone lines are described.

2. Definition and Model of Circuit Interruption

There are two types of measurements which show circuit performance. One type is represented by frequency distortion, amplitude distortion, time (phase) distortion, and their combined effects; and the other is represented by noise, level variation, circuit interruption etc., and concerns itself with reliability. Of these two types, the former has reproducibility and is predictable, so we are able to compensate for the distortion. But the latter type has no reproducibility or predictability so we are not able to compensate for it at the receiving end without using statistical methods. The latter type may be subdivided into additive disturbances and multiplicative disturbances. The existence of multiplicative disturbances depends on the fact that there

* MS in Japanese received by the Electrical Communication Laboratory, on November 18, 1960. Originally published in the *Kenkyû Zituyôka Hôkoku* (*Electrical Communication Laboratory Technical Journal*), N.T.T., Vol. 10, No. 5, pp. 851–865, 1961.

† Communication Network Section.

are nonlinear parts or multiplying devices in an ordinary transmission system, such as multipliers or modulators, which are connected in tandem in the transmission system as shown in Fig. 1. In Fig. 1, block B re-

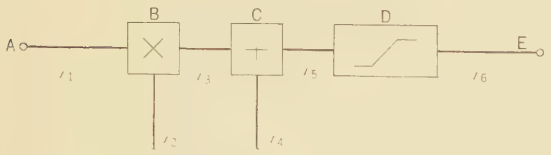

Fig. 1—Block diagram of transmission system

presents a multiplier, and i_3 is equal to $i_1 \times i_2$; C represents an adder and i_5 is equal to $i_3 + i_4$. Block D represents ordinary filters, frequency converters, phase shifters etc. Current i_4 is ordinary noise current, and i_2 indicates a kind of function current which expresses the level variation or circuit interruption. B is a nonlinear element or control element which may be considered to represent amplifier overload, core saturation, contact resistance variation, variation of cable constants, propagation fading etc. In Fig. 1, the arrangement of B, C, and D on the transmission system is obviously changeable. The schematic diagram illustrates a simple tandem configuration but it can be changed to an automatic-control loop configuration. For instance, in a line with AGC, when interruption occurs a pilot current is modulated by the function current (e.g. circuit interruption) and when the line recovers to normal the signal on the line will not recover to its normal value immediately. This occurs because of the AGC loop operation. Furthermore there are variations because of frequency selectivity, but these variations may be expressed by parallel connection of many tandem circuits of corresponding to B,C, and D for each frequency band.

The function current i_2 in Fig. 1 is divided into 3 classes (a), (b), and (c) according to the direct current component, as shown in Fig. 2. In (a), the function current is of the ripple

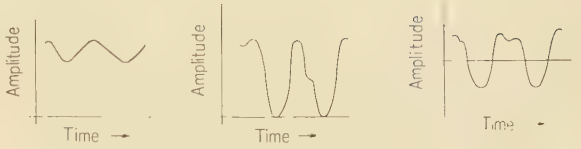

Fig. 2—3 types of function current i_2

type and we can compensate for circuit performance if we do not mind S/N depreciation or signal delay, but in (b) the function current is fragmentary and in (c) it is something like alternating current. In both cases current becomes zero in some instances so we cannot compensate for circuit performance completely. Waveforms of the function current itself would be of many types such as pure sinusoidal wave, rectangular pulse, random noise etc. Any of these undoubtedly reduce the channel capacity of the transmission circuit, and in order to retain accuracy we should define circuit interruption as a phenomenon in which channel capacity becomes zero. But in a communication system for digital transmission such as that with which we are concerned, reduction of channel capacity does not necessarily correspond to the occurence of signal error and this correspondence depends on detector characteristics. Therefore we would like to define circuit interruption as a phenomenon which nullifies the channel capacity of a communication system and includes the signal detector characteristic, which differs from system to system.

3. Detection of Circuit Interruption

If circuit interruption stems from a multiplier element such as shown in Fig. 1, there are problems similar to those in the modulator and demodulator in carrier telephony. For instance, when the frequency spectra of the carrier or signal current i_1 and interruption current i_2 in Fig. 1 are close together, the waveform of the interruption current is affected by spurious or quadrature components and we are unable to obtain the exact envelope waveform of the interruption

current. Therefore, as long as we use a rectifying detector, the information obtained from the received current is insufficient in waveform reproduction accuracy. This indicates that homodyne detection by a multiplier is best, and the obtainable information capacity at the receiving terminal depends upon the location of the carrier or on the type of transmission system; that is, whether the transmission system is a vestigial-sideband system, a single-sideband system, or a double-sideband system.

Slicing after detection is similar to that in carrier telegraphy. At first we set the slice level to an optimum value according to the purpose of communication (or measurement) and by using a feedback detector we change the probability distribution of the amplitude information and slice most effectively. In this case we should consider the problem of miss and error due to noise or long term variation of net loss but this is a problem of data analysis. In another kind of system, for instance in a phase modulation system, the situation is quite similar and it will be satisfactory to select the detection method according to the purpose of the measurement. However, a detector now in use on a communications circuit should not be diverted for use as a measuring instrument, although it may seem to be practical, because the result obtained by such a method would be a quite limited and causality between the definition of circuit interruption and the choice of detecting method will be inverted. We should not forget that the purpose of circuit interruption measurement is to estimate i_2 in Fig. 1 and we should set the slice level with this fact in mind. Therefore the problem of misjudgement is more important than the problem of time distortion in interruption measurement, and it is common to all measurements of infrequent phenomena.

4. Supervision and Recording of Circuit Interruption

Generally speaking, to supervise infrequent phenomena of the order of $10^{-4}\sim10^{-6}$ through human sense-organs, much endurance is required. Of course it is possible to mechanize a continuous supervisory operation or to alarm automatically when circuit interruption occurs, but if we require human intervention for recording or for other assistance after the occurence of the interruption, then this measuring method must be a very uneconomical one. Therefore it is natural to use an automatic recording system for supervision of infrequent phenomena and when recorded data are necessary, the system should be able to supply the necessary records promptly. This requires an automatic supervisory system to abandon worthless data and to retain valuable data which are obtained at infrequent intervals. This function is very important for the purpose of improving the accuracy of collected data. Important data concerning circuit interruption are time of occurence, duration, and interval between successive interruptions. Autocorrelation and crosscorrelation to other phenomena are derived from these data. If the data recording method is not appropriate, the data will become useless when we analyze it later, so we must make records in as much detail as possible. In order to retain generality it is very important to take much data as it is. There are many recording instruments which we can make use of, and digital recorders are supposedly more accurate than analog recorders but we must beware of loss of information, especially when we encode data into digital form.

There are many problems in reliability of an automatic supervisory system itself. This is simply because the parts of the supervisory system are identical with parts of the systems which are the objects of our measurements, and the probability of trouble may be of like order in each. To overcome this difficulty the supervisory system must have ability as complex as the human brain. Otherwise the supervisory system must have an alarm equipment to report trouble within the system itself. Then what kind of alarm equipment is required? The problem may be solved easily if we realize that the purposes of this alarm are to delete the time in which the measuring equipment does not work well from the total measuring period and to dis-

card false data caused by failure of the measuring equipment. In practical use it may be impossible to do this completely. To meet this situation we must take special care when we analyze the collected data, as in the case of misjudgement illustrated in Section 2.

5. Analysis of Circuit Interruption

It is very hard work to analyze the data which are collected by this incomplete measuring set and to attain the object of measurement. It is difficult to enhance the detecting efficiency by controlling the main factors which affect circuit interruption and to improve the accuracy of measurement by increasing the number of repetitions.

The only practical method is to obtain a large quantity of data about the most effective factors and to study correlations between them. It is very dangerous to draw conclusions by examining data from only one point of view and estimating the type of circuit interruption distribution. Especially when we have no idea about factors which influence circuit interruption, it is essential to store much data by long term measurement and to accept them frankly. It is often said that most circuit interruptions are caused by operators, but we should not forget that this conclusion was arrived at under very limited conditions.

6. Construction of a Circuit Interruption Measuring Set

We should use a continuous supervisory system to obtain data on circuit interruption and therefore should record the data continuously. The simplest C.I.M.S. is made of a rectifying detector and recording ammeter, which is a good and reliable method, but its recording speed is rather slow; therefore we are apt to overlook detailed data. Usually in order to obtain detailed data, recorder bandwidth should be as wide as the transmission band. We may use a photographic or magnetic tape recorder for this purpose and the recording speed will reach several megabits per sec, but for the sake of playback we should adopt an intermittent recording system. This means that it is necessary to maintain the balance of data density. The usual recorder takes some time to start, therefore if we want to record data intermittently, a delay apparatus is required. The delay apparatus may be thought of as a memory device, and it is used to increase the information capacity of the recorder. Selection of the recording system should depend on its reliability, but if we use a magnetic tape recorder for playback we should encode the data into appropriate form. The most costly method is to sample the received current at an interval of $T(\leq 1/2W; W$ bandwidth) and to record the sequence after encoding it into a digital form, but practically it is very difficult to develop such a system. Analog recording by photography is not bad. It is very useful because we can inspect the contents of the data directly with our eyes. If we use static-electric photography, which has been widely advertised recently, we can erase the data easily; therefore it may be also used as a storage, memory, or delay apparatus. As a low speed recorder, a discharge breakdown recorder or carbon printer is useful. In short, it is important that the system be simple and free from trouble. In orber to record the time of occurence, duration, and interval of interruption we must use a clock. To record the time of occurrence we may use a normal watch in the case of the photographic recorder but in the case of a magnetic tape recorder we must encode the time into digital form or record a vocal record of a "time-signal service" directly. To record the duration of interruption we must use a counting apparatus, such as a stop-watch, which has a resetting mechanism. The method of disposition of the recorded data is one of the factors to be considered in selection of a recording system. Usually it is convenient to handle the recorded data by an electrical method so it might be better to convert the data into a form which is easily changeable to electrical form.

An adequate measure of trouble within the set itself is the same as in the case of a general

communication system. There are two adequate measures, one is the correction method and the other is the detection method. In the correction method the measuring set works well, as if there were no trouble, even when a part of the measuring set is defective. But in the detection method, if the measuring set finds trouble, it stops the measurement and informs the operators. We should decide which method is preferable, depending upon operating conditions.

7. An Example of a Circuit Interruption Measuring Set

We want to illustrate a C.I.M.S. which was developed in our laboratory. In designing this system we considered the following facts:

1) Measuring period is very long (1 to 6 months).
2) It must record the data as automatically as possible.
3) The purpose of the measuring set is not to find causes of interruption and it will therefore be satisfactory if we can obtain the data at some later time.
4) Detailed analysis of the envelope of the interrupted current is not necessary.
5) It must work from the A.C. power supply and alarm automatically when the current is off.
6) Accuracy of the duration measurement must be of the order of a few ms.

Taking into consideration these facts a normal AM-type magnetic tape recorder was adopted as a recording device. This recorder is divided into a recording element and a playback element. Their actions are as follows. A continuous sinusoidal wave is sent through the telephone or the telegraph circuit which is set up for interruption measurement. At the receiving end, after being detected by a rectifier-type detector, the signal is connected to the slicing circuit. The slicer has a hysteresis characteristic and the slice level can be fixed at any value according to the desired purpose. The waveform at the output of the slicing circuit is rectangular, and this output drives the pulsed oscillator. On the other hand the time and date data are encoded into a seven-unit binary PPM code of four digits by using an electrical watch and a group of relays. When the circuit is interrupted, a constant width rectangular pulse is generated from the beginning of the interruption and the information that the interruption occurred is transmitted to the group of relays through a polar relay by using this constant width rectangular pulse. Receiving this signal, the timing motor begins to drive and after about 1 sec (the tape recorder reaches normal speed during this time) the time and date data are sent to the input of the No. 2 track recording amplifier. Of course, the data are converted to the form of amplitude modulated waveforms, with a 1.7 kc carrier. These time and date signals consist of four digits and it takes about 5 sec to send them serially. Therefore the tape recorder recording time when a single interruption occurs is 7 sec. If another interruption occurs within this 7 sec the tape recorder will continue to turn for another 7 sec from the beginning of the second interruption. And so if interruptions occur successively the tape recorder continues to record them until the interruption cease. This operation is brought about by the following process. At first a timing motor is used to count 7 sec corresponding to the first interruption and if the second interruption occurs in the course of the first 7 seconds the other timing motor automatically begins to count another 7 seconds. The output signal from the timing motor controls the pinch roller of the magnetic tape recorder and causes the recorder to start and to stop. The time and date signals are recorded only once for each successive recording and just before the end the discriminating signal is recorded. This discriminating signal consist of 1.7 kc carrier of several hundred msec. It can easily be discriminated from the time signal according to its length. Therefore the commencement of an interruption is noticed by the time and date signal and the end is noticed by the discriminating signal on the No. 2 track (cf. Fig. 5). On the other hand, the interruption signal modulates 1 kc carrier and after 1 sec delay it is re-

corded on the No. 1 track of the magnetic tape. In this case the time length of the interruption is counted in msec. The error introduced by the delay circuit is less than 1 or 2 msec. The tape recorder to record the data is an ordinary one. It has 3 heads, 3 motors, 2 tracks; and a monitoring speaker and a level meter which are common to both tracks. The vacuum tube circuits are constructed on U-type plug-ins, and the construction is very smart. Start and stop of the recording can be controlled externally through a relay contact by pushing a botton. When the C.I.M.S. is used, electrical power is supplied to all parts. The tape is kept motionless but is ready to record. The tape speeds are 3.75 inch/sec and 7.5 inch/sec. For measurement purposes the slower speed is used and 450 interruption can be recorded on a 1200-foot long (7 inch) reel. The dynamic range of the tape recorder is about 40 dB, and therefore we can record the necessary items such as the date, the name of line and so forth before beginning the measurement. To indicate that the tape reel is finished or the tape is cut we provided a safety switch and an alarm contact making use of the tension arm. The 3 dB bandwidth of the tape recorder is 170 c/s~7 kc/s at the higher speed and 200 c/s~3.8 kc/s at the lower speed. Fig. 3 indicates the schematic diagram of the recording apparatus and Fig. 4 show the front view of all apparatus necessary for measurement. In Fig. 3 the time indicating panel is used to monitor the stored data concerning the date and time. In this panel there are 7 push buttons to reset "day", "hour", and "month", and to test the apparatus by manual interruption. In order to test the apparatus, we may push the "breakdown" button; then the tape recorder begins to run and records the time and discriminating signal on one track but the pulsed-oscillator is not driven and no interruption signal is recorded. This is helpful to indicate the "commencement time" and "end time". An electric clock is also located on this panel and the setting of the minute hand is made by a knob on the surface.

In the case of a cut tape, the red lamp on

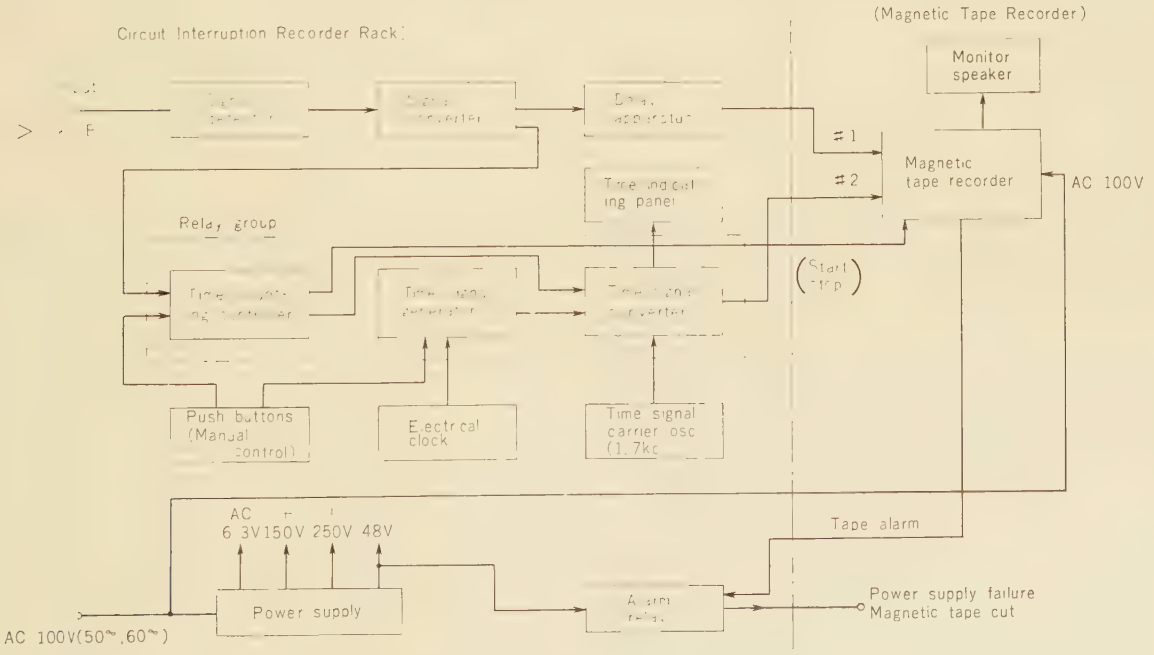

Fig. 3—Schematic diagram of a recording apparatus.

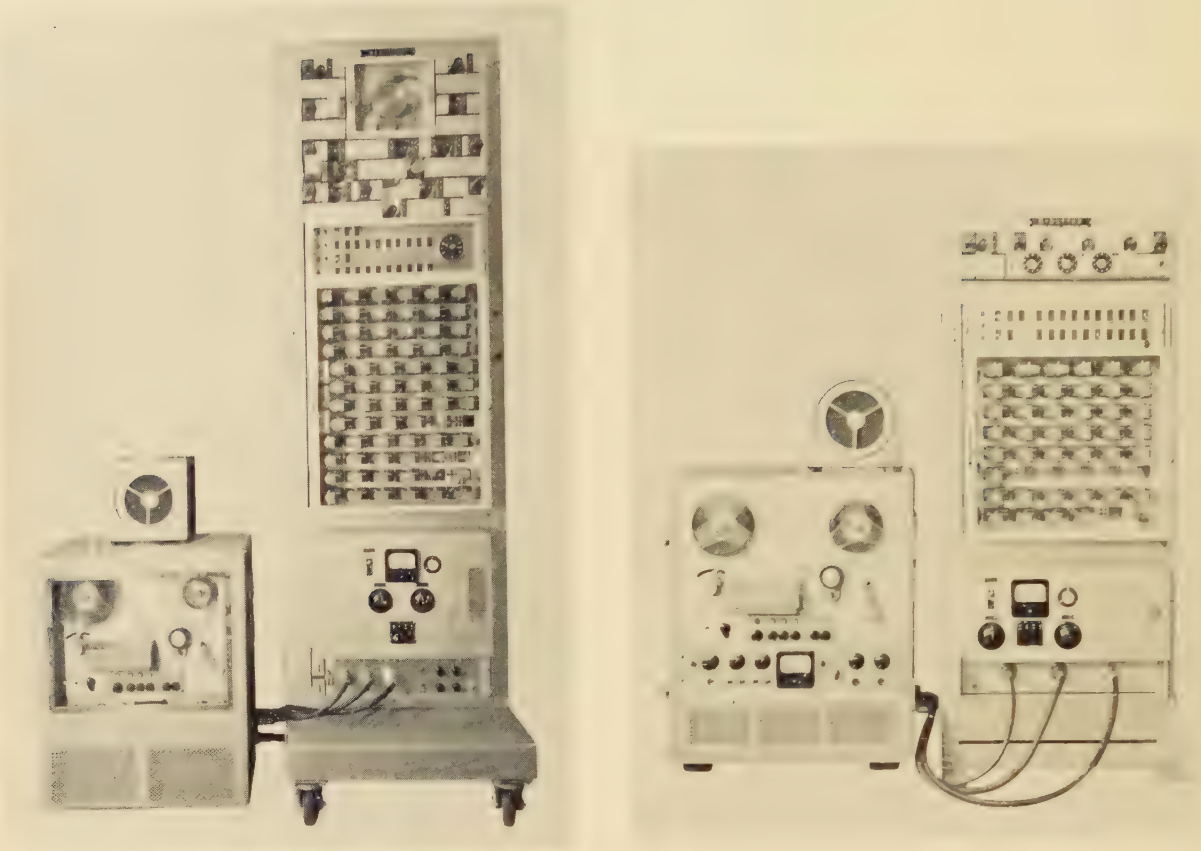

(a) Circuit Interruption Recorder (b) Circuit Interruption Analyzer

Fig. 4—Front view of Circuit Interruption Measuring Set.

the terminal panel at the lower part of the bay is turned on and the relay contact of the bay alarm is closed. The rectified voltage at the filter choke of the −48 V rectifying circuit is used to indicate power supply failure. This voltage is supplied to a horizontal relay and whenever the power supply fails, the contact of the relay is opened and we can easily know it. The relay operates within the interval of power supply failure which affects the keep-relay operation of the relay-group. Short power supply failure (less than 20 ms) will not affect the operation at all because the capacity of the filter circuit is large enough. We omitted an alarm for faulty operation due to tube deterioration. On the terminal panel there are outlets for a power supply cord and a signal control cord, and if we put the ALM OFF switch to the OFF side then the power supply failure ALM relay is set.

In Fig. 5 waveforms and timing relationships of several parts of the recording apparatus are illustrated. From this figure it is easily recognized that successive interruptions within 7 sec are recorded at once. Furthermore, it will be seen that interruptions lasting over 7 sec are recorded only for 7 sec.

In Fig. 6 a schematic diagram of an analyzing apparatus is shown. This apparatus is used to measure the durations of the interruptions which are recorded according to

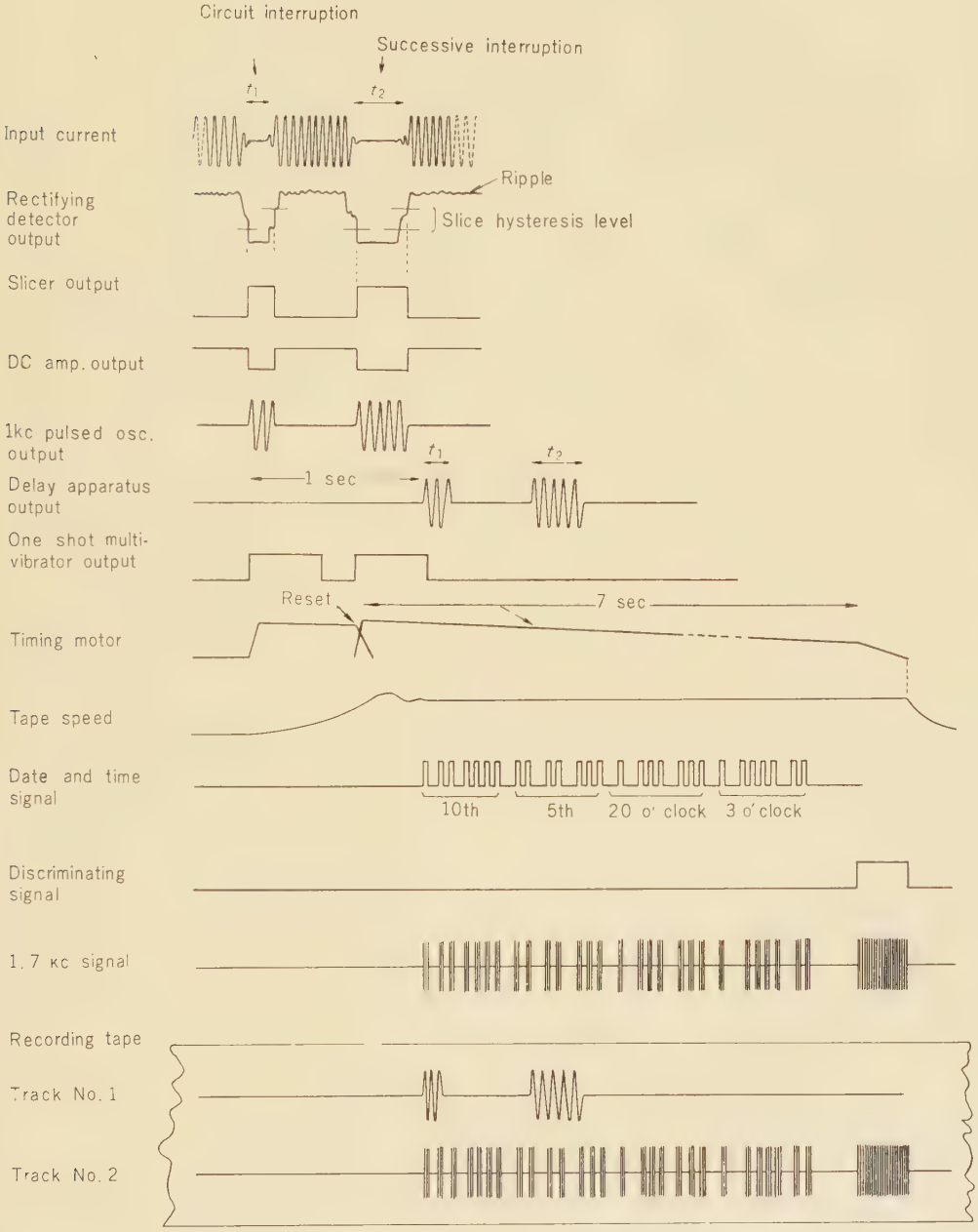

Fig. 5—Timing Chart of Circuit Interruption Recorder.

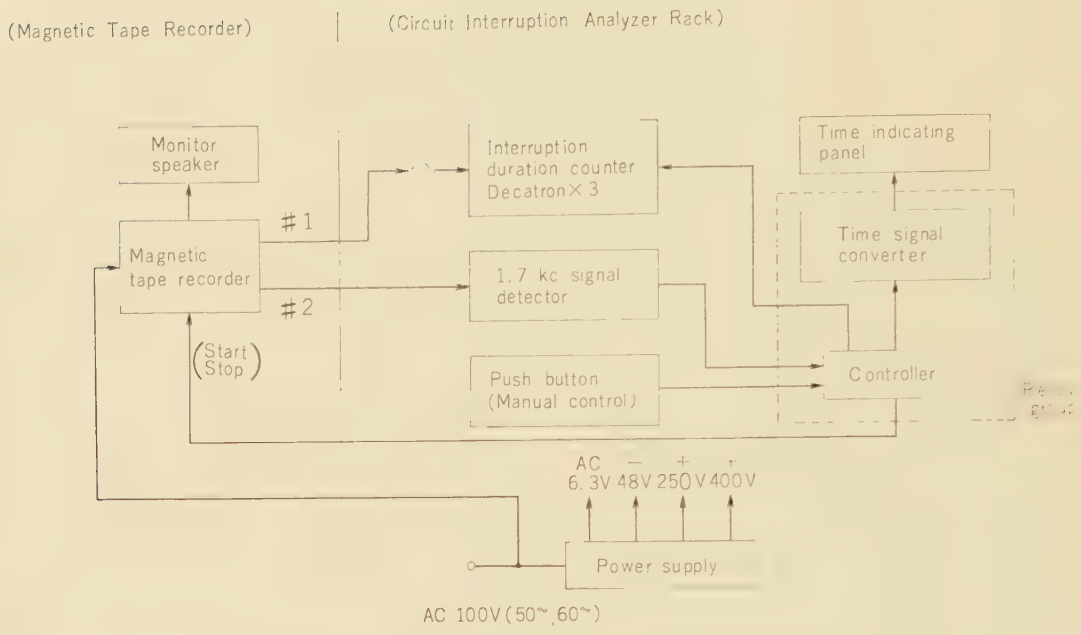

Fig. 6—Schematic diagram of an analyzing apparatus.

the principles described above and to indicate the dates and times when the interruptions occured. The 1 kc signal which was recorded on the No. 1 track is directly connected to a 3-stage decatron counter and this counter indicates the length of the interruptions in msec. The 1.7 kc signal from the No. 2 track is amplified and rectified and then connected to a relay group. This relay group decodes the signal and indicates the dates and times on the time indicating panel. Start of a playback is controlled manually by pushing a button and the end of the playback is automatically controlled by the discriminating signal. Therefore each interruption can be analyzed separately.

8. Results of Circuit Interruption Measurements for Typical Japanese Telephone Lines

Tests were carried out with the object of obtaining data on circuit interruption. Figs. 7∼11 show results which were measured on a telephone circuit between Tokyo and Osaka. The measuring period was 1083 hours. Fig. 7 shows the frequency of interruptions for the days of the week; multiple means the interruptions occur successively within 7 sec.

In Table 1, interruptions on SHF radio links are shown. In this case causes of interruptions are analyzed, too.

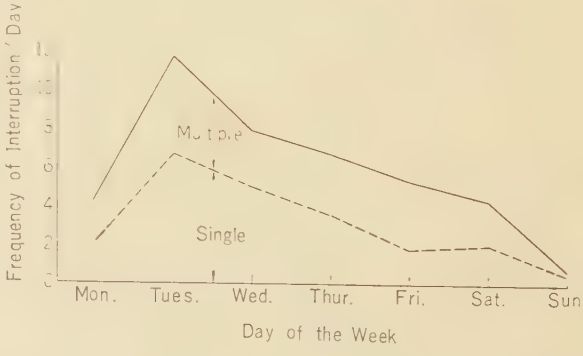

Fig. 7—Frequency of interruptions by day of week.

Fig. 8—Frequency of interruptions by hour of day.

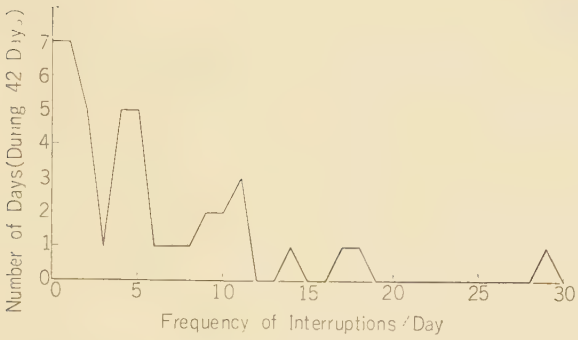

Fig. 9—Frequency of interruptions by day during 42 days.

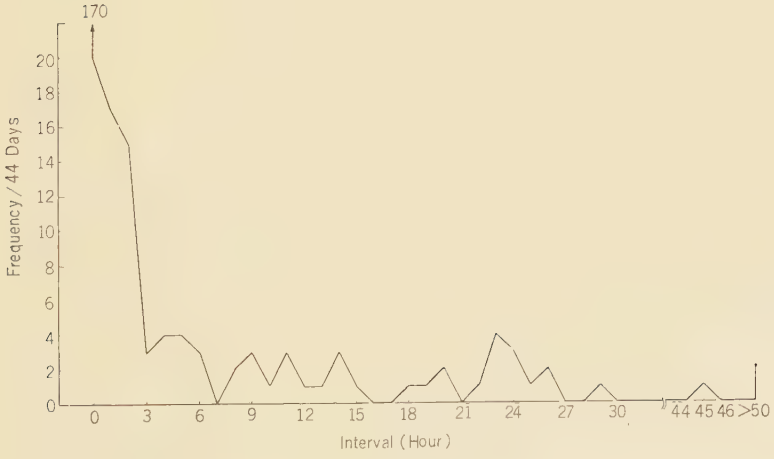

Fig. 10—Intervals between successive interruptions.

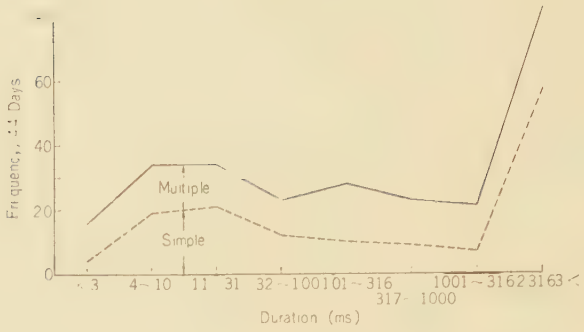

Fig. 11—Duration of interruptions.

Table 1

CIRCUIT INTERRUPTION IN SHF RADIO RELAY LINKS
BETWEEN TOKYO AND SENDAI
(1958. 8. 14 ~ 1958. 9. 15)

Cause	Frequency of Interruptions	Duration of Interruptions (m sec)				
		0 ~ 9	10 ~ 99	100~999	1000~4999	5000<
Fading	15	0	2	10	3	0
Transmitting and Receiving Apparatus	1	0	0	1	0	0
Modulator Changeover	14	1	13	0	0	0
Demodulator Changeover	23	15	8	0	0	0
Auxiliary Apparatus	1	0	1	0	0	0
Power Supply Failure	24	0	13	10	0	1
System Changeover	7	0	5	2	0	0
Other Apparatus	3	1	2	0	0	0
Faulty Operation	4	0	0	0	0	4
Unknown	10	2	5	2	0	1
Total	102	19	49	25	3	6

Conclusion

There are two reasons for research on circuit interruption. One is to find the causes of the interruptions and reduce them as much as possible. And the other is to collect data on circuit interruption such as the frequency of occurrence, duration, and interval. These data will be used when an efficient error correcting system for data transmission is constructed. Here, the problem of construction of a circuit interruption measuring set is investigated and test results of circuit interruptions in typical telephone lines are analyzed from various viewpoints, and some of causes of interruption in SHF radio relay links clarified.

However, more data are neccessary to solve the problem of interruption and this kind of research should be continued in the future.

* * * *

REVIEW OF THE ELECTRICAL COMMUNICATION LABORATORY
VOLUME 9, NUMBERS 9-10, SEPTEMBER-OCTOBER, 1961

U.D.C. 621.395.31

A Study on the Efficiency of Graded Multiple Delay Systems through Artificial Traffic Trials

*Eiichi GAMBE**

With the expansion of common controlled telephone exchange systems, arrangements of devices with a delay system have become widely used. These arrangements are generally the graded multiple system, the link system or the multi-stage waiting system.

On the graded multiple delay system with sequential hunting, a series of artificial traffic trials was performed by means of an electronic digital computer, as one of the studies of these complex delay systems. This computer uses parametrons for logical elements and was developed in our laboratory.

The difficulty of theoretical treatment of the equilibrium equations of states is discussed for a graded multiple delay system with two subgroup and sequential hunting as an example. The method of the artificial traffic trials used in this study are discussed, and some results of the two-subgroup and four-subgroup gradings, with ten-availability and sequential hunting, are shown.

These results are illustrated by the figures in this paper. It should be noted that these results are within the limiting curves which are the load curves of two different full-availability groups.

Further, the analogy to the graded multiple loss system is discussed and the approximate methods for estimating the efficiency of gradings with a delay system, with the knowledge on the same gradings for a loss system are introduced.

Using the results of loss systems, which are obtained by means of an electronic artificial traffic analyzer, the curves of the probability of delay and average waiting time are estimated, and compared with the above results by the computer. The analyzer was installed in our laboratory and is exclusively used for the graded multiple loss systems with sequential hunting.

In the case of two-subgroup gradings, the measured traffic carried by common trunks of a loss system is compared with that of a delay system.

When the situation that some of delayed calls depart without being served is not negligible, the proportion of departed calls will sometimes be taken as a grade of service. Finally these are discussed and an approximate method of estimating this proportion is introduced for the case of the graded multiple delay systems.

1. Introduction

In recent times, common controlled automatic telephone exchange systems are rapidly expanding anddelay systems are becoming more widely used. In the past the delay system has been used mainly in manual type exchanges. In such cases, a comparatively long waiting time may be allowed and the time is only the grade of service for the subscribers.

In the arrangement of common devices, in a common controlled exchange system, the length of waiting time has a direct effect on

* MS received by the Electrical Communication Laboratory on 15 June 1961. Originally published in the *Review of the Electrical Communication Laboratory*, Vol. 10, No. 9-10, pp. 564-580, 1961.

† First Switching Research Section.

This paper was submited to the 3rd. International Congress of Teletraffic held in Paris on 11～16 Sep. 1961.

the required number of waiting devices. This must be taken into consideration in the design of the arrangement of these devices. Therefore, a long waiting time will not generally be allowed. Also, the arrangement of common devices include fundamentally a complicated traffic problem which is called "multistage waiting." For example, as shown in Fig. 11, the waiting time that B waits for C is included in the holding time of B, and the waiting time that A waits for B is included in the holding time of A, and so on. In an example of common controlled exchange systems, A is an incoming register, B is a marker and C is a translator. Therefore, all successive arrangements from incoming lines to the last devices must be treated as one traffic system. However, the multistage waiting systems, even in very simple cases, are not yet completely or precisely solved.

In practical use the arrangement of each stage is regarded as an independent traffic model, and is compensated so that the mean operating time of the considered device, added to the average waiting time in the later stages, is used as the average holding time of the devices.

Such approximations are inevitable, but there is one more problem. That is, since many connection wires are necessary for the connection of the successive different devices, the full availability arrangements are sometimes not economical. Then the link system or the graded multiple system is generally

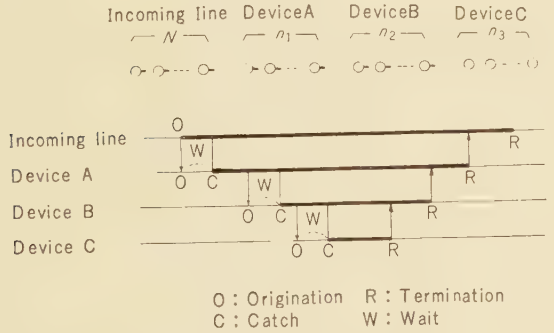

Fig. 1.1—Multistage waiting.

used. Moreover these are generally delay type systems.

The traffic problems with link systems or graded multiple systems have hardly been investigated in detail for delay type systems. A graded multiple delay system has also been used at the multiple of line switches in Strowger exchange system and at the arrangement of operators in the manual recording boards.

This study attempted to determine the efficiency of the graded multiple delay systems with sequential hunting. The theoretical treatment is very difficult, as it will be described first. Therefore, a series of artificial traffic trials was performed by means of an electronic digital computer in our laboratory. These method and results are shown in this paper.

It may be possible that traffic load curves with many usable grading forms can be obtained by the above method, but it would be very laborious. However, the detailed experimental results concerning graded multiple loss systems with sequential hunting are known. Therefore, the analogy between delay systems and loss systems with the same grading forms will be discussed.

An approximate method is introduced in this paper estimate the traffic capacity of delay type systems from that of the loss systems with the same grading forms, where the results obtained by means of the electronic antificial traffic analyzer for loss type systems are used.

2. Equation of State with 2-Subgroup Grading

The required size for a graded multiple delay system is smaller than for a graded multiple loss system. However, it is similar to the loss system in that the traffic problems are very difficult to solve theoretically because of the hypercomplex functions.

The delay system with grading becomes more complicated because the restriction with the servicing of calls waiting simultaneous in several subgroups must be taken into consideration. Therefore, even for a simple case

such as the delay system with 2 subgroups; 2-availability; and 3 trunks; the theoretical analysis is very difficult.

These circumstances will be discussed by introducing the equations of states in equilibrium for the graded multiple delay system with 2 subgroups and sequential hunting, as shown Fig. 2.1.

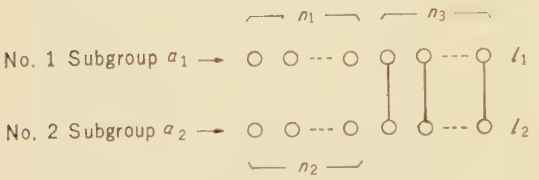

Fig. 2.1—Two-subgroup grading.

Let n_1 be the number of individual trunks of No. 1 subgroup, n_2 be that of No. 2 subgroup and n_3 be the number of common trunks.

In practical use, generally

$$n_1+n_3=n_2+n_3=n_0$$

where n_0 is the availability of the grading.

It will be assumed that all calls are similar and independent of each other, both origination and termination of the calls are pure chance, there is no early departure of delayed calls and that the number of sources, the maximum number of delayed calls and the maximum length of waiting time are infinite.

Let a_1, a_2 be traffic offered to No. 1, No. 2 subgroups respectively. Let $p(i, j, k, l_1, l_2)$ be the, in equilibrium, probability of state (i, j, k, l_1, l_2) that i out of n_1, j out of n_2 and k out of n_3 trunks are busy and the number of delayed calls of No. 1 and No. 2 subgroups are l_1, l_2 respectively.

Now, some other assumptions are necessary concerning the servicing order of the delayed calls. When it is desired to determine the probability of delay or the average waiting time, it will not always be necessary to consider the servicing order in the case of a full-availability group.

In the present case, it is necessary to determine which subgroups should be served when one of the common trunks which are all busy, will become free at the state ($l_1\geq 1$, $l_2\geq 1$).

The following three different methods may be found.

Restriction (1); It is discriminated for all calls that in which subgroups the call is waiting, but all of the delayed calls in the different subgroups are in order according to their arrival times. The delayed calls are then allocated to common trunks in the arrival order.

Restriction (2); In the case of state ($l_1\geq 1$, $l_2\geq 1$), each subgroup is chosen in the probability of 1/2 independently of the values of l_1 and l_2. Let $g_1(l_1, l_2)$, $g_2(l_1, l_2)$ be the probabilities that No. 1 and No. 2 subgroups are served respectively, and then

$$g_1(l_1, l_2)=g_2(l_1, l_2)=1/2 \quad (l_1\geq 1,\ l_2\geq 1)$$

$$g_1(l_1, 0)=g_2(0, l_2)=1 \quad (l_1\geq 1) \text{ or } (l_2\geq 1)$$

Restriction (3); Each subgroup is chosen in the probability proportional to l_1 and l_2. That is

$$g_1(l_1, l_2)=\frac{l_1}{l_1+l_2}, \quad g_2(l_1, l_2)=\frac{l_2}{l_1+l_2}.$$

In the case of an automatic telephone exchange system, etc., it is generally very difficult to identify the arrival order of all calls.

Therefore, the restriction (1) is not appropriate.

Considering restriction (3), then the equiribulium equations of state will take the following forms.

For simplicity, put

$$p(i, j, k, 0, 0)\equiv P(i, j, k)$$

$$p(n_1, j, n_3, l_1, 0)\equiv Q_1(j, l_1)$$

$$p(i, n_2, n_3, 0, l_2)\equiv Q_2(i, l_2)$$

$$p(n_1, n_2, n_3, l_1, l_2)\equiv R(l_1, l_2)$$

and use the notations as

$$\delta(i=n_1)=\begin{cases}1 & (i=n_1)\\ 0 & (i\neq n_1)\end{cases}.$$

(1) $0\leq i\leq n_1,\ 0\leq j\leq n_2,\ 0\leq k\leq n_3;\ l_1=0,\ l_2=0$

$$\begin{aligned}&(a_1+a_2+i+j+k)P(i,j,k)\\&=a_1P(i-1,j,k)+a_2P(i,j-1,k)\\&\quad+\{a_1\delta(i=n_1)+a_2\delta(j=n_2)\}P(i,j,k-1)\\&\quad+(i+1)P(i+1,j,k)+(j+1)P(i,j+1,k)\\&\quad+(k+1)P(i,j,k+1)+\delta(i=n_1)\delta(k=n_3)\\&\quad\times(n_1+n_3)Q_1(j,1)+\delta(j=n_2)\delta(k=n_3)\\&\quad\times(n_2+n_3)Q_2(i,1).\end{aligned}$$

(2) $i=n_1,\ 0\leq j\leq n_2-1,\ k=n_3;\ l_1\geq 1,\ l_2=0$

$$\begin{aligned}&(a_1+a_2+n_1+j+n_3)Q_1(j,l_1)\\&=a_1Q_1(j,l_1-1)+a_2Q_1(j-1,l_1)\\&\quad+(i+1)Q_1(j+1,l_1)+(n_1+n_3)Q_1(j,l_1+1).\end{aligned}$$

(3) $0\leq i\leq n_1-1,\ j=n_2,\ k=n_3;\ l_1=0,\ l_2\geq 1$

$$\begin{aligned}&(a_1+a_2+i+n_2+n_3)Q_2(i,l_2)\\&=a_1Q_2(i-1,l_2)+a_2Q_2(i,l_2-1)\\&\quad+(i+1)Q_2(i+1,l_2)+(n_2+n_3)Q_2(i,l_2+1).\end{aligned}$$

(4) $i=n_1,\ j=n_2,\ k=n_3;\ l_1\geq 0,\ l_2\geq 0$

$$\begin{aligned}&(a_1+a_2+n_1+n_2+n_3)R(l_1,l_2)\\&=a_1\delta(l_1=0)Q_2(n_1-1,l_2)\\&\quad+a_2\delta(l_2=0)Q_1(n_2-1,l_1)\\&\quad+(a_1+a_2)\delta(l_1=0)\delta(l_2=0)P(n_1,n_2,n_3-1)\\&\quad+a_1R(l_1-1,l_2)++a_2R(l_1,l_2-1)\\&\quad+\left(n_1+\frac{l_1+1}{l_1+l_2+1}n_3\right)R(l_1+1,l_2)\\&\quad+\left(n_2+\frac{l_2+1}{l_1+l_2+1}n_3\right)R(l_1,l_2+1)\end{aligned}$$

where probabilities $P(-1,j,k)$, $P(n_1+1,j,k)$, $\cdots$ that over the ranges, are zero.

The supplementary equation is provided by the normalizing condition:

$$\begin{aligned}&\sum_{i=0}^{n_1}\sum_{j=0}^{n_2}\sum_{k=0}^{n_3}P(i,j,k)+\sum_{j=0}^{n_2-1}\sum_{l_1=1}^{\infty}Q_1(j,l_1)\\&\quad+\sum_{i=0}^{n_1-1}\sum_{l_2=1}^{\infty}Q_2(i,l_2)+\sum_{l_1=0}^{\infty}\sum_{l_1=0}^{\infty}R(l_1,l_2)\\&\quad-R(0,0)=1.\end{aligned}\tag{5.1}$$

In the case when restriction (2) is used, only equation (4) is replaced by the following:

(4)′ $i=n_1,\ j=n_2,\ k=n_3;\ l_1\geq 0,\ l_2\geq 0$

$$\begin{aligned}&(a_1+a_2+n_1+n_2+n_3)R(l_1,l_2)\\&=a_1\delta(l_1=0)Q_2(n_1-1,l_2)\\&\quad+a_2\delta(l_2=0)Q_1(n_2-1,l_1)\\&\quad+(a_1+a_2)\delta(l_1=0)\delta(l_2=0)P(n_1,n_2,n_3-1)\\&\quad+a_1R(l_1-1,l_2)+a_2R(l_1,l_2-1)\\&\quad+\left\{n_1+\frac{1+\delta(l_2=0)}{2}n_3\right\}R(l_1+1,l_2)\\&\quad+\left\{n_2+\frac{1+\delta(l_1=0)}{2}n_3\right\}R(l_1,l_2+1).\end{aligned}$$

In the case of a loss system with the same grading form, only equations similar to equation (1) remain. Even in such a simple case the analysis is very complex as solved by C. Palm.[1]

In the present case, the analysis becomes more complicated due to equation (4). Tentatively, let $\Psi(x,y)$ be the generating function with $R(l_1,l_2)$. Then equation (4) is converted into the following first order partial differen-

tial equation.

$$x\{a_1(1-x)xy+a_2(1-y)xy-(n_1+n_3)(1-x)y$$
$$-n_2(1-y)x\}\frac{\partial\Psi(x,y)}{\partial x}+y\{a_1(1-y)xy$$
$$+a_2(1-x)xy-(n_2+n_3)(1-y)x-n_1(1-x)y\}$$
$$\times\frac{\partial\Psi(x,y)}{\partial y}-xy\{a_1(2x-1)+a_2(2y-1)$$
$$-(n_1+n_2+n_3)\}\Psi(x,y)+F \qquad (5.2)$$

$$F=a_1xy\sum_{l_2=0}^{\infty}(l_2+1)Q_2(n_1-1,l_2)y^{l_2}-n_1y^2\frac{\partial\Psi(0,y)}{\partial y}$$
$$+a_2xy\sum_{l_1=0}^{\infty}(l_1+1)Q_1(n_2-1,l_1)x^{l_1}-n_2x^2\frac{\partial\Psi(x,0)}{\partial x}$$
$$+(a_1+a_2)xyP(n_1,n_2,n_3-1).$$

$\Psi(0,y)$ and $\Psi(x,0)$ are included in F, and these do not vanish by using equations (2) and (3). Regarding $\Psi(x,0)$, $\Psi(y,0)$ as known functions, it is then possible to reduce (5.3) to ordinary differential equations, but the equations will be non-linear. Their general method of integration is not yet known.

This difficulity is similar in the most simple case when $n_1=n_2=n_3=1$.

However exact solutions for simple structures with a small number of trunks may be investigated by solving the matrix equations of states, the performance will also be more difficult than for the case of loss systems with grading.

If required, these equation could be solved numerically with the help of computers, by similar method as used by N. I. Bech[2] for loss systems. Also, in the case of such a computer method[3] for solving the equations of states, there will be the added difficulty due to the number of states being infinite for delay systems.

3. Method of the Trials

It is known that an artificial traffic trial using a digital computer is an extremely valuables method for solving the traffic capacity of complicated arrangements of exchange device groups.[4] Detailed investigations of two-stage link systems, using this method have been reported.[5]

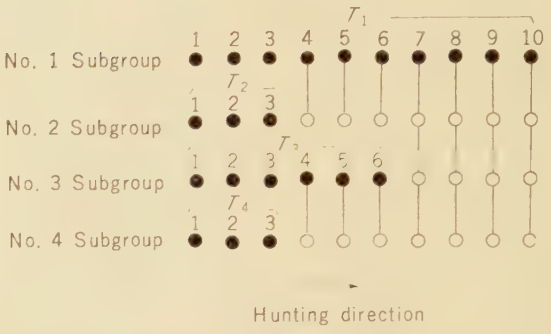

Fig. 3.1—Example of graded multiple delay systems experimened (number of subgroups: $g=4$, availability: $n_0=10$, sequential hunting).

Therefore, some of the methods described here are not original, but the outline of the methods of trials used to obtain the results mentioned in the next section will be stated.

The experiments have been limited to step-up graded multiple delay systems with g subgroups, n_0-availability and sequential hunting as shown in Fig. 3.1. The trunks are devided into g groups corresponding to each subgroup. Let Ti be the number of trunks of the trunk group corresponding to No. i subgroup ($i=1, 2, \cdots, g$). Traffic sources are infinite and the assumptions for calls are simply, equal to those in the Erlang's model. The following notations are used:

a_i: traffic offered to No. i subgroup
a: sum of a_i
C_i: the number of calls offered to No. i subgroup during a measuring interval.
C: sum of C_i
L_t: the number of simultaneous waiting calls of No. i subgroup
L: sum of L_i
$C_{\omega i}$: the number of calls of No. i subgroup delayed during a measuring interval
C_ω: sum of $C_{\omega i}$.

A delay system is treated. Therefore, if it is

desired to obtain the distribution of waiting time, the time of origination or termination of all calls will have to be taken into consideration during the traffic trials. For the present, our object of this research is to determine the average waiting time and the probability of delay. Then only the events of origination and termination of calls will be considered in the trials.

A series of pseudo-random numibers, R_1, R_2, $\cdots\cdots$ is used, and

$$R_{n+1}=5^{13}R_n \pmod{2^{39}}$$

where R_0 is an arbitrary odd number and generally

$$R_0=2910\ 5181\ 6899 \quad \text{or}$$
$$R_0=95\ 2049\ 3187$$

are used. R_0 is changed in the case when many experiments are repeated.

R_n is divided, successively from the first binary digits, per the required number of binary digits for the effecting of events.

The subdivisions are successively used and R_n is used until the remaining number of digits becomes smaller than the required number of digits. Then next number R_{n+1} is originated. The required number of digits is predetermined for each experiment.

Let Q be the number shown by the subdivision.

The origination of a new call from No. i subgroup ($i=1, 2, \cdots\cdots, g$) is effected, when

$$\sum_{j=0}^{i-1} a_j \leq Q < \sum_{j=0}^{i} a_j \quad (a_0=0).$$

The termination of one of the busy trunks in No. i trunks group is effected, when

$$\sum_{j=0}^{g} a_j+\sum_{j=1}^{i-1} T_j \leq Q < \sum_{j=0}^{g} a_j+\sum_{j=1}^{i} T_j,$$

where each trunk of the group corresponds, one by one, to Q within the above range.

The different locations on R_n are used for every requirement in order to effect the subgroup, in which one of the delayed calls will be connected, according to an assumed restriction.

Restriction (3), mentioned in the preceding section, was used in the first stage. That is, each subgroup is chosen in the probability proportional to the number of waiting calls of the concerned subgroups. Concerning the delayed calls of each subgroup, no-pseudo-random number is used for the allocation of the delayed calls to a trunk became free.

R is not referred to, for effecting the sampling of the numbers L_i, L of simultaneous delayed calls, but the sampling is effected every time a call is originated. It is considered that the randomness of sampling will not be disturbed because of the assumptions of pure chance calls and infinite sources.

The average waiting time, W, and the probability $M(0)$ of delay are calculated by,

$$W=\frac{\bar{L}}{C}, \quad M(0)=\frac{C_w}{C}.$$

Every time the number of originated calls amounts to specified numbers, the transit results are printed without releasing the states of holding or waiting calls. Then one experiment is finished after a predetermined number of calls.

Gradings with various numbers of trunks and various forms of multiple were tried. Of course, the conditions are designated on multiple patern memories, and the designation is very simple because the number of each multipled outlet corresponds to the same number of the subgroup in the case of a step-up multiple. A simplified flow chart for the trial is shown in Fig. 3.2.

The computer was used the degital electronic computer named M1-B which was developed in our laboratory several years ago. The computer uses parametrons for logical elements and the calculating speed is a little slow. Therefore, about 2 hours were needed for one trail series of 10,000 calls.

4. Experimental Results

In the case of graded multiple delay systems with 10-availability, the results obtained for

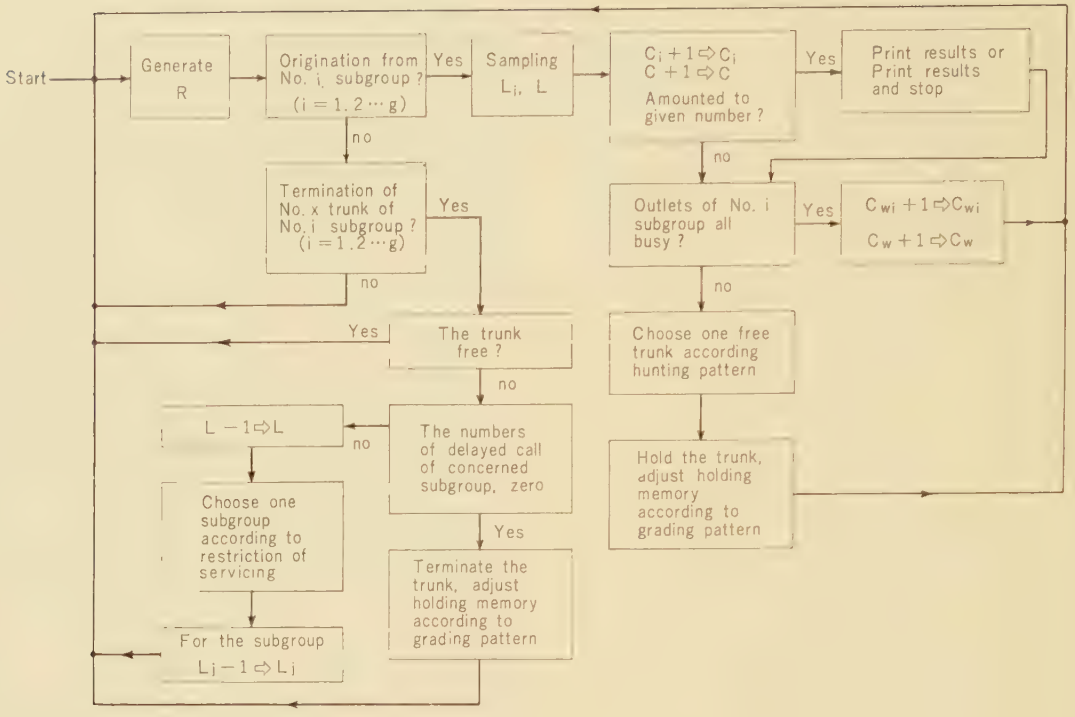

Fig. 3.2—Simplified flow chart for the trials.

two-subgroup gradings and four-subgroup gradings are shown in Table 4.1 and 4.2 respectively.

In order to exclude trangent states, the first 1000 calls were not used in differentiating the experiment conditions.

These results are ploted by black dots in Figs. 4.1∼4.7 which show the variations of the probability $M(0)$ of delay and those of average waiting time W/h with the average efficiency a/n of trunks.

The curve of a full-availability group with n_0 trunks ($n_0=10$: availability of the researched gradings) and that of a full-availability group with the same number of trunks as the corresponding grading group are simultaneously shown, as the upper and lower limiting curves. It is considered that the curve for a grading group will be placed between both curves, like in the case of loss systems.

The curve shown by a broken line in each figures is the value estimated from the case of a loss system with the same grading form, obtained by the approximation method which

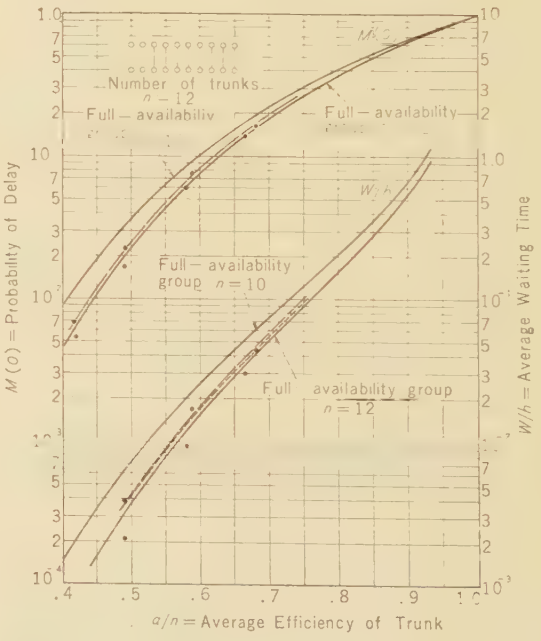

Fig. 4.1—Experimental results shown on the limiting curves given by full-availabillty groups ($n=12$, 2 subgroups).

Table 4.1.

THE EXPERIMENTAL RESULTS FOR 2-SUBGROUP GRADINGS

Number of trunks n	Predetermined traffic	Number of offered calls C	Obtained offered traffic a in Erl.	Traffic carried by common trunks	Probability of delay $M(0)$	Average waiting time W/h	Average efficiency of trunk a/n %	Grading form
12	5	10000	5.02	2.37	.0053	.00052	41.8	Fig. 4.1
		//	4.98	2.34	.0067	.00094	41.5	
	6	//	5.88	3.08	.0167	.00206	49.0	
		//	5.92	3.13	.0223	.00383	49.3	
	7	//	6.98	3.99	.0599	.00933	58.2	
		//	7.06	4.08	.0755	.0169	58.8	
	8	//	8.00	4.86	.139	.0298	66.7	
		//	8.18	5.01	.162	.0529	68.2	
14	7	//	6.90	1.76	.0111	.00107	49.3	Fig. 4.2
		//	7.12	1.86	.0245	.00498	50.8	
	8	//	7.98	2.43	.0423	.00691	56.9	
		//	8.10	2.50	.0508	.00923	57.9	
	9	//	8.91	3.01	.0910	.0180	63.6	
		//	9.00	3.09	.113	.0263	64.3	
	10	//	9.85	3.65	.164	.0379	70.3	
		//	10.10	3.84	.208	.0634	72.2	
16	9	//	8.96	1.24	.0368	.00590	56.0	Fig. 4.3
		//	8.78	1.21	.0332	.00458	54.9	
	10	//	9.95	1.69	.0752	.0134	62.2	
		//	9.90	1.66	.0653	.0132	61.8	
	11	//	11.15	2.23	.167	.0390	69.7	
		//	10.77	2.13	.137	.0264	67.3	
	12	//	11.84	2.58	.245	.0861	74.0	
		//	12.15	2.76	.286	.0987	75.7	
18	11	//	10.95	0.74	.0812	.0159	60.8	Fig. 4.4
		//	10.93	0.73	.0898	.0240	60.8	
	12	//	11.79	0.94	.134	.0313	65.5	
		//	12.02	1.02	.148	.0387	66.8	
	13	//	12.70	1.15	.188	.0551	70.6	
		//	13.09	1.21	.245	.0897	72.6	
	14	//	13.74	1.37	.300	.106	76.4	
		//	13.96	1.42	.337	.161	77.5	

Table 4.2

THE EXPERIMENTAL RESULTS FOR 4-SUBGROUP GRADINGS

Number of trunks n	Predetermined traffic	Number of offered calls C	Obtained offered traffic a in Erl.	Probability of delay $M(0)$	Average waiting time W/h	Average efficiency of a/n %	Grading form
16	6.5	10000	6.38	.0020	.00031	39.8	Fig. 4.5
	8.0	〃	7.99	.0194	.00586	49.9	
	9.5	〃	9.33	.0444	.00876	58.3	
	11.0	〃	11.20	.1731	.0515	76.2	
	12.5	〃	12.80	.359	.127	80.0	
	14.0	〃	13.88	.528	.247	86.7	
22	8.0	〃	8.04	.0009	.000025	36.7	Fig. 4.6
	10.0	〃	9.94	.0047	.00110	45.2	
	12.0	〃	11.82	.0184	.00258	53.7	
	14.0	〃	13.98	.0832	.0170	63.5	
	16.0	〃	15.84	.176	.0376	71.1	
	18.0	〃	18.22	.436	.207	82.9	
	20.0	〃	20.34	.706	.442	95.0	
28	10.0	〃	9.88	.0010	.000111	35.3	Fig. 4.7
	12.5	〃	12.56	.0042	.00039	44.9	
	15.0	〃	14.73	.0144	.00301	52.6	
	17.5	〃	17.95	.0833	.0151	64.1	
	20.0	〃	19.79	.159	.0360	70.7	
	22.5	〃	22.32	.347	.113	79.7	
	25.0	〃	25.12	.621	.363	90.2	

will be mentioned in the next section.

A few results, indicated by dots, are placed out of the lower limiting curve. These are found to occur in the case when the initial number, R_0, of the pseudo-random numbers, was one special value, but which may be chance despersion.

In each Figs. 4.5～4.7, let a_0, a_1 be the offered traffic for the upper and lower limiting curve respectively, for the case when $M(0)$ or W/h is arbitrarily fixed.

The intermediate curve shown by a chain line is given by

$$\frac{a}{n}=\frac{1}{2}\left(\frac{a_0}{n_0}+\frac{a_1}{n}\right) \qquad (4.1)$$

for both of $M(0)$ and W/h.

In the case of $M(0)$ in Figs. 4.5 and 4.6, it was interesting to find that most of the experimental results are located on the chain curve, while the experimental values of W/h

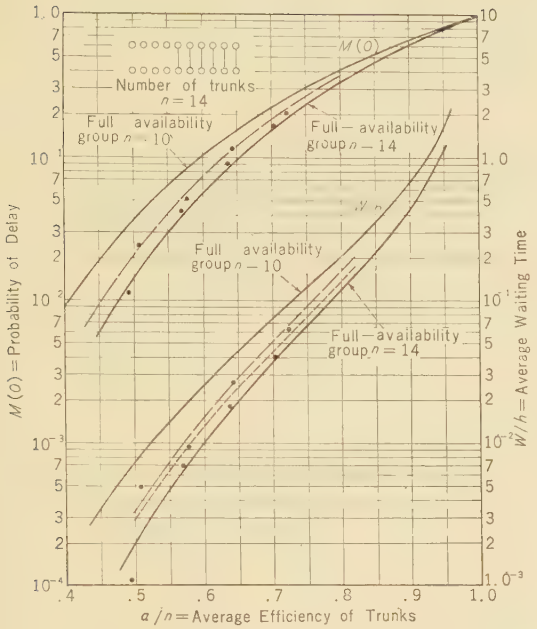

Fig. 4.2—Experimental results shown on the limiting curves given by full-availability groups ($n=14$, 2 subgroups).

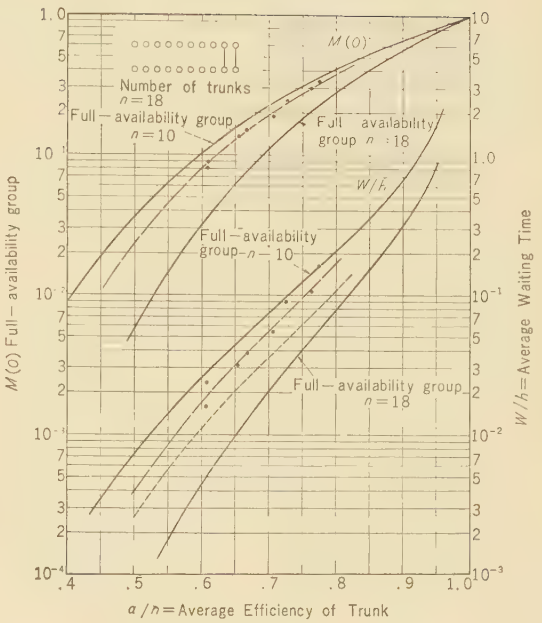

Fig. 4.4—Experimental results shown on the limiting curves given by full-availability groups ($n=18$, 2 subgroups).

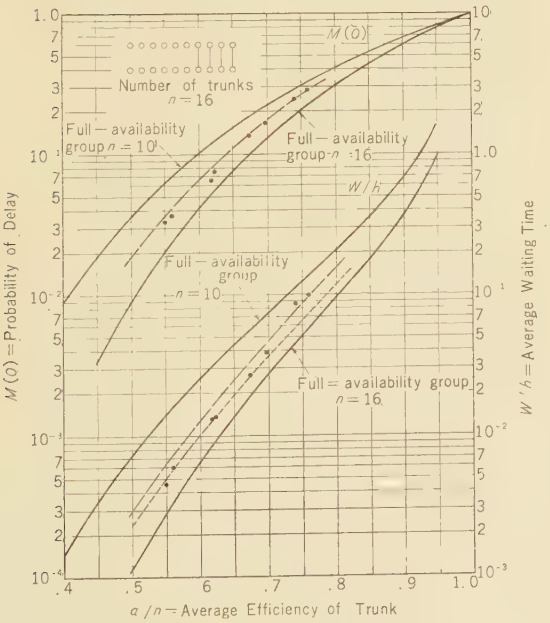

Fig. 4.3—Experimental results shown on the limiting curves given by full-availability groups ($n=16$, 2 subgroups).

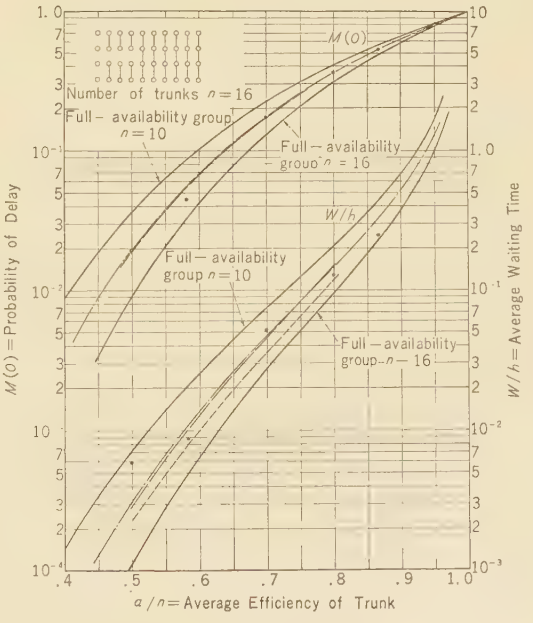

Fig. 4.5—Experimental results shown on the limiting curves given by full-availability groups ($n=16$, 4 subgroups).

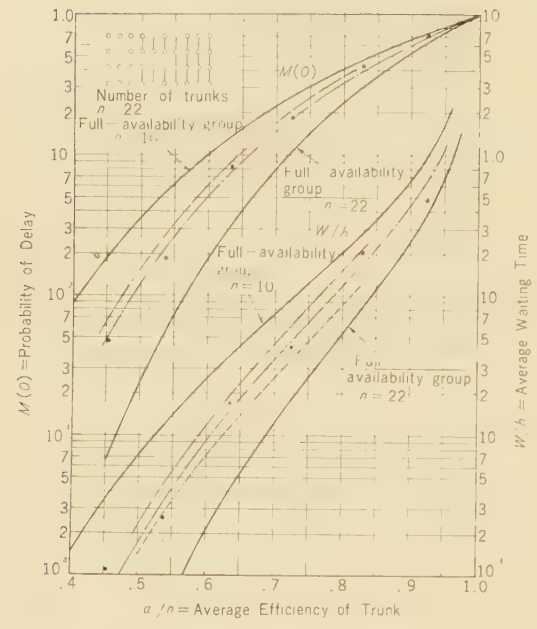

Fig. 4.6—Experimental results shown on the limiting curves given by full-availability groups ($n=22$, 4 subgroups).

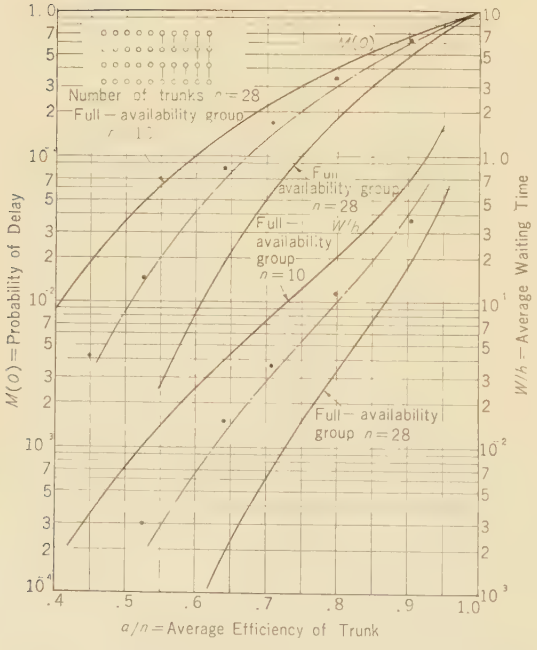

Fig. 4.7—Experimental results shown on the limiting curves given by full-availability groups ($n=28$, 4 subgroups).

do not fall on this curve. It is thought that additional experiments using more calls are necessary.

5. Analogy from Loss Systems

Consider a full-availability group with n trunks and offered traffic a. Let $E_{2,n}(a)$ be the Erlang delay formula and W be the average waiting time in the case when the group is a delay system. Let $E_{1,n}(a)$ be the Erlang loss formula in the case when the group is a loss system. Following relations are known.

$$E_{2,n}(a)=\frac{nE_{1,n}(a)}{(n-a)+aE_{1,n}(a)} \tag{5.1}$$

$$\frac{W}{h}=\frac{1}{n-a}E_{2,n}(a) \tag{5.2}$$

where h is the average holding time.

Let γ be the rate of the increase in the congestion when a loss system is changed into a delay system in the full-availability group, and $\eta(n,a)$ be the average efficiency of the trunks in the case of a loss system. From (5.1)

$$\gamma\equiv\frac{E_{2,n}(a)-E_{1,n}(a)}{E_{1,n}(a)}$$

$$=\frac{\frac{a}{n}\left\{1-E_{1,n}(a)\right\}}{1-\frac{a}{n}\left\{1-E_{1,n}(a)\right\}}=\frac{\eta(n,a)}{1-\eta(n,a)} \tag{5.3}$$

That is, γ can be expressed as a function of only $\eta(n,a)$. Therefore, as one approximate method to determine the traffic capacity of a graded multiple delay system, it may be determined that the relationship of (5.3) can be adapted to the transition of the congestion in the case when a loss system is changed into a delay system in a graded multiple group.

Graded multiple loss systems with sequential hunting have been investigated for a long time by many investigators. In recent years, many detailed numerical relationship have

been determined by using artificial traffic analysers.[6][7] The good approximate method called "equivalent random theory" is also known.[5]

Likewise, in our laboratory, an artificial traffic analyser exclusively usable for graded multiple loss systems with sequential hunting was developed in 1956, which uses thermal noise in a resistor for the call sources and decatrons for counters. And the researches using this analyser has been used for many investigations.[10]

Some examples of the results obtained, using the analyser, are shown in Table 5.1 with some of the grading forms (10-availability) which were determined to be most efficient by using the analyser.

The load curves estimated from the results are shown in Figs. 5.1 and 5.2, which show the variation in the loss with the average offered traffic per trunk. For reference, similar curves of full-availability groups with ($n=10$, $n=22$) ($n=10$, $n=30$) are shown in the figures, respectively. It is well known that the curve of a grading group will be found between the curves of the full-availability groups.

Curve M is the estimated probability of delay (in same scale as loss) for the delay system with the same form of grading, which is obtained by adapting (5.3) to curve B. Curves for corresponding full-availability groups are also shown.

The curve of $M(0)$ shown by a broken line in each of the Figs. 4.1∼4.6, was estimated by the above method. The experimental results of loss systems are not shown here, but those are based on curves of loss obtained by means of artifical trials on the analyser with several hundred thouthand calls offered.

In the case of average waiting time, it appears that (5.2) can not be adapted to the $M(0)$ estimated by the above method. Whereas, if the number of individual trunks of each subgroup increases, $a \to g\, a_0$ ($n \to g\, n_0$) and then

$$\frac{W}{h} \to \frac{1}{g} M(0)$$

It is clearly illogical.

Therefore, let us put

$$\frac{W}{h} = \frac{1}{n_1} \cdot \frac{1}{1-a/n} M(0) \qquad (5.4)$$

Where n_1 is the number of trunks in a full-availability group which will have the same $M(0)$ as the considered graded multiple group has for the same average efficiency of trunks. n_1 is not always represented by one value for all a/n. For example, $n_1=12.8$ for $a/n=0.5$, but $n_1=12.0$ for $a/n=0.8$ in Fig. 4.8.

The curve of W/h shown by a broken line in each of the Figs. 4.1∼4.6 was ploted by (5.4). For reference, a curve ploted by (5.2) is shown by a dotted line.

That we make use of (5.3) and (5.4) for the estimation, is finally the same as the following. That is, the number of trunks, n_1 of a full-availability group which will have the same probability of loss as the considered graded multiple loss system for a given average efficiency of trunks is first determinated. Then the $M(0)$ and W/h of the full-availability group with n_1 trunks are regarded as those of the delay system with the same form of grading.

As indicated in Figs. 4.1∼4.6, the above estimating method may be considered nearly adoptable but lies a little on the safety side.

On the other hand, it must be noticed that the restriction of servicing of delayed calls is not taken into consideration. More researches through artificial traffic trials will be necessary in order to determine the effect of the restriction.

Now the traffic carried by trunks will be considered. On a full-availability group with n trunks and offered traffic a and with sequential hunting, let the traffic carried by trunks latter than No. r outlet be $A_L(r+1)$ in the case of a loss system and be $A_W(r+1)$ in the case of a delay system.

It is well known[10] that these are given by

$$A_L(r+1)=a\{E_r(a)-E_n(a)\}$$

Table 5.1

THE RESULTS BY THE TRAFFIC ANALYSER WITH GRADED MULTIPLE LOSS SYSTEMS

Grading form	Number of trunks	Total numder of offered calls (1000)	Offered traffic (Erl.)	Probability of loss	Confidence rate limit with 95% coefficient for the loss
		730×2	10.00	.00399	
		〃	11.99	.0148	
Fig. 5.1	22	〃	13.99	.0373	±3%
		〃	16.01	.0719	
		〃	17.98	.0113	
		1180×2	12.00	.00095	
		〃	15.00	.00716	
Fig. 5.2	30	〃	18.02	.00269	±8%
		〃	21.03	.0610	
		〃	23.99	.106	

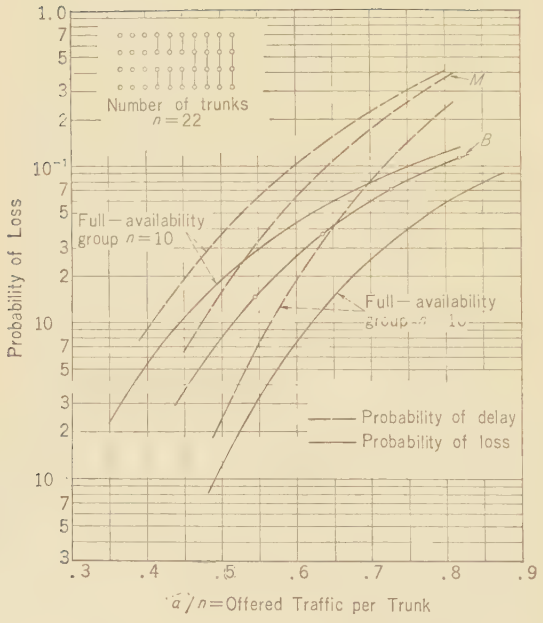

Fig. 5.1—Probability of loss in a graded multiple loss systems obtained by means of an artificial traffic analyser.

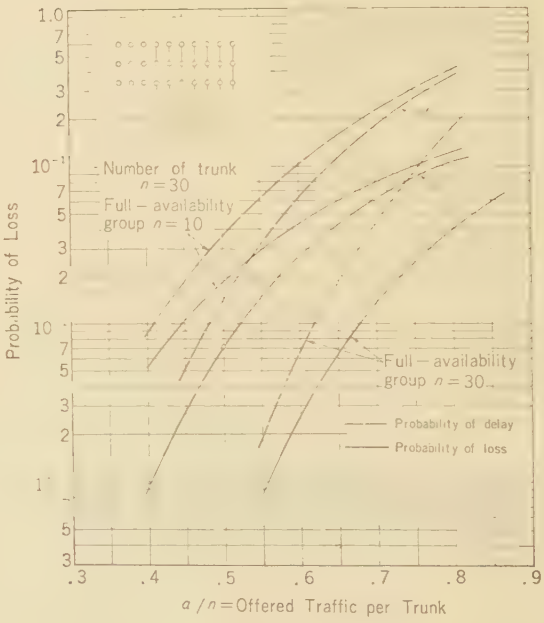

Fig. 5.2—Probability of loss in a graded multiple loss systems obtained by means of an artificial traffic analyser.

$$A_W(r+1)=\frac{a\{E_r(a)-E_n(a)\}+(n-r)\frac{a}{n-a}E_n(a)}{1+\frac{a}{n-a}E_n(a)} \qquad (5.5)$$

Consider the case when traffic a is offered to each subgroup of a 2-subgroup graded multiple group that latter outlets than No. r are commoned. Let half of the traffic carried by the common trunks be $A_{LG}(r+1)$ in the case of a loss system, and be $A_{WG}(r+1)$ in the case of a delay system. Generally

$$A_L(r+1)<A_{LG}(r+1),\ A_W(r+1)<A_{WG}(r+1)$$

Some of the value of $A_{LG}(r+1)$ and $A_{WG}(r+1)$ were obtained by the artificial trials. These are shown in Fig. 5.3 and also the value obtained by (5.5) are shown simultaneously for comparison. Within the range of the experiment, the following was found.

$$A_L(r+1)\fallingdotseq A_{WG}(r+1).$$

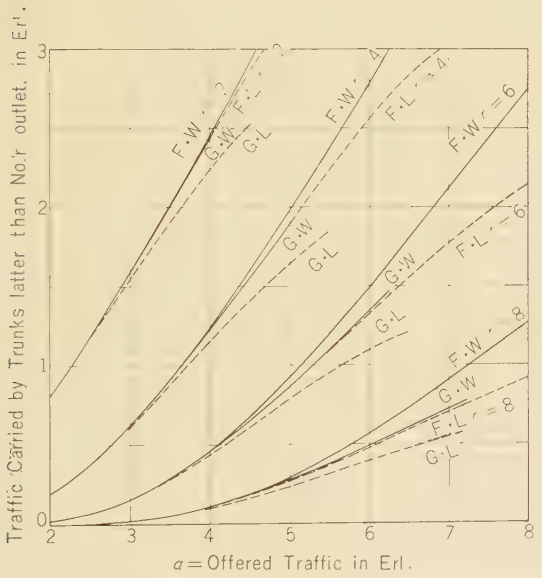

F: full-availability group with 10 trunks
G: graded multiple group with 2 subgroups and 10-availability
W: delay system
L: loss system.

Fig. 5.3—Comparison of traffic carried by trunks latter than No. r outlet (availability $n_0=10$).

6. Analogy for Early Departure

In the preceding sections, it was one of the basic assumptions that all delayed calls wait until served. However, consideration must sometimes be given to the situation where some of the delayed calls depart without being served, such as cases where originating registers are waited in common controll exchange systems. Also in some cases the measure of grade of service may not be the average waiting time or the probability of delay, but the propotion of departed calls will be taken as the measure in some cases.

In the case when the distribution of time until departure may be assumed to be a negative exponential distribution, with mean h/s, the stationally queuing problems on a full-availability system $M/M/n$ was solved exactly.[10] Let R be the proportion of departed calls, and then[11]

$$R=\frac{s}{a}\cdot\frac{E_{1,n}(a)\sum_{l=1}^{\infty}l\prod_{i=1}^{l}\frac{a}{n+is}}{1+E_{1,n}(a)\sum_{l=1}^{\infty}\prod_{i=1}^{l}\frac{a}{n+is}} \qquad (6.1)$$

The expression is illustrated in Fig. 6.1 as an example which shows the variation of R with s for various values of n where a is given with the various values of n to be $R=E_{1,n}(a)=0.01$ when $s=\infty$. Of course, R varies with n. It is, however, interesting to notice that the variation of R for the variation of n decreases rapidly as n becomes larger.

In the exchange systems of transit or terminal offices which receive subscriber dial pulses through incoming trunks, the connection to the incoming registers is generally controlled during the pause between successive pulse trains. In such cases of queuing problems, the consideration of the proportion of departed calls is very effective.

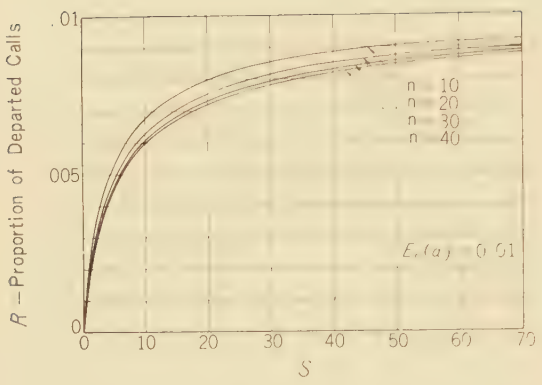

Fig. 6.1—Variation of the proportion of departed calls with S.

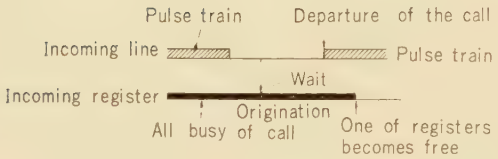

Fig. 6.2—Early departure in the case of dial pulse incoming register.

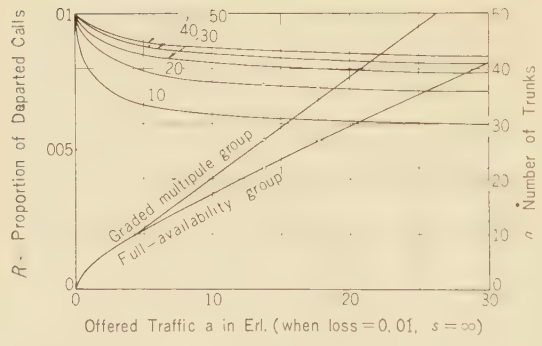

Fig. 6.3—The method of estimating the properties of departed calls with graded multiple delay systems (grading with 10-availability and step-up multiple form).

The arrangement of incoming registers is generally designed as a delay system. If the delay time for a call becomes longer, and the next pulse train begins before a register is prepared to receive it, then a busy signal will be sent in order to avoid a wrong connection. The probability that the busy signal will be sent, may be used as a grade of service.

In such a case, as shown in Fig. 6.2, the event that the next pulse train begins may be regarded as the early departure. Therefore, if it may be assumed that the length of remaining pause and the holding time of the register are distributed exponentially with means τ and h respectively, the problem will be adapted to the model of (6.1).

For example, put $\tau=500$ ms, $h=15$ sec, and then $s=30$. Since s is generally large like this, the delay system is close to a loss system.

Now consider the case when the registers are arranged with graded multiples. It will also be required to determine the proportion of departed calls in the graded multiple delay system.

Corresponding to Fig. 6.1, as shown in Fig. 6.3, the variation of R can be illustrated with the offered traffic a which is so given that $R=E_{1,n}(a)$ becomes a given constant when $s=\infty$. The traffic load curves for a given loss are practically usable for graded multiple loss systems where $s=\infty$.

The following approximate method using them may be considered to be useful. That is, the proportion of departed calls for $s=s_1$ in a graded multiple delay system with n_1 trunks to which is offered the same traffic as for a given loss B when $s=\infty$, is assumed to be equal to the R for $s=s_1$ in the full-availability group with n_2 trunks ($n_2<n_1$), to which the above same traffic is offered for the above same loss B when $s=\infty$.

The traffic load curves for a full-availability loss system and for a step-up graded multiple loss system with 10-availability and sequential hunting are shown simultaneously in Fig. 6.3.

For example, in the case of the full-availability group with $n=27$ to which the same traffic $a=17.7$ Erl. as for $E_{1,n}(a)=0.01$ when

$s=\infty$ is offered, it will be found that the proportion $R_1=0.0073$ for $s=20$. On the other hand, according to the above method, it can be found that the proportion $R_2=0.0074$ for $s=20$ in the case of the grading with $n=27$, because $a=13.7$ E.l. for $B=0.01$ when $s=\infty$ in the grading and the corresponding full-availability group is that with $n=22$,

When s is larger than about 20, it may be no hindrance for practical use that the proportion of departed calls of a grading is put more roughly to be equal to that of a full-availability group with the same number of trunks and loss as the grading when $s=\infty$, because $R_1 \fallingdotseq R_2$ in the above example.

7. Conclusion

The efficiency of graded multiple delay systems with sequential hunting was discussed, being based on the results of artificial traffic trials by means of a digital computer. For practical use, it was mentioned that the efficiency of the delay system can be estimated from the knowledge of a loss system with the same form of grading.

Since the results obtained are dispersive, especially for the average waiting time, more experiments will be necessary before obtaining a more detailed conclusion.

In the case of graded multiple delay systems, the restriction of servicing of delayed calls must have influence on the probability of delay and the average waiting time. Sometimes distribution of waiting time will also be required. These are thought to be some of the future problems.

In this paper, only the case with sequential hunting was discussed, but a graded multiple delay system with random hunting will also be important in automatic exchange systems.

Finally, the author wishes to state that the following is considered to be one of the problems of this investigation.

How can detailed results be obtained through artificial traffic trials by means of a digital computer, especially on a delay system? It must be investigated further with the development of computers with very large memory capacity and super high speed, where problems on a pseudo-random number will be especially important.

Acknowledgement

The author wishes to acknowledge the encouregement and suggestions of Mr. T. Shimbori: former Chief of the Communication Network Section, Mr. H. Shimada: Chief of the Communication Network Section, Mr. H. Kawasaki: Chief of the Switching Research Section and Mr. Y. Sekiguchi: Chief of the First Switching Section.

The author's thanks are also extended to Mr. K. Takagi who programed and prerformed the trials by a digital computer and Mr. K. Takahasi who performed the experiments by an artificial traffic analyzer and for the co-operation of members of the degital computer research group.

References

(1) Palm, C.; Calcul Exact de le Perte dans les Groupes de Circuits Échelonnés, Ericsson Techn., **4,** (1932) pp. 39–71.

(2) Bech, N. I.; Statistical Equilibrium Equations for Overflow System, *Teleteknik* (*Eng. Ed.*) **1,** (1957) pp. 66–71.

(3) Carlsson, S. G. & Elldin, A.; Solving Equations of State in Telephone Traffic Theory with Digital Computers, *Ericsson Techn.*, **14,** (1958) pp. 221–244.

(4) Neovius, G.; Artificial Traffic Trials using Digital Computers, *Ericsson Techn.*, **11,** (1955) pp. 279–291.

(5) Wallström, B.; Artificial Traffic Trials on a Two-Stage Link System using a Digital Computer, *Ericsson Techn.*, **14,** (1958) pp. 259–289.

(6) Broadhurst, S. W. & Harmston, A. T.; Studies of Telephone Traffic with the Aid of a Machine, *J.I.E.E.*, **100,** (1953) pp. 259–274.

(7) Ekberg, S.; Telephone Traffic Research with the Aid of the Swidish Traffic Analyser, *Tele.*, (*Eng. Ed.*), **1,** (1955) pp. 1–29.

(8) Wilkinson, R. I.; Theories for Toll-Traffic Engineering in the U.S.A., *B.S.T.J.*, **35,** (1956) pp. 421–514.

(9) Gambe, E. & Takahashi, K.; Studies on the Efficiency of the Standard Grading with an Artificial Traffic Analyser, *Reports of ECL., NTT.*, **7,** (1959) pp. 385–392.

(10) Palm, C. ; Research on Telephone Traffic Carried by Full Availability Groups, *Tele. (Eng. Ed.)*, **1,** (1957) pp. 1–107.

(11) Syski, R. ; Introduction to Congestion Theory in Telephone Systems, p. 559, London, (1960).

* * * *

U.D.C. 666.97.03 : 678.674
: 621.315.651.66

Thermosetting Plastic Swelled with Grainy Fillers (Plastic Concrete)

Nobuo MURAI† and *Susumu MIZUNO*†

Polyester resin swelled with grainy fillers is described in this paper. The fillers are different in size, i.e., powder of calcium carbonate of 2–5μ, iron sand of 100–200μ, sand of 300–400μ and stone of 3–5 mm. The mixing ratio for high workability and strength has been determined. The characteristics of the mixture thus obtained after curing, which is called Plastic Concrete (P.C.) are as follows:

Compressive strength……12 kg/mm²; modulas of elasticity……2,000 kg/mm²; flextural strength……3 kg/mm².

P.C. has now been used for crossarms and insulator housings.

1. Introduction

When plastic is used for construction, it usually requires reinforcement. F.R.P., (Fiberglass Reinforced Plastics) for example, has very good mechanical characteristics and is used in motor cars, boats, etc. However, it is so expensive that its use is limited.

Tests heve been made by the authors to swell thermosetting plastic with fillers. Namely, grains such as iron sand, sand and stone were mixed in polyester resin, and then the mixture was cured until P.C. was obtained. Measurements made of the mechanical characteristics of the P.C. indicated that it can be used for compressive materials.

2. Condition of Swelling

In compounding fillers in resin, care must be taken to make the workability of the resin high before curing and its strength after curing high.

2.1. Swelling Limit due to Size of Grains

Supposing that the size of each filler is the same and the grains are of spherical shape, the theoretical limit of compounding fillers in resin is up to f_m of 0.75, which is the maximum value of f, i.e., the ratio of the total volume of resin including fillers to that of the fillers (to be called "filling ratio"). Since, however, the actual fillers such as sand, stone etc. are not of spherical shape, f_m will be a little smaller, something about 0.6–0.5.

When the fillers are different in size, f_m can be approximated as 1. Supposing that N kinds of fillers $A, B, \cdots\cdots N$ markedly diminish in diameter in order of $A, B, \cdots\cdots N$, and putting $f_a, f_b, \cdots\cdots f_n$ for f of the respective fillers and F for the overall filling ratio, the following relation may be obtained.

$$\frac{1}{1-F} = \frac{1}{(1-f_A)(1-f_B)\cdots\cdots(1-f_N)}$$

Whereas the maximum value of $f_A, f_B, \cdots\cdots$

* MS in Japanese received by the Electrical Communication Laboratory on July 5, 1961. Originally published in the *Kenkyû Zituyôka Hôkoku* (*Electrical Communication Laboratory Technical Journal*), N.T.T., Vol. 10, No. 10, pp. 2107–2127, 1961.

† Outside Plant Section.

is about 0.5, value under 0.4 is used in practice for the reasons mentioned later. Where four kinds of fillers are used, the swelling ratio of the resin can be increased up to 7 or more.

2.2. Swelling Limit due to Viscosity of Mixture

When the size of the grains of the fillers used is the same, it may be said, from the viewpoint of the resistance of stirring and the difficulty of casting work (taken altogether, hereinafter to be referred to as workability) at the time when resin and fillers are mixed together, that the greater the size of grain, the higher the workability will be. However, when the size of the grain is great, the strength of the P.C. will not be as high and the value of f_m can not be greater than 0.75, as mentioned later.

When a mixture of grains, which are different in size, is used as a filler, not only a high swelling ratio but also a high workability can be obtained. Fig. 1 shows the viscosity-workability-measured by putting the propeller, with a constant number of rotations, into the mixture, and measuring the value of torque of its shaft.

It may be seen from the figure that fillers ⑦, ⑧ and ⑨, whose particle diameters are distributed, have higher a, but lower viscosity as compared with fillers ①, ②,……⑥, whose particle diameters are the same. It may, further, be said that the resin with lower viscosity can be swollen more easily. In practice, however, the resin is selected in many cases from an economical point of view.

2.3. Relation between Compressive Strength and Swelling of P.C.

When fillers of the same size are added to the resin, the compressive strength, σ_c, of

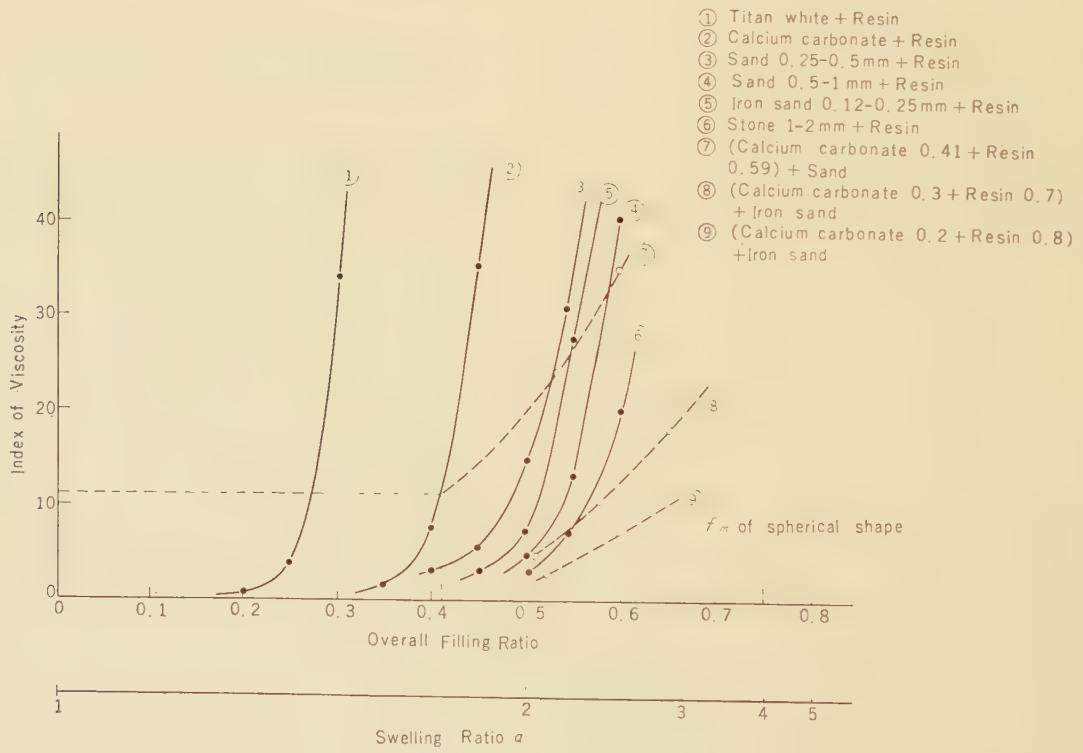

Fig. 1—Index of viscosity with swelling ratio.

P.C. after curing will diminish as the ratio of its swelling is increased. In this case, σ_c will diminish very rapidly, where $f>0.7$.
The compressive strength will also diminish as the particle diameter increases. When, however, two or more kinds of fillers of different size are mixed in the resin, σ_c will be greater than in the case where fillers of the same size are mixed, and this tendency will be conspicuous when $F>0.7$. An example of such a relation with porcelain grains used as the filler, is shown in Fig. 2.

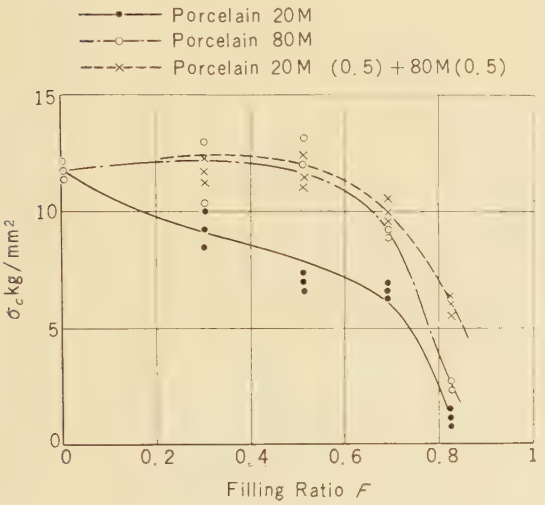

Fig. 2—Compressive strength σ_c with filling ratio F.

The calculated value of this equation is shown in Fig. 4.

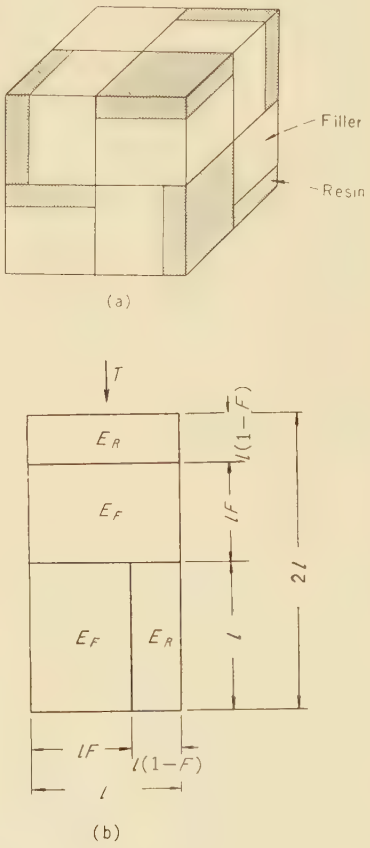

Fig. 3—Unit cube of P.C.

2.4. Relation between Modulus of Elasticity and Swelling

Modulus of elasticity E of P.C. lies between the modulus of elasticity of the resin E_R and that of the filler E_F. Supposing that the composition of the P.C. is microscopically made up of a gathering of unit cubes, in which resin and filler are piled up in series parallel (see Fig. 3),

$$\frac{2}{E}=\frac{1-F}{E_R}+\frac{F}{E_F}+\frac{1}{E_R(1-F)+E_F\cdot F}$$

In practice, however, a smaller value is obtained, since foam, which are intermixed in the P.C. during the course of stirring, still remain after curing.

Now, E_R of polyester resin is usually considered to be about 400 kg/mm², while E_F of a filler to be above 4000 kg/mm². When load is brought to an anisotropic body made up of bodies whose modulus of elasticity markedly differs from each other, it is desirable that E_R and E_F are equivalent in order to avoid the concentration of stress within the body. Tests were made to avoid the concentration of stress by filling the

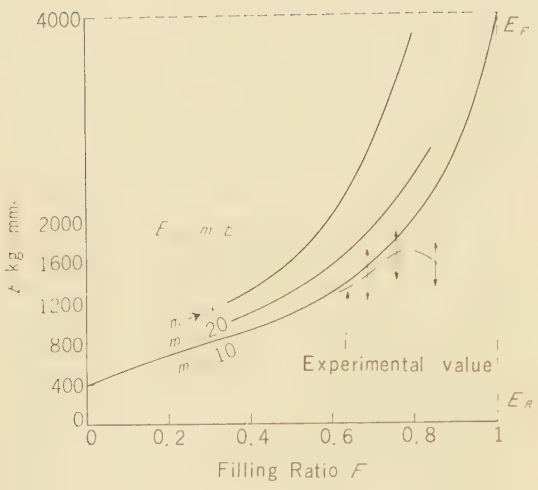

Fig. 4—Modulus of elasticity E with filling ratio.

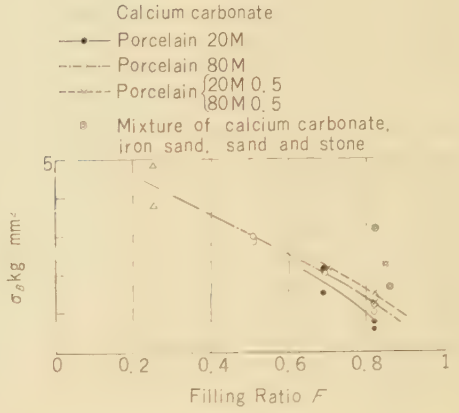

Fig. 5—Flexural strength σ_B with filling ratio F.

resin not only with filler A but also with filler B, which is finer than the former, and making to modulus of elasticity of the filler other than filler A apparently great.

It is also desirable for the economization of swelling, workability and compressive strength to mix two kinds or more of the fillers which are different in grain size.

2.5. Relation between Flexural Strength and Swelling

Since fillers are of grainy nature, its effect an increasing the tensile strength of the mixture can not be hoped for. Therefore, the flexural strength will also be decreased in proportion to the rate of swelling. The experiment made with grains of porcelain show that the flexural strength will, as in the case of the compressive strength, be greater as the grain size becomes smaller and the grain size distribution wider. (see Fig. 5)

3. Material for P.C.

〔**Resin**〕

Epoxy resin and polyester resin are the typical ones as casting resin for P.C. since epoxy resin generally has a low viscosity, it can be swelled greatly. Its mechanical characteristics are also good, and it has various other advantages, but it has also some weak points, namely high cost and long curing time required (some 0.5–1 day). Polyester resin, on the contrary, falls behind epoxy resin in various strong points mentioned above, but offers the advantages of low cost and short curing time (about 1 hour). There are several types of polyesters on the market such as general type, chemical proof type, flexible type etc., and it is necessary to select one according to the usage of the P.C.

〔**Filler**〕

Stone: The grain size is determined according to the size of moldings. In the experiment, 2–3 mm grains were used, where $f_m \fallingdotseq 0.60$.

Sand: In many cases, the sand has the diameter of about 0.25–0.45 mm and it has sharper corners as compared with stone. $f_m \fallingdotseq 0.54$–0.58; specific gravity $= 2.6$

Iron sand: Many grains have the diameter of 100–150μ and are more spherical than the sand or stone. The use of iron sand in P.C. will offer better workability and, at the same time, greater compressive strength as com-

pared with sand. $f_m \fallingdotseq 0.60$; specific gravity $=4.6$

Calcium carbonate: Calcium carbonate is usually used as resin filler, with its diameter being about 2–5 μ. Specific gravity $=2.6$

Porcelain: This is obtained by crushing the insulator for communication use into grains of the magnitude of 0.15–1.0 mm, without giving them surface finishing. When this is used in P.C., its abrasion resistance will be great and insulation good. Specific gravity $\fallingdotseq 2.6$.

〔**Others**〕

In addition to the above, glass powder or metallic oxides are used, in which case, however, the workability, unit price and the characteristics of the filler are taken into consideration.

4. Compounding Ratio and Characteristics of P.C.

The compounding ratio of filler and resin is determined according to the workability and strength required for the P.C. On the other hand, the grain size and viscosity of the P.C. will somewhat vary according to the description of each filler and resin. The exact compounding ratio, therefore, should be determined through experiments. Some examples of the results obtained by experiment, are shown below.

(1) In the case of the compounding ratio of:

Polyester (general type)····about 12 % by wt.
Calcium carbonate····· 〃 18 〃
Iron sand, sand, stone····· 〃 70 〃
Promoter, catalyzer·····a little

the following characteristics were obtained.

Compressive strength·· about 12 kg/mm^2
Modulus of elasticity·· 〃 2000 〃
Flexural strength····· 〃 3 〃

(2) In the case of the compounding ratio of:

Polyester (general type)····about 7 % by wt.
Calcium carbonate····· 〃 9 〃
Iron sand, sand, stone ····· 〃 84 〃

the following characteristics were obtained.

Compressive strength··about 11.5 kg/mm^2
〃 〃
(after boiling at 96°C for 8 hrs.)··8 〃

When resin of lining type was used,

Compressive strength··about 12.5 kg/mm^2
〃 〃
(after boiling at 96°C for 8 hrs.)··12.5 〃

The results of experiments showed that P. C. with a great compressive strength had also a large modulus elasticity, and the reverse relation held good. The flexural strength was about 1/4–1/6 of the compressive strength.

The table attached shows the electric characteristics obtained.

The shrinkage of P.C. due to curing is very small, which can be expressed experimentally by the following equation.

$$s = s_R(1-F)$$

where s : shrinkage of P.C.
s_R : shrinkage of resin

P.C. is not susceptible to cracks or deformations due to shrinkage, therefore, it is suitable for making large-size castings.

It is also chemical and flame proof, and its surface appearance, which varies with the kind of filler, usually has a black or marble tone.

5. Applications

〔**Crossarm**〕

The tensile side of the crossarm is reinforced with steel wire. The moment of destruction M of the crossarm depends upon its sectional shape and the tensile strength of steel wire. M of the P.C. arm of the same gauge as the arm now in use is 120 kg-m in the case of 4 wire type, and 300 kg-m in the case of 8 wire type.

The P.C. arm has the strong point that it is less liable to deformation or rotting as compared with wooden one and its dimensions can be taken precisely, and that it can be

Table

ELECTRIC CHARACTERISTICS OF P.C.

Material		P. C.			Polyester
Dielectric loss tan δ	1 KC	0.15 – 0.21	resin	7 Wt %	1 MC
	50 KC	0.22 – 0.28	resin	7 Wt %	0.01 ~ 0.02
	1 MC	0.19 – 0.21	resin	8 Wt %	
Dielectric constant ε	1 KC	33 – 53	resin	7 Wt %	1 MC
	50 KC	20 – 27	resin	7 Wt %	2 ~ 4
	1 MC	14 – 17	resin	8 Wt %	
Volume resistivity	1.5×10^{7} – 1.7×10^{7} Ω cm		resin	7 Wt %	10^{13} – 10^{16} Ω cm
Dielectric strength	1 KV/mm		resin	7 Wt %	14 – 16 KV/mm

made thin without impairing its serviceability.

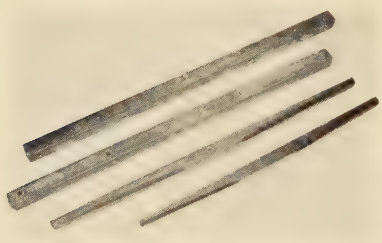

Fig. 6—Four wire type crossarm (upper two) and experimental eight wire type crossarm (lower two).

Fig. 7—Crossarms installed on pole for testing.

〔Terminal housing〕

This is the housing for a terminal board which connects the cable with a drop wire in the underground wiring for a subscriber's line. It is of cylindrical shape, having the diameter of about 50 cm, depth of 60 cm or

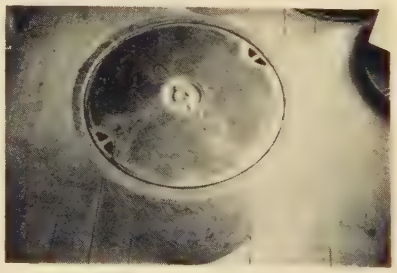

Fig. 8—Terminal housing.

90 cm and thickness of 2.5 cm, in which the terminal board can be installed. It has a weight of about 110 kg or 140 kg, including the cover. By using P.C. a lighter housing can be obtained than that made of cement.

〔**Road eye**〕

Here, porcelain is used as a principal filler, with fibrous material and others mixed to some extent.

Being of white colour, this P.C. has large abrasion resistance. After being molded into a fixed shape, it is fastened to the road with epoxy resin. It will stand a load of about 20 tons.

Fig. 9—Road eye.

Fig. 10—Road eyes with glass beads.

〔**Others**〕

The P.C. manhole cover (Fig. 11), water-meter cover (Fig. 12), cable terminal plate (Fig. 13) etc. have been manufactured for testing, while the P.C. duct, insulating parts etc. are now under test-making.

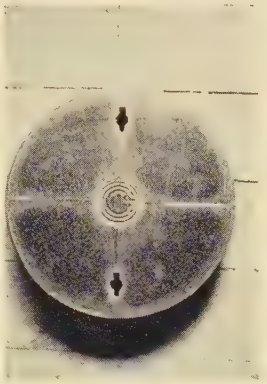

Fig. 11—Manhole cover.

Fig. 12—Meter case cover.

Fig. 13—A hundred-pair cable terminal.

6. Plastic Concrete has Many Distinctive Features, such as

a) it is an insulating material, b) it can be hardened in a short time, c) small shrinkage and little deformation, d) capa-

bility of being casting-molded etc., P.C. is now in commercial use for some purposes. However, in order to make P.C. cheaper and stronger, further experimentation on the swelling technique and, the anisotropic body is necessary. It is also necessary to develop new swelling materials.

* * * *

U.D.C. 681.177.7 : 621.374] : 003.24

An Electronic System for Translating Japanese into Braille*

KIYASU Zen'iti† and *SEKIGUTI Sigeru*‡

A new electronic system for the translation of Japanese into Japanese braille is described in this paper. The system, which is controlled by six-hole paper tape whose codes correspond to the six dots of the braille cells, consists of three parts: the teleprinter, the braille translating unit, and the braille printer.

The codes of the keyboard in the teleprinter are somewhat different from those in conventional teleprinters in order to simplify the translating unit. About 800 Parametrons are used in the translating unit, which is a special-purpose computer.

The translated codes on a braille tape are read by the braille printer and printed in the form of braille cells. Several plans for improving the equipment and for developing a braille service system are also discussed.

1. Introduction

The Japanese orthography currently used is very complicated, because a mixture of Chinese ideographic characters and Japanese 'kana' characters is used. However, a braille system for the blind based 'kana' only has been in use since 1890. Therefore, the orthography for the blind differs quite markedly from that for the not blind, a practice quite different from that followed with European languages.

Until the present, the translation of ordinary writing into braille, that is to say "braille translation," has been performed mostly be "Braille Volunteers" using braille styluses or braille typewriters. And when it was necessary to make many copies the so-called zinc-sheet method, in which braille paper was placed between two zinc sheets, which had been prepared by embossing them with braille symbols, and then compressed between two rollers was used. However in the former method much labor of the "Braille Volunteers" is necessary; and in the latter method the zinc sheets are expensive. To lessen these difficulties we have developed an electronic system for translating Japanese into braille. A photograph of the completed system is shown in Fig. 6

This system consists of three parts: the teleprinter, the braille translating unit, and the braille printer.

First, a sentence is printed in Roman letters on printing paper by the teleprinter, and at the same time a paper tape is perforated.

In the translating unit, Roman letters are translated into braille letters and their codes are perforated on a paper tape. These codes are then read by the braille printer, and are printed in the form of usual braille letters.

With this system even a person with no knowledge of braille can translate Japanese into braille. Moreover, the original cost is

* MS in Japanese received by the Electrical Communication Laboratory on December 9, 1960. Originally published in the *Kenkyu Zituyôka Hôkoku* (*Electrical Communication Laboratory Technical Journal*), Vol. 10, No. 6, pp. 1149–1161, 1961.

† Associate Director of Electrical Communication Laboratory.

‡ Electronics Research Section.

much lower than that of the zinc-sheet method, because in this system paper tape is used instead of zinc sheets.

2. On the Japanese Braille System[1]

The Japanese 'kana' are quite different from Roman letters in that they are not an alphabet, they are a syllabary; that is, each character represents one syllable of a word. As mentioned above, Japanese braille is based on 'kana', and the correspondence is shown in Table 1. Since each braille cell is in the form of a six-digit binary code, it may be represented by a series of ones and zeros in the from $x_1x_2x_3x_4x_5x_6$: for example, ア (a), 100000; カ(ka), 100001; etc. However, as shown in Table 1 Japanese braille consists of several groups: Each cell of the first group, which is called the 'fifty sounds', can be represented by a single code; each cell of the second group can be represented by two codes, a '000010' and a 'fifty sounds' code; each cell of the third group can be represented by two codes, a '000100' code and a 'fifty sounds' code; etc. Parentheses, brackets, the period, etc. are omitted from this table.

It will be seen from this table that the codes of vowels are composed of the three digits x_1, x_2, and x_4,; that is, vowels are represented as follows:

$$x_1 \quad x_2 \quad 0 \quad x_4 \quad 0 \quad 0$$

where x_1, x_2, and x_4, are 0 or 1.

Most of the 'fifty sounds' codes except vowels are composed of vowel codes and so-called "consonant codes": $0\,0\,x_3\,0\,x_5\,x_6$; therefore, (ka) for example, is represented by the following logical notation:

$$(k) \vee (a) = (ka). \qquad (2)$$

However, (ya), (yu), (yo), (wa), and (wo) are exceptions.

Thus, braille cells are constructed in a manner similar to the transliteration of Japanese into the Roman alphabet.

The basic features of the braille orthography will be explained below.*

1) A macron, ⠒, is used to prolong a sound in the following manner:

Braille cells	Roman transliteration
⠁⠒ (a :)	Ā
⠊⠒ (i :)	Ī

2) Assimilated sounds in a word are written by using the cell ⠆ in the following manner:

Braille cells	Roman transliteration
⠅⠆⠉ (ko)(ka)	KOKKA
⠅⠆⠞ (ki)(to)	KITTO

3) Words which mean quantity or order are preceded by the special code ⠼ —which we call the "Figure Symbol Code"— in the following manner:

Braille cells	Roman transliteration
⠼⠑⠓⠝ (5)(ho)(n)	5 HON
⠼⠎⠒⠁⠚⠚⠊⠝ (su)(:)(1)(0)(0)(ni)(n)	SŪ 100 NIN

* Japanese braille are normally written from right to left; however in this paper they are written from left to right for convenience. In the main body of this paper either the corresponding Roman transliteration or Arabic figure is given below each braille cell; in Table 1 the corresponding Japanese 'kana' character is also given.

4) If the first character code of the word following any figure is the same as any figure code – for example, the code of the character (re) is the same as that of (7) – a hyphen should be inserted between them.

Example:

Braille cells	Roman transliteration
⠼⠁⠗⠞⠥	3 RETU
(3) (re) (tu)	

5) Rules of spacing between words are extremely complicated. The following rules are only a small number of the many which must be observed.

a) No space is inserted before some kinds of auxiliary word and auxiliary verbs, which are written directly after the preceding word.
b) One space is inserted after the auxiliary words (TE), (NI), (WO), (HA), etc.
c) Two spaces are necessary after a period, and one space is necessary after a comma.
d) Two spaces are necessary after both a quotation mark and an exclamation mark.

Because rules like 5-a) and 5-b) concern semantic information, it is difficult to translate according to these rules.

3. Outline of the System

Since each braille cell can be specified by a six-digit binary code, the six-hole paper tape which is commonly used in Japan was chosen to control the system. The block diagram of the complete system, which consists of three units—the teleprinter, the braille translating unit, and the braille printer— is shown in Fig. 1. The first step in making a translation is to type the written matter to be translated on the teleprinter, which simultaneously produces a printed copy and a perforated paper tape. The printed copy is

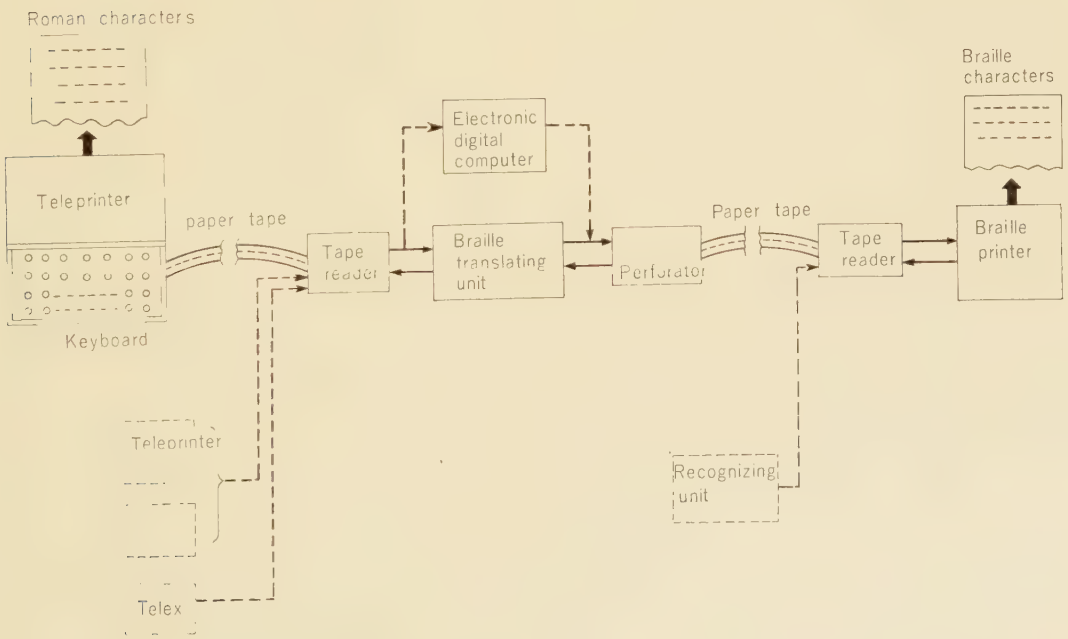

Fig. 1—Block diagram of the complete system, with arrows to show control paths.

Table 2.

TELEPRINTER-CODE PATTERNS.

	X_1	X_2	X_3	X_4	X_5	X_6	LTRS	FIGS
0	○	○	○	○	○	○		
1	○	○	○	○	○	●	K	
2	○	○	○	○	●	○	R	
3	○	○	○	○	●	●	S	
4	○	○	○	●	○	○	Y	
5	○	○	○	●	○	●	·	(Decimal point)
6	○	○	○	●	●	○		
7	○	○	○	●	●	●	W^4	
8	○	○	●	○	○	○	N	
9	○	○	●	○	○	●	H	
10	○	○	●	○	●	○	T	
11	○	○	●	○	●	●	M	
12	○	○	●	●	○	○	/	(Fraction bar)
13	○	○	●	●	○	●	D^4	
14	○	○	●	●	●	○	" ^{4}	
15	○	○	●	●	●	●	Figure	
16	○	●	○	○	○	○	.	'(Apostrophe)
17	○	●	○	○	○	●	$=^1$	
18	○	●	○	○	●	○	—	
19	○	●	○	○	●	●		
20	○	●	○	●	○	○		9
21	○	●	○	●	○	●	B^2	
22	○	●	○	●	●	○		0
23	○	●	○	●	●	●	O^1	
24	○	●	●	○	○	○		
25	○	●	●	○	○	●	$!^1$	?
26	○	●	●	○	●	○		
27	○	●	●	○	●	●	( )	
28	○	●	●	●	○	○	Space	
29	○	●	●	●	○	●	G^2	
30	○	●	●	●	●	○		
31	○	●	●	●	●	●	Z^2	
32	●	○	○	○	○	○	—	
33	●	○	○	○	○	●	—3	×
34	●	○	○	○	●	○	Hyphen	
35	●	○	○	○	●	●	A^1	
36	●	○	○	●	○	○		3
37	●	○	○	●	○	●		5^4
38	●	○	○	●	●	○		4
39	●	○	○	●	●	●	U	
40	●	○	●	○	○	○		
41	●	○	●	○	○	●	P^5	
42	●	○	●	○	●	○		
43	●	○	●	○	●	●		
44	●	○	●	●	○	○		
45	●	○	●	●	○	●		
46	●	○	●	●	●	○		
47	●	○	●	●	●	●		
48	●	●	○	○	○	○		2
49	●	●	○	○	○	●		
50	●	●	○	○	●	○		8
51	●	●	○	○	●	●		
52	●	●	○	●	○	○		6
53	●	●	○	●	○	●		
54	●	●	○	●	●	○		7
55	●	●	○	●	●	●	E	
56	●	●	●	○	○	○		
57	●	●	●	○	○	●		
58	●	●	●	○	●	○	Letters	
59	●	●	●	○	●	●	Carriage return	
60	●	●	●	●	○	○	Line feed	
61	●	●	●	●	○	●	Blank	
62	●	●	●	●	●	○	Back	
63	●	●	●	●	●	●	Delete	

Rules of Code Conversion

1 :	X_5X_6
2 :	$X_2X_3X_4$
3 :	$X_1X_3X_5X_7$
4 :	$X_4X_5X_6$
5 :	X_1

Numbers 1 through 5 refer to superscripts of characters in the main table.

used to check for errors, which are corrected. Then the six-digit codes on the tape are sent to the braille translating unit by the intra-office transmitter.

In the translating unit, the encoded Roman characters are translated into braille, and these braille codes are then perforated on a second paper tape by the intra-office reperforator. The translated codes on the second paper tape are read by the braille printer, and printed in the form of braille cells.

4. The Teleprinter

The keyboard of this teleprinter has keys for Roman letters and Arabic figures, and also keys for other characters such as the period, the comma, etc. It is possible to use a Japanese 'kana' keyboard, but for a 'kana' keyboard more keys are required and the teleprinter is not suitable for typing foreign languages; therefore a Roman-character keyboard has been used. Modification of the code bars of this teleprinter has allowed substantial simplification of the translating unit.

Codes of each key are shown in Table 2. Most of the codes are made in such a way that the code corresponds directly to the respective braille code. Several codes, however, are made by converting them according to the rules shown in the lower part of Table 2. That is to say, these codes are converted into braille merely by negating some digits. For example, braille vowel codes may be obtained from the codes for (A), (I), (U), (E), and (O) by negating digits x_5 and x_6; and (B), (G), Z are transformed into (H), (K), and (S) by negating digits x_2, x_3, and x_4; etc. Moreover, figures are assigned to the upper part of the upper row of keys and the code of the "figure shift" key is made to be the same as the "figure symbol code".

If all the codes of the keyboard were made to correspond one-to-one to braille, the printer would have to be extremely large in size. Therefore, this is not practical. Codes on the tape which are perforated by the perforator unit of the printer are different from the five-unit code used in Europe, they are in the six-unit code as described above.

5. General Features of Translating Unit

As stated in Section 2, the orthography of braille is quite different from the ordinary orthography. Especially, it is difficult to translate according to rules such as those described in 5-a) and 5-b) in Section 2, for in these cases the semantic information of the words should be considered when performing the translation. Therefore, if we try to translate according to such rules, a large scale translating unit which has memories with large capacities and which uses a stored program system would be necessary.

In view of these difficulties translations involving semantic information are not carried out in the translating unit, and the operator must observe the rules when typing the Roman characters. Therefore, this unit can be thought of as a special-purpose computer system. The Parametron, a new type of logical device developed in Japan, is used in this system and all logical operations are of the parallel type. The translating unit consists of code conversion part, a control part, and output equipment as shown in Fig. 2.

The main functions of each part are as follows: In the code conversion part, codes which have been fed into this part by paper tape are sent to Register R_0, and then these codes are decoded by recognition circuit R_E. The control part consists of the three six-digit registers R_1, R_2, and R_3; the main control circuit; and code generator R_G.

The main control circuit sends several kinds of instruction signals according to the flow diagram shown in Fig. 3. In this diagram, the figures in circles and the arrowheads on the flow lines represent numbers of states, and informaiton flows as shown. The letters above and below these arrows illustrate input signals to the main control circuit and instructions produced by that circuit respectively. For example, if the character (K) enters into this circuit, the content of R_1, whose symbol is $C(R_1)$, is transfered into R_2.

When the next character; for example (A),

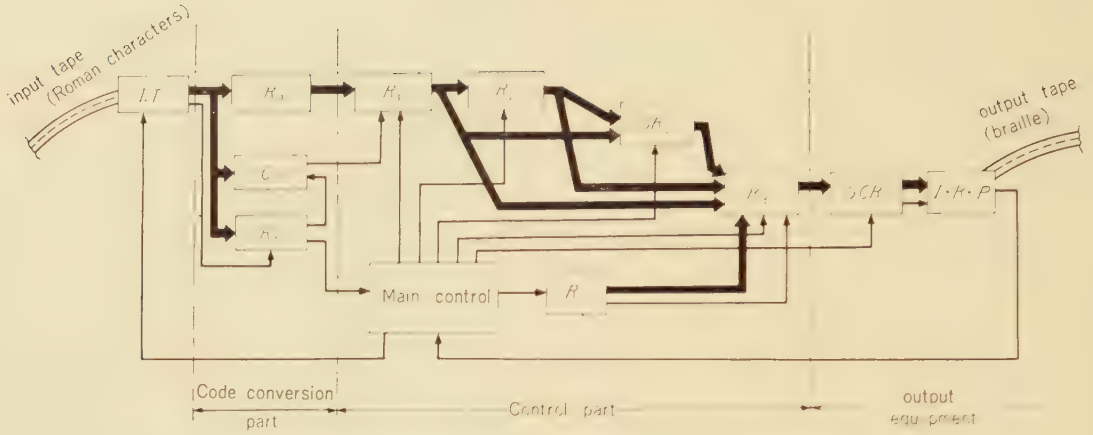

$R_{0\sim3}$: six-unit registers
C_0 : code converter
R_E : recognition circuit
OR_1 : OR circuit
R_G : code generator
→ : information flow
→ : control signal flow

Fig. 2—Block diagram of the translating unit.

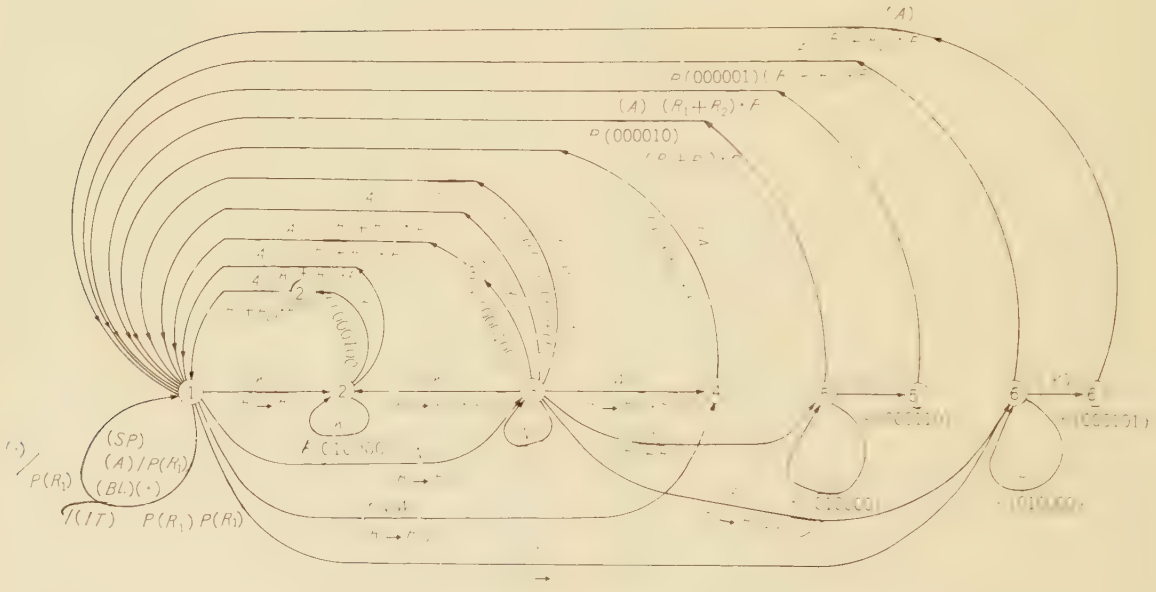

(*A*) : A, I, U, E, O,
(*K*) : K, S, T, H, M, R,
(*G*) : G, Z, D, B,
(*P*) : P,
(*Y*) : Y,
(*W*) : W,
(*N*) : N,

(*SP*) : SPACE
(*BL*) : BLANK, BACK, DELETE,
(.) : Period,
(,) : Comma,

$R_1 \rightarrow R_2$: transfer $C(R_1)+_0C(R_2)$.
R_1+R_2 : add $C(R_1)$ and $C(R_2)$.
$(R_1+R_2).P$: after (R_1+R_2), print the results
$P(X)$: Print the braille code or $C(X)$ illustrated by X.
$(I.T)$: read the next character without printing.

Fig. 3—Flow diagram of the control part.

Table 1.

JAPANESE BRAILLE, AND THE CORRESPONDING JAPANESE 'KANA' AND ROMAN ALPHABET TRANSLITERATION

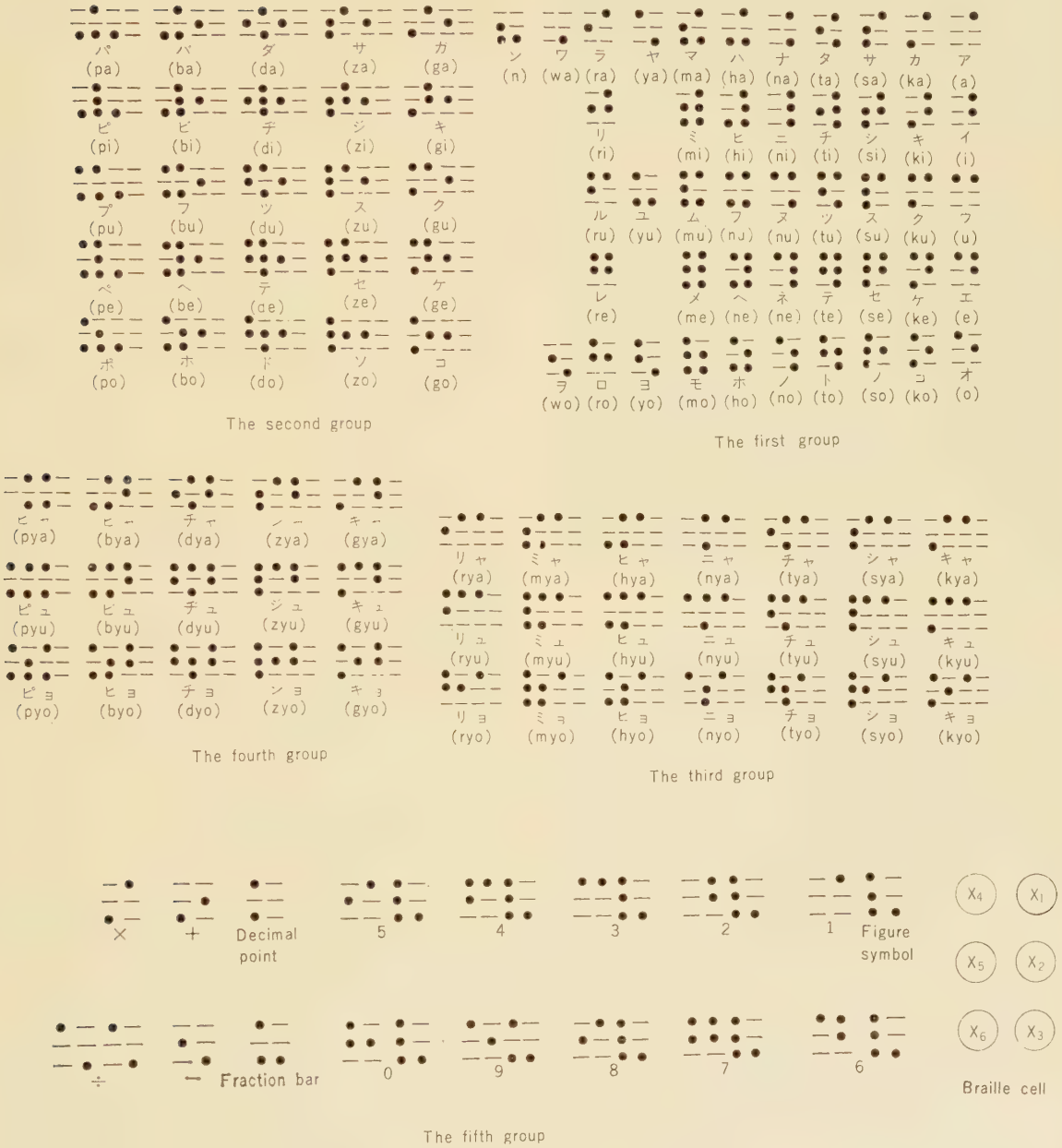

is fed into this circuit the following operation is performed in *OR* circuit OR_1;

$$C(R_1) \wedge C(R_2). \qquad (2)$$

The result of this operation—100001 in this case—is registered in output register R_3 and then, $C(R_3)$ is transferred by the printing signal from the main control circuit,

For the input character series (K) (Y) (A), first a "Contracted-sound code" 000100 is generated in R_G and sent to the output equipment, and then operations similar to those described above are performed. To avoid complication, the translating part for figures is omitted from Fig. 3.

The output equipment consists of eight cold-Cathode grid-control relay tubes (*GCR* tubes) and an intra-office reperforator (*IRP*). The translated codes are perforated on the output paper tape by the *IRP*, in which selection magnets are energized by current through the *GCR* tubes. At the same time, a start signal is sent for the next character to be fed into this unit. The "Carriage return and line feed code" for the braille printer is automatically inserted on the output tape by counting the number of translated braille cells.

As a result of a statistical investigation of the text of several books, the following was made clear: The ratio of the number of Roman characters to braille cells is about 1.6 : 1, and the probability that braille words composed of more than eight cells will occur is less than two percent. Therefore, the "Carriage return and line feed code" for the braille printer is produced by the main control circuit in the following two cases:

i) Whenever a space code appears after the code corresponding to the 22nd braille cell has been counted on any line of braille.
ii) Whenever a long word would be divided between any two lines of braille.

All the operations of the translating unit were simulated on the M-1 electronic computor,[3] and the results showed that a memory of about 200 words, with 40 bits per word, is necessary. To translate Japanese 'kana' into braille almost the same number of words would be necessary. This is because the Japanese braille and the Japanese 'kana' do not correspond exactly, which can be seen by examining the third and fourth groups. For example, the sounds (KYA), (KYU), and (KYO) are written using the 'kana' groups (KI) (YA), (KI) (YU), and (KI) (YO) in the standard orthography, but they are written using the cells ⠈⠡, ⠈⠥, and ⠈⠩ in braille. The braille cell ⠈ is the symbol for a contracted sound, and has no equivalent in the standard orthography. Therefore, when the sounds (KYA), (KYU), and (KYO) are written in braille, both the component characters and their order differ from those used in the standard orthography.

The translation unit contains 800 binocular-type Parametrons[2] which have the small power consumption of about 30 mw, and are operated at the keying frequency of 10 kc/s.

6. The Braille Printer[4]

The braille printer consists of a tape reader and a special page printer. The codes on the tape which was perforated at the output equipment of the translating unit are read by the tape reader. Then in the page printer, these codes are transformed into ordinary braille codes, that is, a pair of three unit codes, and printed in the page form shown in Table 1.

The following are several of the characteristics of the braille printer.

(1) Codes

The "000111" code, which is the only unused code, corresponds to "Carriage return and line feed."

(2) Printing

The dimensions of the braille cell, which are shown in Fig. 4, and the spacing between the cells are almost identical to those currently in use in Japan. (The dimensions of the braille cell were made slightly smaller than the present standard after extensive tests showed that this change would have no abverse effects on the legibillity of the braille.)

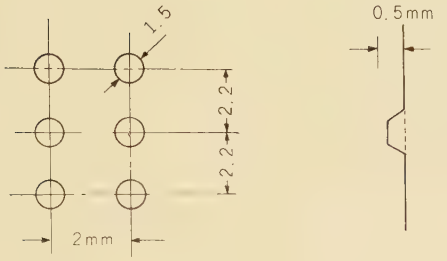

Fig. 4—Dimensions of printed braille cell.

(3) Page Layout

Each line consists of 30 braille cells; there are 17 lines on the front of each page, and 18 lines on the reverse side. The dimensions of the printed page are shown in Fig. 5.

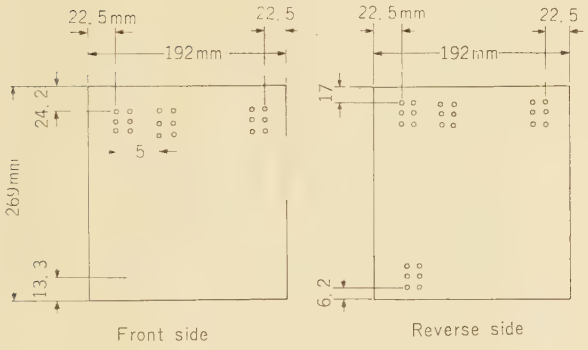

Fig. 5—Layout of page printed in braille.

(4) Printing Speed

The printing speed is about 187 cells per minute; therefore it takes about 3 minutes to print a page. This speed is provisional, and if necessary it is possible to increase the speed.

(5) Power Supply

Power is obtained from the 100-volt ac commercial mains. The braille printer is able to print up to three pages simultaneously, The braille cells on the reverse side of a page are printed between the lines already printed on the

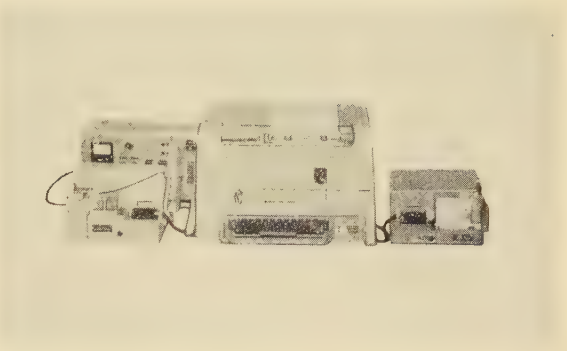

Teleprinter

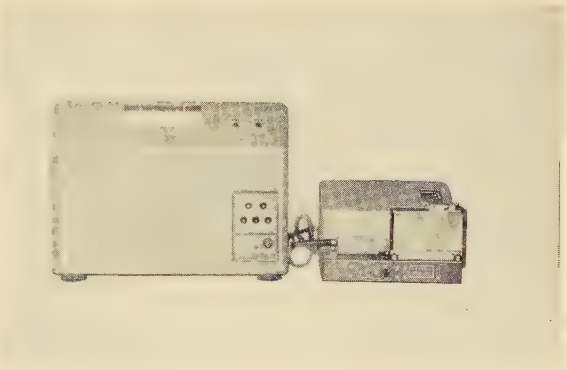

Braille Printer

Translating Unit

Fig. 6—Photograph of the completed system.

front of the page. The cost of the paper tape is about $1.75 per kilometer, which is about one-twentieth the cost of the corresponding quantity of zinc sheets. Moreover, both storage and correction are easier when paper tapes rather than zinc sheets are used.

7. Conclusion

This system was completed by our Laboratories in October 1959 and has been successfully used at the Tokyo University of Education since that time. Several books were transcribed by this system, and as the result of this experience, we have the following plans for improving and automating this equipment, and for developing a braille service system.

1) Further Development of this System

It would be very easy to punch page numbers on the tape automatically. And the following improvements are possible, but expensive: automatic correction of errors due to system error, on the perforated paper tape; and automatic removal of a printed braille page and insertion of the subsequent page. Moreover, if it is necessary to translate Japanese braille into either a Japanese or into a foreign language the whole system should be redesigned with a stored program which would make the system more flexible. It is easily possible to increase the printing speed by about 2 or 3 times, but it would be very expensive to increase the speed by 100 or even by 10 times.

2) Pattern Recognition

If a paper tape which has the same codes as the braille tape produced by this system is made available in some manner. then only the braille printer is necessary to transcribe braille. A simple manual punch was also made, but its use requires a knowledge of braille. Also, it would be possible to make a six-unit perforated tape with braille codes by means of a pattern recognition device if braille is written on paper with a pencil or with magnetic ink. Such a device should be more simple than those which make it possible to read printed or type-written letters.

3) Studies on a Braille Service System

In order to utilize this system efficiently it is necessary to study the utilization of the system, just as in the case of an electronic telephone exchange or an electronic digital computer. We have devised the following plan to assure efficient operation of the system.

The Braille Center Stations where the requirement from the local terminals are received and the translating unit is controlled will, like a computation center, be constructed in a large city. Also, the requirements for the translation of Roman characters into Japanese braille, which are sent from the Telex terminals, will be received. The translated tapes, together with the manually punched tapes which have been received from the "Braille Volunteers", will be printed and edited at the Braille Center Station. The studies described above are one of the important problems in electronic control techniques, and relate to the high speed transmission and processing of the information.

Acknowledgements

We are indebted to Mr. H. Imai and Mr. I. Ozeki, Lecturers at Tokyo University of Education, for valuable suggestions concerning the translating method, and to Mr. S. Amada of this Laboratory for a discussion of the design of the braille printer.

References

(1) K. Homma: A Guide to Braille (in Japanese) *Japanese Braille Library*, 1957.
(2) K. Fukui et al: Binocular Type Parametron, *The Electrical Communication Laboratory Technical Journal*, **8**, 1, 1959.
(3) S. Muroga and K. Takashima: System and Logical Design of the Parametron Digital

Computer MUSASINO-1, *The Journal of I. E.C.E.J.* **41,** 11, 1958.

(4) T. Seki and K. Tobita: Braille Teletypewriter, *OKI REVIEW*, **26,** 3, 1959.

* * * *

Review of the Electrical Communication Laboratory
Volume 9, Numbers 9-10, September-October, 1961

U.D.C. 621.372:517

Stability of Active Circuits*

Shunitsu HAMAO†

This paper describes one or two cases in which the H. Nyquist's Regeneration Theory is not applicable concerning the stability of feedback circuits. It shows that the feedback circuit may become unstable even if the so-called $(\mu\beta)$ locus does not contain $(1+i_0)$. The result of this is used for examining the stability of active driving-point immittance. For example, this paper shows that the driving-point immittance whose numerator and denominator are both Hurwitz's polynomials may become unstable. It throws doubt on the mechanical application of the function theory, which has been recognized as appropriate to the passive circuit, to the solution of the characteristics of the active circuit.

1. Introduction

In introducting negative immittance into the lumped constant circuit theory which is somewhat generalized, a few supplements have been given to the H. Nyquist's Regeneration Theory concerning the examination of the stability required for the introduction. The result of this has been applied to the examination of some active immittances to clarify its characteristics.

2. Relations with Nyquist's Theory

To simplify our discussion, we assume the following:

Assumption **A**

The transfer functions, $W(p)$, and $F(p)$ are those of a lumped constant circuit containing the ideal transformer. They are regular on the imaginary axis of the complex frequency $p(\delta=+i\omega,\ \omega=$real frequency) and on the right half plane.

First, Table 1 shows the relations between this paper and H. Nyquist's Regeneration Theory.

The table mentioned above contains cases in which the H. Nyquist's Regeneration Theory is not applicable. Of these, the case in which max $w(p)=1$ on the imaginary axis of the p plane may have to be treated with other considerations. This case, therefore, is not dealt with in this paper.

The transfer function, $w(p)$, of the loop that can be treated by the application of Nyquist's theory, and must satisfy the following equation.

$$\lim_{\omega\to\infty} \omega\cdot w(i\omega) < \infty^* \qquad (1)$$

Owing to the assumption **A**, $w(p)$ is a rational function, and when it satisfies the equation (1), $w(p)=O(p^{-1})$, $(p\to\infty)$. For the complete examination of the driving point immittance of the active circuit, we must examine cases in which the equation (1) is not satisfied. This paper treats such cases.

3. Supplement I to Nyquist's Theory

In this paragraph, the conditions imposed

* MS in Japanese received by the Electrical Communication Laboratory, on 15 May, 1961. Originally published in the *Kenkyu Zituyôka Hôkoku* (*Electrical Communication Laboratory Technical Journal*), N.T.T., Vol. 10, No. 9, pp. 1991-1995, 1961.

† Communication Network Section.

* References (1) p. 131

on $w(p)$ are shown below.

Condition 1. $w(\infty) \neq 0$,
Condition 2. Max $w(p) = M < 1$,

Only on the imaginary axis of the p plane.

Since $w(p)$, in this case, is regular on the imaginary axis of the p plane and the right half plane, the "maximum principle" is applicable to it on the imaginary axis and right half plane except on the point at infinity. The point at infinity, excluded in this application, has the following relation because of Condition 2: $w(\infty) \leqq M$. Consequently, $|w(p)| \leqq M$ on the imaginary axis of the p plane and the right half plane. From this we can deduce that $1/\{1-w(p)\}$ is regular on the imaginary axis of the p plane and the right half plane.

Now, when the feedback circuit is operated with an input power, the output power after going around the loop acts as the input power again, to repeat this process. The total input power is the sum of this process according to the principle of superposition because of the linear circuit.

Let us, therefore, consider the time response when the feedback circuit having the transfer function $w(p)$ of the loop in this paragraph is operated with the function $F(p)$ satisfying the equation (1). $U_n(t)$ denotes the output power that has gone around the loop n times, then the sum up to N times may be shown in the following equation:

$$\left.\begin{aligned} \sum_{n=0}^{N} U_n(t) &= \sum_{n=0}^{N} \frac{1}{2\pi i}\int_C w^n(p)\,F(p)\,\varepsilon^{pt}dp \\ &= \frac{1}{2\pi i}\int_C \frac{F(p)}{1-w(p)}\varepsilon^{pt}dp \\ &\quad - \frac{1}{2\pi i}\int_C \frac{w^{N+1}(p)}{1-w(p)}F(p)\varepsilon^{pt}dp \end{aligned}\right\} \quad (2)$$

C denotes the Bromwitch path also in the subsequent equations and formulas.

From Assumption **A** and the examination above, it is clear that the integral of right hand side of equation (2) exists for any given N. Put the sequence of functions $w^{N+1}(p)$ in the second term of the right hand side as follows:

$$\left.\begin{aligned} w^{N+1}(p) &= W_{N+1}(p) + w^{N+1}(\infty), \\ \text{only } W_{N+1}(p) &= w^{N+1}(p) - w^{N+1}(\infty) \end{aligned}\right\} \quad (3)$$

$w^{N+1}(\infty)$, the second term of the right hand side of equation (3), converges with 0, and the first term of the right hand side of the equation is $|W_{N+1}(p)| \leqq 2 \cdot M^{N+1}$ on path c, and uniformly convergent with 0. But,

$$W_{N+1}(p) = \{w(p) - w(\infty)\} \sum_{r=0}^{N} w^r(p) \cdot w^{N-r}(\infty),$$

and on path c,

$$|W_{N+1}(p)| \leqq |w(p) - w(\infty)| \cdot (N+1)M^N, \quad (4)$$

So there is a constant A irrespective of N, and about $|p|$ large enough we have

$$|W_{N+1}(p)| \leqq |A/p|, \quad (N = 1, 2, 3, \cdots\cdots)$$

Now we can seek the sum of the input power as the limit of equation (2), which can be shown according to equation (3) as the following equation:

$$\left.\begin{aligned} \lim_{N\to\infty} \sum_{n=0}^{N} U_n(t) &= \frac{1}{2\pi i}\int_C \frac{F(p)}{1-w(p)}\varepsilon^{pt}dp \\ &\quad - \lim_{N\to\infty} \frac{1}{2\pi i}\int_C \frac{W_{N+1}(p)F(p)}{1-w(p)}\varepsilon^{pt}dp \\ &\quad - \lim_{N\to\infty} \frac{w^{N+1}(\infty)}{2\pi i}\int_C \frac{F(p)}{1-w(p)}\varepsilon^{pt}dp, \end{aligned}\right\} \quad (5)$$

Needless to say, the third term in the right hand side of the equation above is 0. The integral of the second term in the right hand side of the equation above is uniformly convergent with relation to t, N because of the assumptions and conditions imposed upon $w(p)$, $F(p)$, and the characteristics of $W_{N+1}(p)$ described with regard to equation (3). More-

Table 1

RELATIONS BETWEEN NYQUIST'S REGENERATION THEORY AND THIS REPORT

Nyquist's theory is applicable			Nyquist's theory is not applicable	
$w(\infty)=0$			$w(\infty)\neq 0$	
If $1/\{1-w(p)\}$ is regular	If $1/\{1-w(p)\}$ is irregular	If max $w(p)<1$ on the imaginary axis of the p plane,	If $w(\infty)>1$	If max $w(p)>1$, on the imaginary axis of the p plane and $w(\infty)<1$
On the right half and the imaginary axis of the p plane,				
the feed back circuit is stable	the feed back circuit is unstable	the feed back circuit is stable*)	the feed back circuit is unstable**)	the stability of feedback circuit is unknown.

where $w(p)$=loop transfer function $(\mu\beta)$, $w(\infty)=\lim_{p\to\infty} w(p)$

* See Section 3. ** See Section 4.

over, $W_{N+1}(p)$ uniformly converges to 0 in regard to p, so we can exchange the order of the limit and the integral to show that the second term is also 0.

Thus, equation (5) has only the first term remaining on the right hand side, and this determines stable response.

4. Supplement II to Nyquist's Theory

In this paragraph, the conditions imposed on $w(p)$ are shown below:

Condition 1, $|w(\infty)|>1$,

Under this condition, the feedback circuit will be unstable.

In general, the time response $U_1(t)$ when the function $w(p)$ satisfying the assumption **A** alone is operated by the function $F(p)$ satisfying equation (1) as well is shown as the following equation:

$$U_1(t)=\frac{1}{2\pi i}\int_C w(p)\cdot F(p)\varepsilon^{pt}dp$$

But when $w(p)$ also satisfies equation (1), which is the condition for the applicability of Nyquist's theory,

since as it has been shown earlier

$$w(p)=O(p^{-1}),\quad (p\to\infty)$$

$$w(p)\cdot F(p)=O(p^{-2}),\quad (p\to\infty).$$

Consequently the integral of the above equation uniformly converges in every closed t interval, and the integrand is continuous. $U_1(t)$ is therefore a continuous function of t.

Since it is clear that $U_1(t)=0$, $(t<0)$ whether $w(p)$ satisfies the conditions of equation (1), when $w(p)$ satisfies equation (1) as in the case above,

$$U_1(0)=0$$

On the other hand, when $w(p)$ does not satisfy equation (1) and $w(\infty)\neq 0$,

$$U_1(0)=\frac{1}{2\pi i}\int_C w(p)\cdot F(p)\,dp$$

The integral of this is shown from equation (3) as

$$U_1(0)=\frac{1}{2\pi i}\int_C W_1(p)\cdot F(p)dp + \frac{w(\infty)}{2\pi i}\int_C F(p)dp \qquad (6a)$$

Since $W_1(p)$ satisfies equation (1),

$$W_1(p)\cdot F(p)=O(p^{-2}),\quad (p\to\infty)$$

$W_1(p)$, $F(p)$ are regular on the imaginary axis of the p plane and the right half plane because of assumption **A**. The value of the first term of the right hand side of equation (6a) is 0. The second term of it, according to Cauchy's principal value, is shown as

$$U_1(0)=w(\infty)\frac{\sum R_F}{2}, \qquad (6b)$$

where $\sum R_F$ = the sum of every residues of the pole of $F_1(p)$

When $\sum R_F \neq 0$, that is, $F(p)$ satisfies equation (1) and p's point at infinity is zero of order 1, namely the waveform of the input power is discontinuous, the waveform $U_1(t)$ of the output power is also discontinuous and $U_1(0)$ takes the value described above.

Thus, the time response differs between the one satisfying equation (1), the condition for the applicability of Nyquist's theory, and the one not satisfying equation (1). Utilizing this characteristic, we shall examine the following.

Now let us consider the time response when the feedback circuit having the transfer function $w(p)$ of the loop satisfying condition 1, in this paragraph is operated by the function $F(p)$ where p's point at infinity is zero of order 1 among the functions satisfying equation (1).

From equation (3) the total output power, up to N times, is shown by following expression:

$$\sum_{n=0}^{N} U_n(t)=\sum_{n=0}^{N}\left\{\frac{1}{2\pi i}\int_C w^n(p)\cdot F(p)\varepsilon^{pt}dp\right\} = \sum_{n=0}^{N}\left\{\frac{1}{2\pi i}\int_C W_n(p)F(p)\varepsilon^{pt}dp + \frac{w^n(\infty)}{2\pi i}\int_C F(p)\varepsilon^{pt}dp\right\} \qquad (7)$$

where $U_n(t)$ dentes the output power that has gone n times around the loop, can be shown by examinating expressions (when $t=0$). The value of the above expressions (3), (6a), and (6b) as follows:

$$\sum_{n=0}^{N} U_n(0)=\frac{\sum R_F}{2}\sum_{n=0}^{N} w^n(\infty)$$

Since $\sum R_F \neq 0$, if $|w(\infty)|>1$,

$$\lim_{N\to\infty}\sum_{n=0}^{N} U_n(0)$$

diverges and the circuit is unstable.

The feature of this instability is that, if the condition $|w(\infty)|>1$ is satisfied, the instability does not depend on whether $1/\{1-w(p)\}$ is regular or not on the imaginary axis of the p plane and the right half plane. Even if it is regular and negative feedback on all real frequency, the instability is not changed.

Some base the stability on the regularity mentioned above*, but it is impossible to apply Nyquist's theory to this condition.

5. Application to Active Immittance

Let us realize negative impedance by a simple impedance converter as shown in Fig. (1), and apply the result of our examinations described earlier.

In the firgure, the transfer function $w(p)$ of the loop will be represented by following equation.

$$w=2R/(R+\rho)$$

If $\rho>R$, $|w|<1$, so the circuit is stable as has been shown in our examination in the third section (3. Supplement I to Nyquist's Theory), and if $\rho<R$, $|w|>1$, the circuit is unstable by reason of our examination described in

* References (2) p. 155.

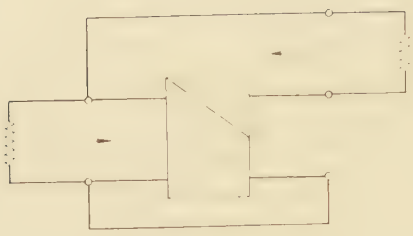

Input impedance of the amplifier	∞
Output 〃	0
Voltage gain of the amplifier	+2

Fig. 1—Impedance converter.

section 4. When $\rho > R$, and the circuit is stable, and w is not subjected to very by measurement, the impedance considered serially with R is the negative resistnce $R-\rho$ of the inverse current type, and the impedance considered parallelly with ρ is the negative resistance $R\rho/(R-\rho)$ of the inverse voltage type. If we open the terminal of the former measured, or if we short the terminal of the latter measured, $w=2$ in both cases, and the circuit becomes unstable because of what we have examined in Section 4.

In connection with this, I would like to point out that, although the negative resistance of the inverse current type and that of the inverse voltage type are sometimes respectively called the negative resistance of the short-circuit stable type and that of open-circuit stable type, this correspondence cannot be considered to be a general rule. Concerning our examination described in Section 4, examples can be given for cases in which the instability occurs for both short and open circuits in either type of the inverse current type and inverse voltage type. If we have to use the term related to the stability, (since it is impossible to operate the negative resistance of the inverse current or voltage type by means of a constant current or voltage source) it would be more appropriate to call the inverse current type the open-circuit unstable type, and the inverse voltage type the short-circuit unstable type.

Now, in Fig. (1), if we replace R with the passive driving point impedance $Z(p)$ of which both numerator and denominator are Hurwitz's polynomials, the transfer function w of the loop is represented as

$$w(p)=2Z(p)/\{\rho+Z(p)\}$$

and $Z(p)$ is small enough to satisfy $\max w(p)<1$, on the imaginary axis of the p plance, the circuit is stable for the reason we have shown in Section 3. In this case, if we denote the impedance considered serially with $Z(p)$ with $\zeta(p)$,

$$\zeta(p)=Z(p)-\rho,$$

and the real parts of $\zeta(p)$ and $1/\zeta(p)$ are negative on the imaginary axis of the p plane, and the $\zeta(p)$ and $1/\zeta(p)$ are driving point impedance functions which are regular on the imaginary axis and right half plane.

However, if we open the terminal measured, $w=2$ and the circuit is unstable because of what we have clarified in our examination in Section 4.

Similarly, we can point out that like function which have the negative resistance of the inverse voltage type as their real parts are short-circuit and unstable, and that dual relations are to be found concerning the admittance.

The foregoing described those having negative real parts. Next, we shall examine cases in reverse. For example, in Fig. (1) let us consider the case in which the sign of the gain of the amplifier is negative. If we replace ρ with $Z(p)$ and R with a constant voltage source, the impedance further to the right is $Z(p)/3$. This has a positive real part, and as a type of function, is nothing but the passive driving point impedance. Nevertheless, if we open the source, $w=-2$, and the circuit is unstable because of what we have examined in Section 4. Similarly, there are those that are short-circuit unstable.

The foregoing exposition makes it hard for us to agree with the view that holds that negative or positive driving point immittance functions to be both short-circuit stable and open-circuit stable.*

* References (2) p. 188.

Conclusion

As has been clarified in the foregoing, it is not always proper to apply, without reservation, the method of the function theory established with passive network, to the examination of active immittance.

In this paper no reference has been made to negative inductance $(-L)$ and negative capacitance $(-C)$, because I know nothing about their existence.

Acknowledgment

In this study I am indebted to Mr. Yoshiyuki Araki, chief of the Training Section at the Head Office of Nippon Telegraph and Telephone Public Corporation, who was formerly chief of the section I belong to, Prof. Akio Matsumoto and Prof. Ryoichi Miura of Hokkaido University, Mr. Takashi Omori of the Electrical Communication Laboratory, and others. I wish to express my deep gratitude to these people.

References

(1) H. Nyquist: Regeneration Theory, *B.S.T.J.*, Jan., 1932.
(2) H. W. Bode: Network Analysis and Feedback Amplifier Design.

* * * *

REVIEW OF THE ELECTRICAL COMMUNICATION LABORATORY
VOLUME 9, NUMBERS 9-10, SEPTEMBER-OCTOBER, 1961

U.D.C. 621.396.647.2.029.63:621.317.351]
:621.317.79 182.3

Microwave Amplitude Characteristics Measuring Equipment*

Masamitu OTA† and *Ituo SUGIURA*‡

The development of the multi-channel microwave transmission system created a necessity for accurate measurement of the amplitude characteristics of repeaters.

This work describes the development of amplitude characteristics measuring equipment having an accuracy of 0.1 dB over a ±15 Mc band.

To obtain high accuracy, the authors utilized an automatic power control system using a barretter detector as a reference for the sweeper, designed the circuit arrangement, and investigated the details of the circuits theoretically and experimentally.

Maximum loop gain of 70 dB was obtained for the AC components of the sweeper output.

Amplitude characteristics measuring equipments for the 4000 Mc and 6000 Mc bands were designed, and it was proved that the equipments satisfied the initial objectives.

Introduction

The performance of microwave repeaters has been improved remarkably since the microwave transmission system was first installed in Japan. The number of telephone channels in a repeater system has been increased successively, and actual equipment can transmit from 600 to 1200 channels. Furthermore, a microwave amplifier repeater system for more than 1800 channels will be developed soon.

The larger number of channels requires the stricter transmission line and repeater standards, and it means that higher accuracy is required for measuring equipment. For the amplitude characteristics measuring equipment, the actual newest transmission line requires accuracy of 0.1 dB over a ±15 Mc band, while the microwave amplifier system needs more accurate equipment.

In measurements of the amplitude characteristics of repeaters, the largest interruption for improvement of the accuracy is that the repeater output frequency differs from the repeater input frequency. The frequency difference is 40 Mc for the 4000 Mc system and 252 Mc for the 6000 Mc system. And the characteristics between receiver input terminal and intermediate frequency amplifier output terminal are measured usually in heterodyne type repeaters. Moreover, such nonlinear circuits or elements as limiters and traveling-wave-tubes are included in repeaters. Then, we can not obtain the bare characteristics of the system under test from the difference between the measured values of when the measuring system contains the system under test and the values of when it does not. Therefore, the output power of measuring equipment and the sensitivity of detector must be constant over the desired band

* MS in Japanese received by the Electrical Communication Laboratory, May 11, 1961. Originally published in the *Kenkyû Zituyôka Hôkoku* (*Electrical Communication Laboratory Technical Journal*). N.T.T., Vol. 10, No. 9, pp. 1757–1825, 1961.

† Assistant Section Chief, Communication Network Section.

‡ Radio Section.

width.

In the old type equipment, the greater parts of errors in the measurement of amplitude characteristics were the output deviation of the sweeper and the sensitivity deviation of the detector, therefore the authors concentrated on these two items in order to develope the new and more accurate equipment.

In the new equipment, a barretter is used as a detector instead of a crystal detector as in the old one, and the barretter is also used as a reference detector for the automatic power control (APC) circuit which was newly developed. Thus the foregoing problem was solved, and we succeeded in significantly improving the accuracy of measurement. In the following, the detector and the APC circuit using barretters are described, and outlines are given about amplitude characteristics measuring equipment which uses these circuits.

1. Detector

The sensitivity of the detector used in an amplitude characteristics measuring equipment must be constant over the band width to be measured (from ± 15 Mc to ± 25 Mc). Next, it is necessary that the relation between the level variation of input signal and the variation of output voltage is constant, because, if the relation changes, it becomes a factor of errors when the detector output is read on the scale of the cathode ray tube. Of course, the sensitivity itself is required to be more than a given value, because the gain of the amplifier following the detector is limited.

Besides, it is also necessary that the input impedance of detector be matched as well as possible.

Up to this time, the crystal detector was principally used for the purpose described above. The merit of a crystal detector is its high sensitivity. The structure of a crystal detector is also very simple. It needs only a crystal diode and a mount; no other circuits are required. It is, however, very difficult to obtain excellent frequency characteristics. In spite of the repeated efforts which have been made up to the present to improve its performance, it has a sensitivity deviation of about 0.05–0.1 dB over a 30 Mc band. Therefore, it is not suitable for high accuracy measurements of amplitude characteristics. Large input standing wave ratio and poor interchangeability of crystal diode are also defects of the crystal detector.

However, barretters which have been used for microwave power measurement have some defects such as low sensitivity and long time constant.

But, their frequency characteristics are very excellent. Therefore, the authors used a barretter as a detector in the amplitude characteristics measuring equipment.

1.1. Barretter Element

The type of barretter which is used as detector is the SR-6, which is very similar to the Sperry Type 821. Characteristics are shown in Table 1.

Table 1

THE SPECIFICATION TYPE SR-6 BARRETTER

Type	SR-6
Shape	Bar type
Frequency Range	500 ~ 12,000 Mc/s
Operating Resistance and Balancing Current	200 Ω at 25° C with 8.75 ± 0.25 mA
Cold Resistance	117 ± 10 Ω
Sensitivity	4.8 Ω/mW at 200 Ω
Max. Safe Operating Power	32.5 mW at 25° C
Burn-Out Power	80 mW at 25° C
Size	4.9 ϕ × 20.6 mm
Weight	1.5 g

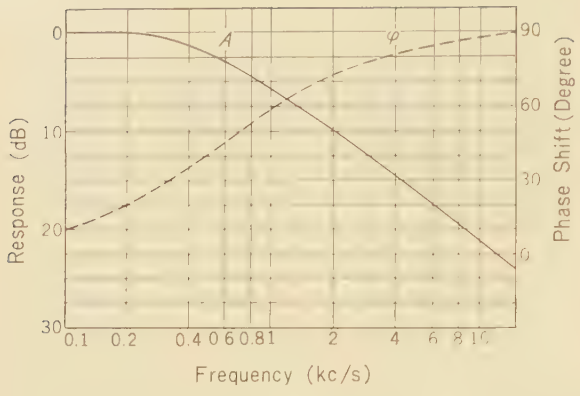

Fig. 1—Thermal Response Characteristics of Type SR-6 Barretter.

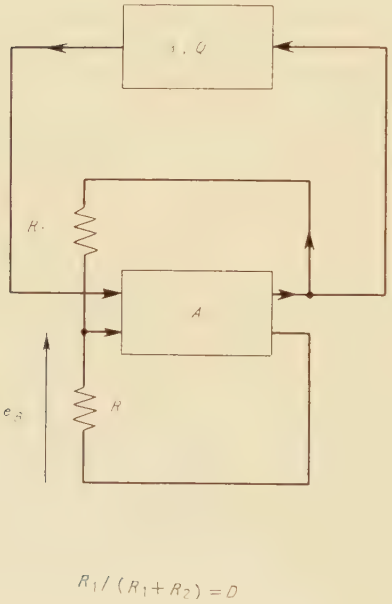

Fig. 2—Oscillator circuit containing a barretter.

1.2. Frequency Response Characteristics[1]

The detector circuit is essentially the same as the usual power meter of the self-balancing, low frequency substitution type.[2] A block diagram of the circuit is shown in Fig. 2. If we assume circuit is linear, the response of this circuit for the envelope frequency of the microwave input signal is represented by the following equation:

$$\frac{\Delta P_2}{P_1}=\frac{1}{1+j\left(\frac{Q_0}{1-1/D}\cdot\frac{p}{\lambda\omega}+\frac{Q_0}{(1-1/D)}\cdot\frac{p^2}{\lambda\omega p_c}\right)} \tag{1}$$

where P_1 = external power added to the barretter,
ΔP_2 = variation of low frequency power,
p = envelope angular frequency,
p_c = thermal cutoff angular frequency of barretter,
Q_0 = Q value (quality factor) of positive feedback circuit,
D = dividing ratio of negative feedback circuit,
ω = oscillation angular frequency,
λ = power sensitivity of barretter, which is given by the following equation:

$$\lambda=\frac{\Delta R_B/R_B}{\Delta P_0/P_0}, \tag{2}$$

where R_B = operating resistance of barretter,
ΔR_B = variation of R_B when P_0 is changed by ΔP_0,
P_0 = balancing power of barretter for normal R_B,
ΔP_0 = power variation.

We know that Eq. 1 shows the characteristics of a second order vibration system. The natural angular frequency ω_n and the damping factor ζ of the system are represented as follows:

$$\omega_n=\sqrt{\frac{1-1/D}{Q_0}\lambda\omega p_c}, \tag{3}$$

$$\zeta=\frac{1}{2}\sqrt{\frac{Q_0}{1-1/D}\cdot\frac{p_c}{\lambda\omega}}. \tag{4}$$

As the relation between ω_n and ζ is given by

$$\zeta\omega_n=1/2\cdot p_c, \tag{5}$$

It is not possible to vary ζ and ω_n independently.

In the usual power meter, the circuit constants are selected such as $Q_0=1/3$, $D=3$, $\omega/2\pi\approx$ 10 kc, and $\lambda=0.34$, $p_c/2\pi\approx 300$ c/s for the type SR-6 barretter, therefore $\omega_n/2\pi\approx 1.5$ kc/s is obtained.

In this case the flat region is less than 500 c/s, which is not wide enough for the present requirement.

From Eq. 3 it is clear that if higher ω_n is desired it is necessary to use higher ω or lower Q_0. As the oscillation is usually unstable when Q_0 is very low, high $\omega/2\pi$ of 200 $\sim$500 kc/s is used and Q_0 remains at the same value as in the usual power meter.

1.3. Sensitivity Characteristics

Next, we consider the detection sensitivity characteristics.

The low frequency voltage e_B that is added to the barretter is given by the next equation:

$$e_B=\sqrt{R_B(P-P)}=e_{B0}\sqrt{1-P_\mu/P_0'}, \qquad (6)$$

where $P_0'=P_0-P_D$, P_D=superposed DC power,

$$e_{B0}=\sqrt{R_B P_0'}\,.$$

The variation of voltage, e_B', is shown by

$$e_B'=e_{B0}-e_B=\sqrt{R_B P_0'}=R_B(P_0'-P_\mu),$$

and if we substitute as follows:

$$P_0'=K P_{\mu 0}$$

$$P_\mu=\alpha P_{\mu 0}$$

where $P_{\mu 0}$ is the maximum value of P_μ, e_B' may be expressed as

$$e_B'=\sqrt{R_B P_{\mu 0}}(\sqrt{K}-\sqrt{K-\alpha}\,). \qquad (7)$$

For $K=\infty$, linearity is maintained between α and e_B'; therefore, the variation of substituted low-frequency voltage corresponds directly to the microwave input power. Namely, we obtain square law detection. As the value of K becomes smaller, the characteristics depart further from exact square law detection. The relation between α and normalized e_B' for several values of K is shown in Fig. 3.

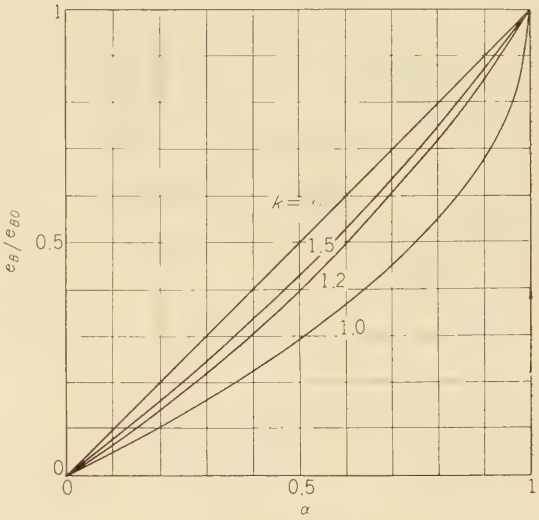

Fig. 3—Relation between microwave power and substitution voltage.

From the relation mentioned above, it is possible to show the following:

1) When multiple ranges are used and if the DC superposed powers are selected such that K is constant over all ranges, the detection characteristics remain identical. In other words, one scale can be used for all ranges.
2) When the substitution power is very large compared with the maximum value of microwave power, the characteristics more closely approximate square law detection.
3) Otherwise, with the increase of substitution power over the maximum value of microwave power the sensitivity decreases.

1.4. Harmonic Distortion of Barretter Detector

When we determine the DC superposed power, we must also consider the distortion factor of the detected signal. The relation

between P_D, P_μ and distortion versus modulation factor of the microwave signal are shown in Fig. 4. In this figure, it is assumed that the modulation signal is a single sine wave, and distortion is calculated only for the second harmonic.

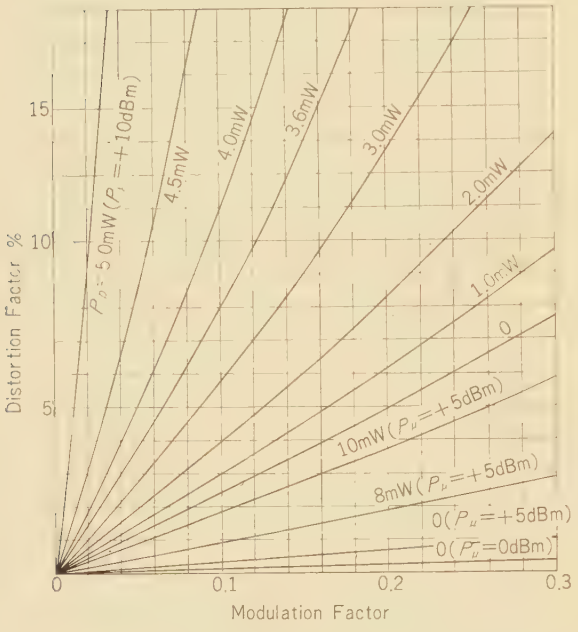

Fig. 4—Relation between modulation factor and distortion.

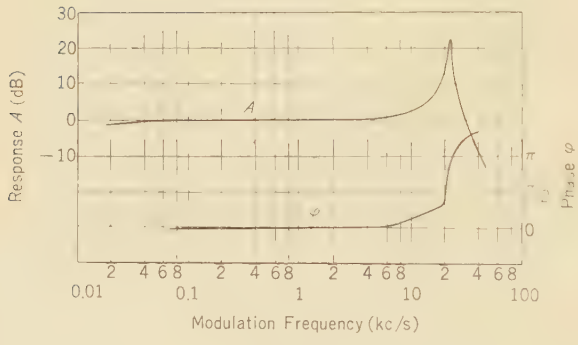

Fig. 5—Typical characteristics of barretter detector.
(Q_0=0.04, ω=200kc/s, P_μ=5dBm, P_D=0)

1.5. Typical Characteristics

Typical characteristics of a barretter detector are shown in Fig. 5. In this example, however, the extremely low Q_0 of 0.04 is used. This very low value of Q_0 is close to the practical lower limit.

2. Automatic Power Control of Microwave Sweeper

Because the usual microwave sweep oscillator has an output deviation of the order of 0.2–0.5 dB over a ±15 to ±25 Mc band, it is not enough to use for the accurate measurement of amplitude characteristics.

Therefore the writers applied APC, which used a barretter as a reference detector, to the sweeper. For this purpose the new AP C circuit described here has been developed.

The APC circuit is constructed so that the oscillator power is divided and detected, and fed back to the control grid of the klystron after the necessary amplification. In the present case, it is assumed that only the alternating component of power variation is treated, and there is no response to the absolute value, or the DC component.

The alternating component of power deviation is formed from the repetition frequency component of the sweeper and its harmonics. As the harmonic content depends on the original output deviation of the sweeper, it seems to be necessary to consider frequencies up to 500 c/s for a 50 c/s of repetition frequency. For instance, the harmonic contents of the envelope waveform of a repeater output, when the sweep signal is applied, are described in the following section. However, it may be considered the harmonic contents of the sweeper are equal to or less than those of the repeater output.

Because the output deviation of the sweeper, in the APC circuit, is constrained to the deviation of sensitivity characteristics of the reference detector, the sensitivity of the detector must be sufficiently constant with frequency over the needed band. Therefore, the barretter is best for this purpose. In a self controlled system, however, the relation $S=$

$1/(1+G)$ exists. (S: supression factor, G: loop gain), accordingly, the phase versus frequency characteristics of the detector must also be considered with the amplitude versus frequency characteristics.

2.1. Self-oscillating Type Barretter Detector as APC Reference Detector

The self-oscillating type barretter detector described in the previous section may be applied as an APC circuit reference detector. However, as described in section 1. 2., its amplitude and phase versus modulation frequency characteristics vary markedly near its natural frequency. Moreover, it is not feasible in practice to obtain a high enough natural frequency of the self-oscillating type barretter detector used for a APC circuit that requires sufficiently high frequency response and large enough gain. Therefore the self-oscillating type circuit is not suitable for use in an APC circuit which has rigorous requirements.

It is suitable, however, for the case where the requirements are not so strict, and the construction is relatively simple compared with the external oscillator type circuit described in the following section.

Experimentally and also theoretically, it is possible to obtain a maximum loop gain of up to 40 dB with a frequency response of up to 500 c/s (−3 dB) when an oscillation frequency of about 200 kc/s is used.

2.2. External Oscillator Type APC Circuit[1]

In the foregoing, it has been shown that the response of the oscillator circuit limits the performance of the self-oscillating type barretter detector as the reference detector in an APC circuit, and the maximum practical loop gain is about 40 dB. Consequently, in order to remove this limitation, it is necessary to see that no closed circuit for the APC signal is formed in the detector circuit.

A new circuit satisfying the above condition has been developed. A maximum loop gain of more than 70 dB in the 50–500 c/s (−3 dB) band, which is required for measurement of amplitude characteristics, is obtained.

In followings, the make-up and function of each component are described, the conditions needed for them are studied; moreover, the experimental results are shown.

2.2.1. Circuit

In order that no closed circuit for the APC signal is formed in the detector circuit, the following is necessary: A carrier signal source independent of the detector circuit containing the barretter must be available, and the APC signal must be obtained as a modulated signal at the bridge circuit by means of substitution with microwave power. Also it is necessary that the carrier input to the bridge circuit be controlled in order to maintain the constant microwave input impedance of the barretter mount by keeping the barretter operating resistance at its normal value.

Therefore, the circuit, although it cannot be clearly separated, consists of two parts. One is the closed circuit which includes the klystron, whose power must be controlled. The other is the closed circuit which keeps the barretter resistance constant. The block diagram of the complete circuit that realizes the above conditions is shown in Fig. 6. The operation of this circuit is as follows:

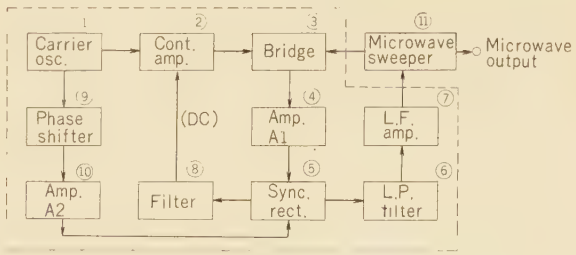

Fig. 6—Block diagram of external oscillator type APC circuit.

The carrier signal generated in ① is amplified by ② and drives the bridge ③ containing the barretter. Some modulated signal

is obtained from this bridge due to the unbalance of the bridge based upon the resistance variation with the variation of microwave input power. This modulated signal is amplified by amplifier ④. From this signal, the variation of amplitude and phase of the microwave input are detected by the synchronous detector ⑤ driven by the carrier signal coming through ⑨ and ⑩. The alternating component is amplified to the necessary voltage level by ⑦, and controls klystron control-grid voltage. On the other hand, because the DC component of the output of ⑤ corresponds to the variation of the average power, the barretter resistance is kept constant by controlling the bridge driving voltage, that is, applying a DC voltage which is obtained by eliminating the alternating component and carrier component from the output of ⑤ through the filter ⑧.

2.2.2. Circuit Design

1) APC Circuit.

i) Gain of APC Signal Loop.

The total gain necessary for the APC loop is given by the following equation:

$$G_l \simeq \frac{\delta}{S}\left\{2\eta_p \lambda' m P_\mu K(n+1)\sqrt{\frac{P_0-P_{s0}}{R_0}+\frac{\alpha_0}{\lambda}}\right\}^{-1}, \tag{8}$$

where, δ=initial power deviation (dB, p-p),
S=sensitivity of control electrode of klystron (dB/V),
η_p=efficiency of synchronous detector defined as the ratio of the DC voltage at the filter output to the rms value of the input carrier frequency signal,
λ'=sensitivity of barretter: $\lambda/(1+jP/P_c)$,
λ=static sensitivity of barretter,
m=modulation factor of microwave input power by the residual deviation,
P_μ=average microwave power,
n=resistance ratio of barretter series arm of bridge to normal barretter resistance,
P_0=balancing power of barretter for the normal resistance,
P_{s0}=total superposed power; $P_{s0}=P_\mu+P_D$ (P_D=DC superposed power),
R_0=normal barretter resistance,
α_0=deviation factor of barretter, $\alpha_0=\Delta R/R_0$ (ΔR=deviation from the normal value),
K=sensitivity of bridge;

$$K = e_B \cdot l \cdot \alpha_0 \sim n/(1+n)^2$$

(e_B=bridge driving voltage, e_a=unbalanced output of bridge),

In Eq. 8, if each constant is as given below:

$\delta=0.5$ (dB)
$S=0.5$ (dB/V)
$\lambda=4.5\cdot 10^3$ (Ω/W)
$n=1.0$ or $K\approx 1/4$
$R_0=200$ (Ω)
$m=2\times10^{-3}$ ($\simeq 0.01$ dB, p-p)
$\alpha_0=0.01$ and $P_D=0$,

the relation between P_μ and G_l is as shown in Fig. 7.

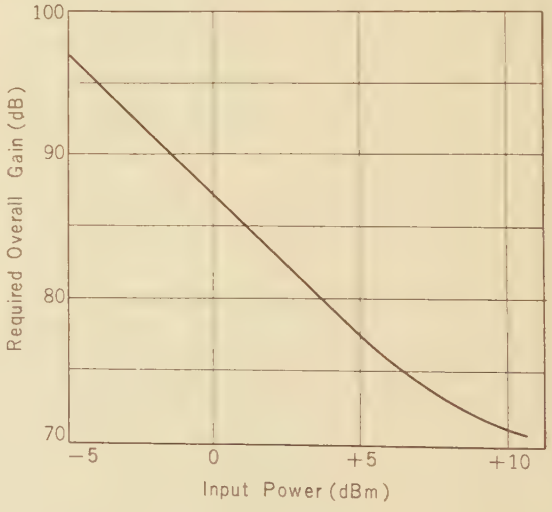

Fig. 7—Required overall gain versus barretter input power.

ii) LF Amplifier

The total gain of APC circuit given by Eq. 8 is assigned to the carrier frequency amplifier ④ and the LF amplifier ⑦. The maximum gain of the LF amplifier is limited because of the noise of the amplifier, especially by vacuum tube flicker noise. When the APC circuit is closed, the residual noise level of microwave output signal depends on the overall characteristics of APC circuit. But a limit may be given by the modulation factor of microwave output signal due to the LF amplifier output noise.

In order to limit the modulation factor due to LF amplifier noise less than ε (dB, $p-p$), if the LF amplifier grid equivalent noise voltage is e_{Ng} (V. $p-p$), the LF amplifier maximum gain $G_{A.\mathrm{Max}}$ must be less than $G_{A.\mathrm{Max}} \leqq \varepsilon/(e_{Ng} \cdot S)$.

Also the factor λ' in Eq. 8 must be considered for amplitude and phase characteristics of LF amplifier.

The necessary open circuit overall characteristics to obtain the required loop gain and to obtain the required frequency band width are given by the adjustment of the characteristics of LF amplifier.

iii) Low Pass Filter Eliminating Carrier Component

A residual carrier component will not hinder the measurements of amplitude characteristics if it is not so large that the modulation of the microwave output is remarkable. However, the residual carrier component may cause unstable operation of the APC, and may cause error due to the mutual conversion of AM and PM; therefore it is advisable that the residual be as small as possible.

The desired attenuation of the n-th harmonic of the carrier signal for the residual modulation of less than ε_c(dB, $p-p$), A_{Fn}, is given by

$$A_{Fn}=20\,\mathrm{Log}_{10}\left[\frac{\sqrt{2}\,A_n\alpha_0 R_0}{\eta_p \lambda' m P_\mu}\,\frac{\delta}{\varepsilon_c}\right]\ (\mathrm{dB}), \quad (9)$$

where A_n is the harmonic attenuation at the synchronous detector output.

2) AGC Circuit

i) Desired Gain of AGC Circuit

In order to maintain the low input standing wave ratio of the barretter mount, it is necessary to keep the barretter operating resistance within a small deviation from the normal resistance.

The block diagram of AGC circuit is shown in Fig. 8. In this figure, G_1 is the gain of the control amplifier, G_c is the gain of the carrier frequency amplifier and E is the DC output or AGC voltage. The symbol γ represents the gain control factor of the control amplifier.

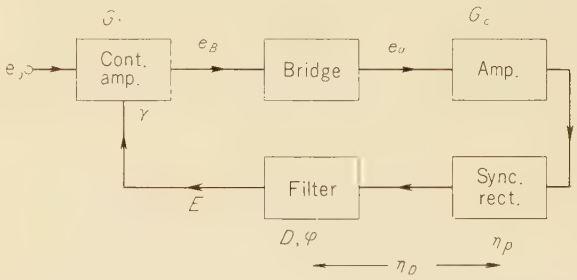

Fig. 8—Block diagram of AGC circuit.

According to Fig. 8, the desired gain of the AGC circuit or the gain of the carrier frequency amplifier for a given deviation of barretter operating resistance is represented by

$$G_c=\frac{e_B-e_{B0}}{e_B e_{B0}\eta_D \alpha_0 K \gamma} \quad (10)$$

where $e_{B0}=e_0 G_{10}$ and G_{10}=initial gain of control amplifier.

Generally, however, γ is a function of E; accordingly, it is a function of G_c. For example, for the 6CB6 vacuum tube, the characteristics of G_m versus E_g and γ versus E_g are shown in Fig. 9. An approximate equation for γ is derived from Fig. 9:

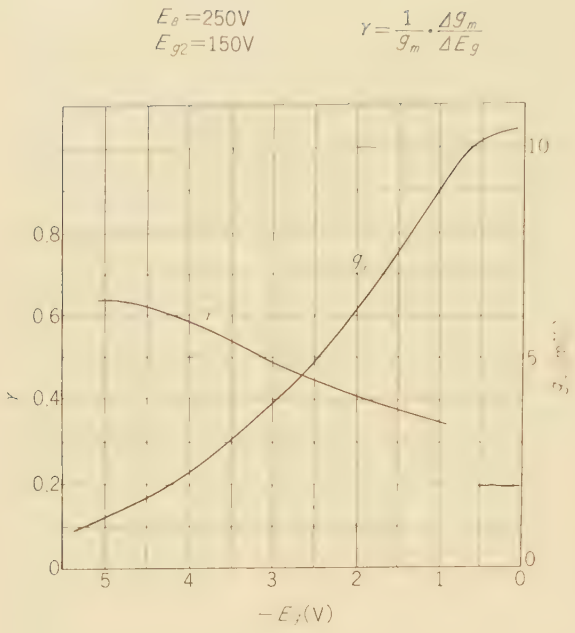

Fig. 9—g_m and γ versus grid bias E_g for 6CB6 vacuum tube.

$$\gamma \simeq -0.077E_g + 0.273 \quad (-1 > E_g > -5)$$

and $E_g = E_{g0} - E$, $\gamma = \gamma_0$ when $E_g = E_{g0}$. (11)

From equations 10 and 11, the following equation is derived:

$$G_c = \frac{-\gamma_0 + \sqrt{\gamma_0 - 0.308\,(1 - e_B/e_{B0})}}{0.154\,\eta_p\,D\,\alpha_0\,K\,e_B} \qquad (12)$$

where D is the transmission factor of the filter.

For $E_g = -2$(V), it becomes

$$G_c = \frac{-0.43 + \sqrt{0.49 - 0.31\,e_B/e_{B0}}}{0.154\,\eta_p\,D\,\alpha_0\,K\,e_B}, \qquad (13)$$

where

$$e_B \simeq (n+1)\sqrt{(P_0 - P_{s0} - \alpha_0 R_0/\lambda)R_0}\,, \qquad (14)$$

When the following constants are substituted in Eq. 13, the results may be represented as shown in Fig. 10:

η_p=0.6 (experimental value)
e_{B0}=3.5 (V) (r.m.s.)
K=1.4 (n=1)

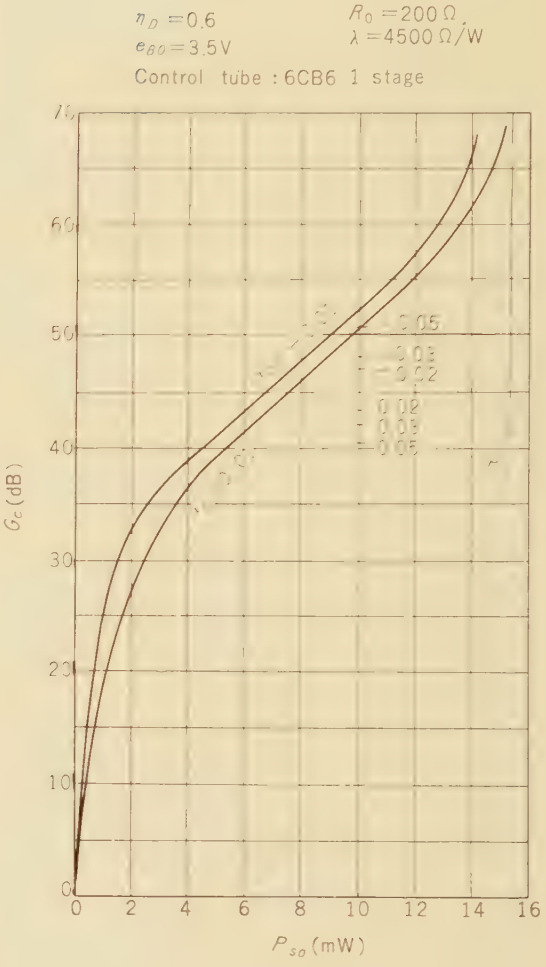

Fig. 10—Required gain of AGC circuit.

ii) Filter Circuit

The AGC circuit theoretically passes only the DC component and completely stops the signal, but it is impossible to realize such a filter. Accordingly, it is true that a loop circuit is formed in the detector or the AGC circuit. But in this case, the loop is significant only at very low frequencies far from the fundamental frequency of

the APC signal. The block diagram of the AGC circuit is shown in Fig. 8, and from Fig. 8, the APC signal component of the detector output is represented as

$$e_p=\frac{C \sin (pt+\theta)}{1-CD\gamma \sin (pt+\theta+\Phi)}, \qquad (15)$$

where $C=\eta_D \lambda' m P_\mu K e_{B0} G_c/R_0$, D is the transmission factor of the filter, and ϕ is the phase shift in the filter.

From Eq. 15, it is clear that in the frequency region of $1 \gg CD\gamma$, the alternating components of microwave input will be reproduced exactly, but near the frequency of $1=CD\gamma$, the amplitude and phase of the detector output differ considerably from those of the deviation of microwave input. Actually, the side-band energy is increased rapidly and the carrier component will be decreased, and the amplitude and phase of envelope frequency will jump near $CD\gamma=1$.

Therefore, the attenuation characteristics of the AGC low pass filter circuit must be determined to obtain the condition $CD\gamma=1$ at such very low frequency that the attenuation of main APC circuit are large enough satisfying the required maximum loop gain. In other words, if the APC main circuit does not have sufficient attenuation at a high enough frequency, the time constant of the AGC circuit becomes very large, and long period will be needed before the barretter attains the normal or balanced state when the mean value of the microwave input power is changed.

3) Common Circuits

i) Carrier Oscillator

The requirements for the carrier oscillator are as follows:

a) It must be considerably higher frequency than the maximum frequency of the APC signal in order that the APC signal can be easily separated from the detector output.

b) Because of the capacity of barretter mount and cable reactance, it is not advisable to select such a high frequency that the reactance becomes not negligible compared with the barretter resistance.

c) Carrier to noise ratio must be as good as possible, in order to obtain good signal to noise ratio in the output signal.

d) If the frequency stability of carrier is not good, the signal to noise ratio will be deteriorated by phase detection in the synchronous detector.

Conditions a) and b) are contrary to one another, and the carrier frequency must be determined from considerations of the operating frequency band-width of the APC circuit, maximum loop gain, and the circuit constants of the detector bridge circuit.

Generally, it is suitable to select a frequency in the range between 100 and 500 kc/s.

The carrier to noise ratio of the carrier signal, C/N, necessary to obtain the signal to noise ratio of the output signal, S/N, is given by

$$C/N=C/P \cdot S/N \qquad (16)$$

where, $C/P=\sqrt{2}\, A_1 \alpha_0 R_0/\eta_p \lambda' m P_\mu$.

ii) Control Amplifier

Because the signal through the control amplifier is theoretically an unmodulated wave, the control amplifier is not needed for wide-band characteristics. However, because of the variation of amplitude and phase of the carrier signal due to the fluctuation of carrier frequency or the variation of circuit constants of the control amplifier itself, the signal to noise ratio of the APC signal will decline, and the balance of the detector bridge will be degraded.

Accordingly, very sharp amplitude and phase characteristics are not advisable. Also it is harmful to transmit harmonics of the carrier or generate any harmonics in the control amplifier itself. Of course a good signal to noise ratio must be maintained. High gain is not necessary, but it is desirable to use a vacuum tube with large γ.

iii) Carrier Frequency Amplifier

Because this amplifier handles modulated signals, it should have good amplitude and

phase characteristics over a sufficiently wide frequency band-width. Therefore it is advisable to use a resistance-coupled circuit. The gain, G_c, must satisfy the following condition:

1) It must be larger than the value subtracted the gain of the LF amplifier from the total gain represented by Eq. 8.

2) It must be larger than that given by Eq. 10 or Eq. 12, Eq. 13.

3) In Eq. 15, G_c is included and therefore, a lower G_c is desirable.

Therefore, it is desirable to employ the minimum value of gain in the range that keeps the barretter operating resistance within the allowable deviation, and does not require that the gain of amplifier exceed the limit due to its noise level.

iv) Unbalance Detector

A differential amplifier with grid and cathode input (shown in Fig. 11) is most simple as the unbalance detector and satisfactory results are obtained with a suitable vacuum tube.

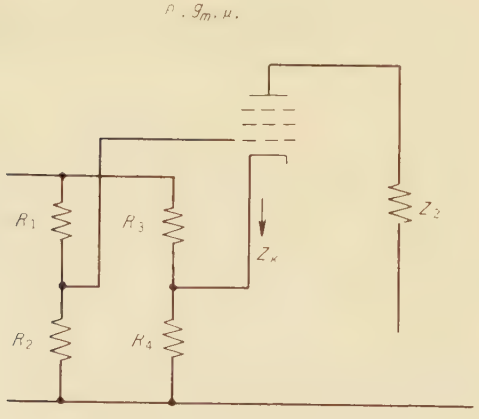

Fig. 11—Unbalance detector.

About Fig. 11, when the ratio M of the residual output at the balanced condition of bridge to the unbalanced output of bridge is taken as a factor which shows the performance of unbalance detector, M is represented as follows:

$$M=\frac{[\mu(\beta-1)-1][\rho+(1+\mu)Z_k+Z_2]}{2(\rho+\mu Z_k)(1-\beta)}, \quad (17)$$

$$\simeq 1-\frac{\alpha}{2}\mu, \text{ when } \mu\gg 1 \text{ and } \rho\gg Z_2,$$

where, $\beta=2(1+\alpha)/(2+\alpha)$

Therefore, the input impedance of the unbalance detector must be high enough to avoid reaction with the barretter. The input impedance of the grid side is generally high enough. The input impedance $Z_{in\,k}$ of the cathode input is shown by

$$Z_{in\,k}\simeq\frac{\rho+(1+\mu)Z_k+Z_2}{\mu(1-\alpha)}, \quad (18)$$

$$\simeq Z_k+1/g_m, \text{ when } \rho\gg Z_2 \text{ and } 1\gg\alpha$$

Accordingly, as shown by Eqs. 17 and 18, high μ and high ρ tubes are suitable.

Of course, transformers are useful for this purpose. But now the frequency is comparatively high, so the unbalance factors of the transformer itself such as the leakage inductance and the stray capacitance must be considered.

v) Synchronous Detector

Suitable results are obtained by utilizing a half wave synchronous detector using four semiconductor rectifiers as the amplitude and phase detector. The detector efficiency is

$$\eta_p=\sqrt{2}/\pi\simeq 0.45,$$

when the operation is considered to approach that of an ideal switching circuit. Experimentally η_p was about 0.6.

2.2.3. Experimental Results

Due to the foregoing theoretical considerations, experimental work was performed, and the following results are obtained: Maximum loop gain of over 70 dB is required to achieve residual power deviation of 0.001 dB without spoiling the needed operating frequency band of 50~500 c/s (−3 dB) when the initial de-

viation is 0.5 dB. Typical experimental characteristics are shown in Fig. 12 (a) and (b). Fig. 12 (a) is an open circuit overall characteristics of higher frequency side of band, and Fig. 12 (b) is an open circuit overall characteristics of lower frequency side of band of the same circuit.

2.3. Power Modulation Sensitivity of Klystron

2.3.1. Power Modulation Sensitivity and its Deviation

The APC signal, detected by the barretter detector and amplified, is applied to the control grid of the klystron, and the power deviation is suppressed. Therefore, the relation between the variation of output power and grid input voltage, in other words, the modulation sensitivity of control grid, is important.

The sensitivity S is given by

$$S=\Delta P_0/\Delta E_{gk}\ (\mathrm{dB/V}), \qquad (19)$$

where, ΔP_0=variation of oscillation power,
ΔE_{gk}=variation of control grid voltage.

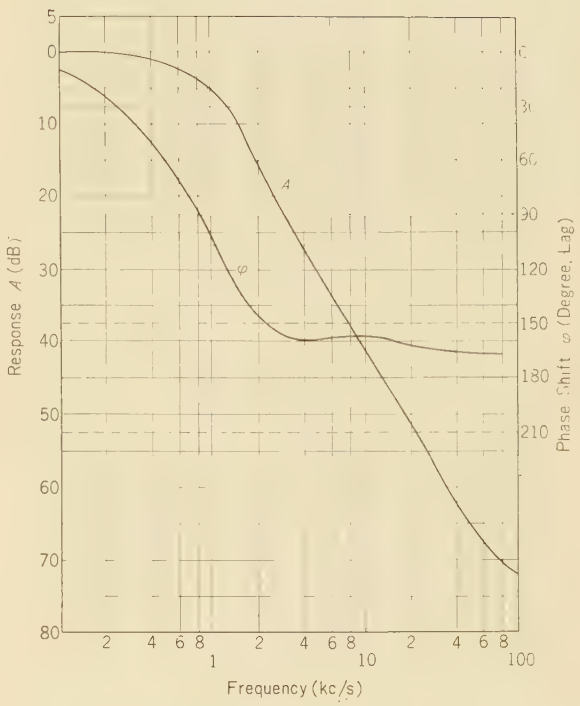

Fig. 12 (a)—Overall characteristics of higher side.

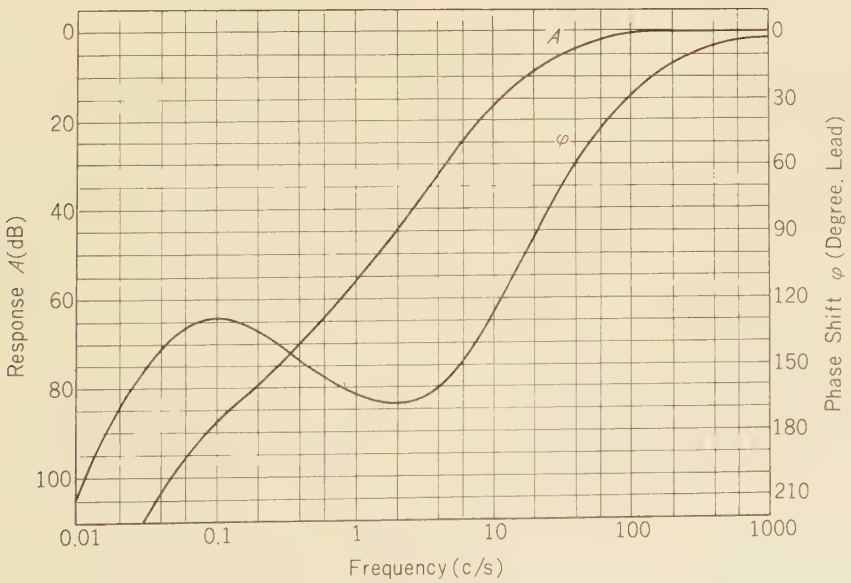

Fig. 12 (b)—Overall characteristics of lower side.

If S is larger, lower maximum APC signal output voltage and lower APC circuit gain are allowable. However, if S is too high, the value of the grid voltage becomes critical; accordingly, the power supply stability requirements become severe.

Next, variation of sensitivity due to the variation of static and dynamic state of the klystron must be considered, namely;

(1) variation of sensitivity due to the variation of value of grid voltage with constant frequency and constant output coupling,
(2) variation of output coupling with constant frequency and constant grid voltage,
(3) variation of oscillation frequency with constant grid voltage and constant output.

In the following, the modulation sensitivity characteristics of the 4V27 klystron (similar to 5837) for 4000 Mc and the 5721 klystron for 6000 Mc are discussed.

2.3.2. Characteristics of the 4V27 klystron

1) Variation of sensitivity due to variation of grid voltage is about 6 dB at practical output powers (about 5 dBm, 10 dB padded).
2) Frequency characteristics of sensitivity is about 6 dB too.
3) When the other conditions remain constant, the variation of sensitivity, following a change of output coupling, is about 6 dB with maximum power of about 20 dBm (without padding).
4) The experimental value of S is about 0.1–0.3 (dB/V).

From the above, if the output power of the sweeper is controlled by changing output coupling, some 10 dB of excess margin of APC loop gain is desirable.

2.3.3. Characteristics of the 5721 klystron

1) Variation of sensitivity caused by the variation of output power with constant frequency and constant grid voltage is less than 6 dB in usual tubes.
2) Deviation of sensitivity with change of frequency is about 3 dB when the output power is less than 20 dBm to matched load.
3) The actual sensitivity is about 0.2–0.5 dB/V.

Therefore, the desirable excess gain margin of APC, due to the deviation of modulation sensitivity of the klystron, is as large as for the 4V27, or about 10 dB.

3. Measuring Equipment for Relay Station

In this section, the measuring equipments using the barretter detector and APC which were described in the foregoing section, are explained.

3.1. Measuring Equipment for 4000 Mc Band Relay Station (Type WJ-310 Measuring Equipment)

3.1.1. Functions and Make-up

The measuring functions which have been performed up to this time in relay stations are as follows:[3]

(1) amplitude characteristics,
(2) delay characteristics,
(3) input and output impedance (VSWR) of repeater and TWT,
(4) noise figure,
(5) level (μ and IF),
(6) performance as standard signal generator,
(7) impedance matching of antenna system,
(8) field intensity.

These measurements are for a heterodyne repeater system. However, with the increase of channel capacity due to the improved performance of the repeater, accuracy requirements have become more severe.

On the other hand, the stabilities of repeater characteristics have been improved and measurement of some quantities is unnecessary. Therefore, the items measured have been changed and the advance of performance is planned about needed items.

Namely, the unnecessary measurements are those in items (2), (3), and (4). Also, about amplitude characteristics, because the characteristics of μ–IF are needed chiefly by the relation of adjustment, IF–μ, IF–IF, and μ–μ are omitted.

Thus, the functions required of the new equipment are as follows:

(1) measurements of amplitude versus frequency characteristics of receiver part of repeater (μ–IF);
  (a) output level of microwave (repeater input level): $-20 \sim -35$ dBm,
  (b) IF detector input level: -2 dBm (standard level),
  (c) precision: 1 dB or ∞ dB full scale (80 mm) on five-inch cathode ray oscilloscope,
  (d) accuracy: 0.1 dB.
(2) performance as standard signal generator;
  (a) level: -5 -60 dBm, continuously variable by reactance attenuator,
  (b) accuracy: 1 dB, below -5 dBm,
(3) level of IF;
  (a) level: $+6 \sim -5$ dBm, direct reading on meter,
  (b) accuracy: 0.5 dBm,
(4) level of microwave;
  (a) level: $+10 \sim -5$ dBm, direct reading on meter,
  (b) accuracy: 0.5 dBm,
  and more by the using of adapter,
(5) input and output impedance matching of repeater; VSWR: 1.04 to 3, accuracy: 1.02,
(6) overall amplitude characteristics (μ–μ);
(7) frequency measurements of microwave.

Adapters are installed at only main stations or terminal stations, and they are movable if they are required at any other station.

In the above items, (1), (5), and (6) are displayed on the cathode ray oscilloscope over the ± 15 Mc band width.

The block diagram of this equipment is shown in Fig. 13.

The main equipment contains the detector and display unit, microwave sweep signal oscillator, and power supply; and the adapter contains the microwave detector, 200 kc/s modulation signal generator, 200 kc/s amplifier, 200 kc/s detector, and power supply.

The external appearance and construction are shown in Fig. 14. The most important quantity measured by this equipment is amplitude characteristics of μ–IF. The amplitude characteristics of repeaters are required to be within 0.5 dB of specifications; accordingly the measuring equipment must have an accuracy of better than 0.1 dB. The barretter detector and APC described in the previous

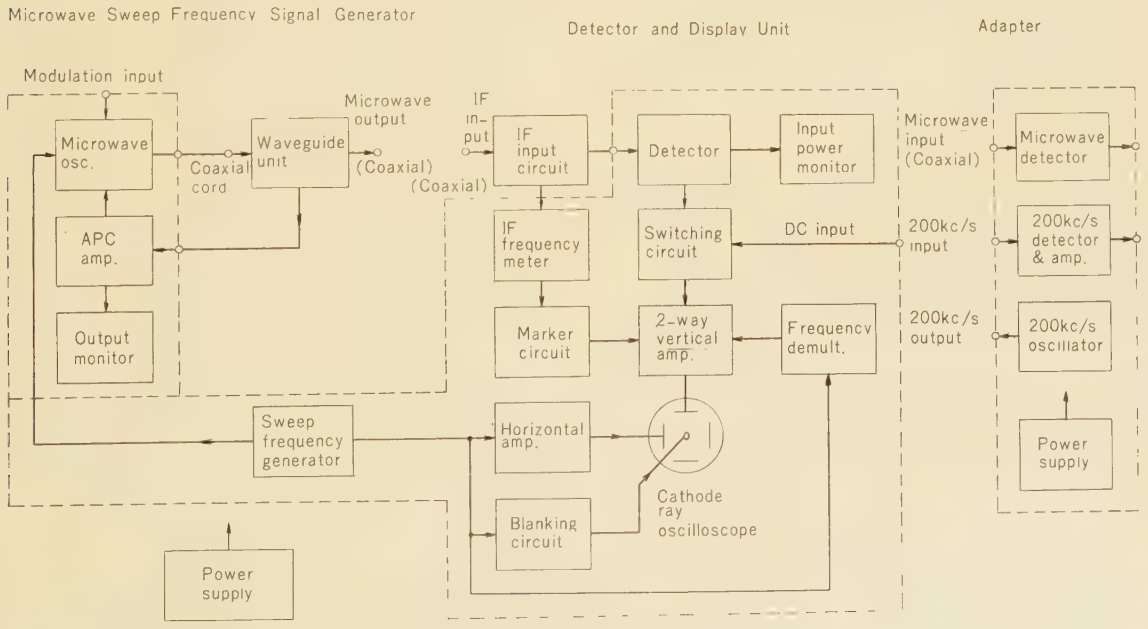

Fig. 13—Block diagram of type WJ-310 measuring equipment.

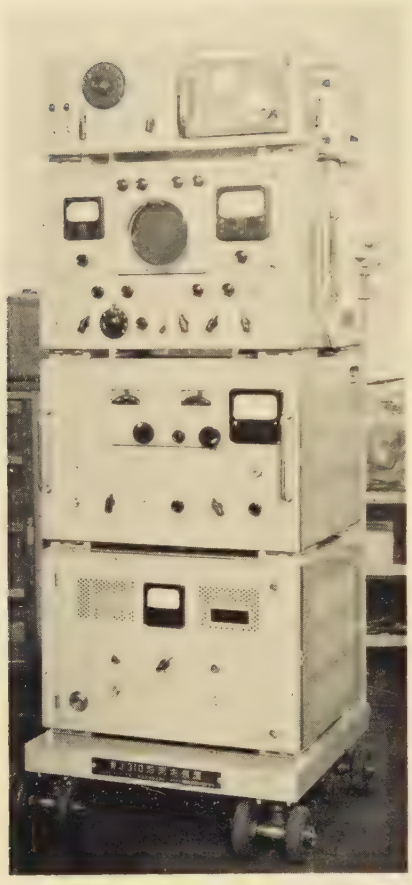

Fig. 14—External appearance of measuring equipment for 4000 Mc relay station.

sections are utilized in order to realize this requirement.

3.1.2. Performance Requirements

The following are the performance requirements of the important components:

1) IF Detector

i) Input Impedance

If the input impedance of barretter mount varies with frequency, the declined frequency characteristics of detector sensitivity will be caused. Also, if it is mismatched, even it is constant over the rated band width, it causes the long line effect when the output impedance of the equipment under test is mismatched, and causes some error in the measurement. In this equipment a VSWR less than 1.2 is provided over the bandwidth of 70 ± 15 Mc/s.

ii) Frequency Response Characteristics

The required frequency response characteristics of a detector depend on the degree of how fine structures are necessary for the displayed pattern on the screen of cathode ray oscilloscope.

The envelope waveform of the output signal of the equipment under test is somewhat distorted, so the harmonic contents become important.

Then, the necessary frequency response characteristics of the barretter detector were determined from the results of some experiments; harmonic contents of envelope waveform for actual repeaters were measured. Measuring methods are as follows: a swept microwave signal is applied to the repeater under test, and its IF output or microwave output is detected by a crystal detector, the detector output recorded on the tape, is analyzed by sonergraph, and its integrated energy is measured by filter method. Various characteristics of several repeaters were measured by the above method. Examples are presented in Fig. 15 (a), (b) and (c).

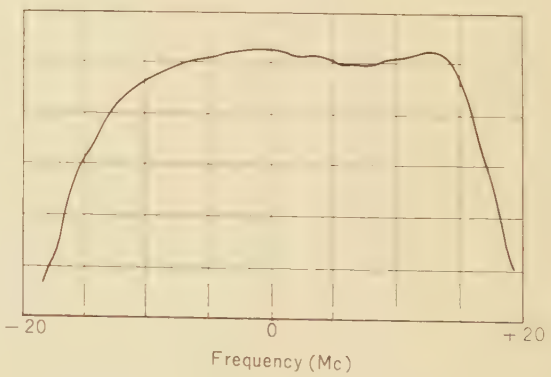

Fig. 15 (a)—Amplitude characteristics of repeater.

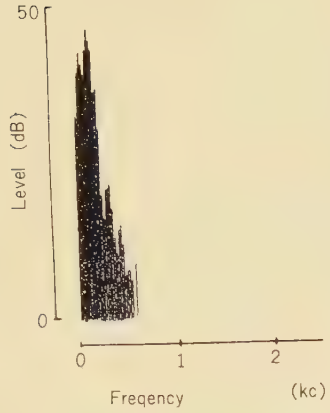

Fig. 15 (b)—Pattern of soner graph.

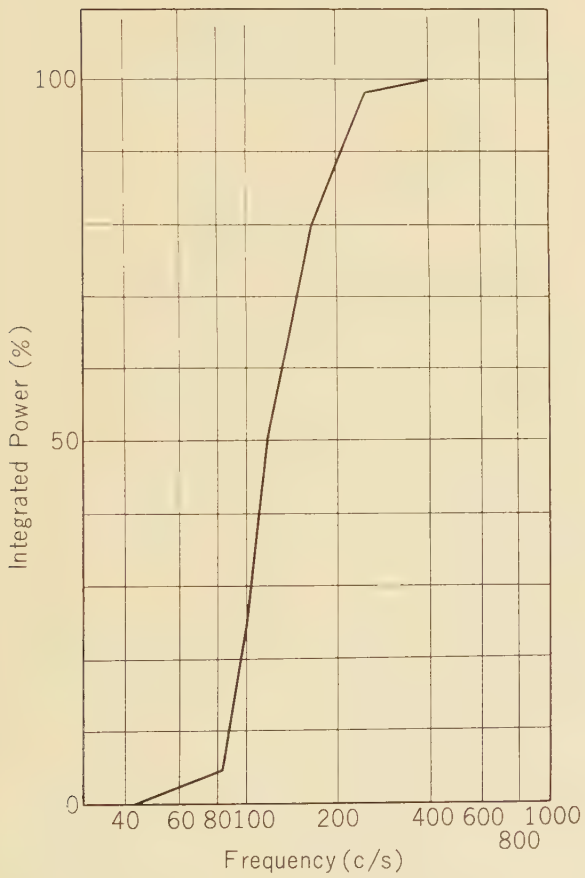

Fig. 15 (c)—Integrated power.

Fig. 15—Harmonic contents due to amplitude characteristics of repeater.

It was understood from the results of experiments that; the upper limit frequency of the band containing the 99% of total energy of the envelope components or the sideband components of repeater output signal, was less than 800 c/s for the repeater having bad characteristics, and it was also less than 500 c/s for the repeater having normal characteristics.

Due to the above results, the standard for the detector was determined as shown in Fig. 16.

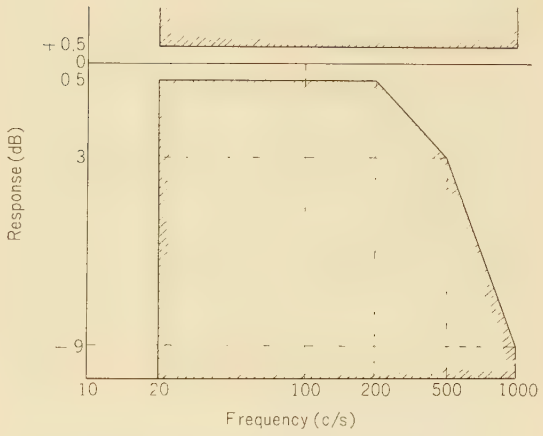

Fig. 16—Standard frequency response of IF detector.

iii) Noise level

The fluctuations of the base line due to the hum and the noise outputs of the measuring equipment itself are respectively less than 2 mm on the scale of a cathode ray oscilloscope, whose vertical amplifier gain is adjusted in order that the variation of deflection is 80 mm when the intermediate frequency detector input level changed from −2 dBm to −3 dBm.

3.1.3. Microwave Sweep Frequency Signal Generator

1) Sweep Oscillator

i) Frequency Range

Type 4V27 klystron is used, and frequency range is 3600 to 4200 Mc/s.

ii) Deviation of oscillator output

It must be less than 0.5 dB without APC over the ±15 Mc bandwidth.

2) APC Circuit

i) APC loop gain

When the input level of the APC reference detector is 5 dBm, APC loop gain must be larger than 25 dB and the gain margin of the APC circuit must be more than 10 dB.

ii) Frequency Response of Reference Detector

The deviation of the frequency response must be less than 3 dB in the frequency range of 50 to 500 c/s when the IF input level is 5 dBm.

To the IF detector, a somewhat complex amplitude-modulated wave caused by the repeater characteristics is applied. But in the case of APC the signal is the sweep oscillator output itself. Therefore, it is possible to consider that the harmonic content is less than that in case of the IF detector.

3) Output Circuit

The output of the microwave sweeper is introduced to a waveguide component through a cord and applied to the APC detector.

Moreover, the sweeper output is divided by a directional coupler included in the waveguide component, and is introduced to the input terminal of the repeater through a cord or directly. Accordingly, the frequency characteristics of the coupling factor of the directional coupler and the long line effect due to the coaxial cord enter into the error factor. The coupling of the directional coupler is 25±1 dB over the frequency band of 3600~4200 Mc. The long line effect has been decreased by using a lossy cord.

4) Adapter

i) Modulation Signal

The measurement of input and output impedance of repeater requires considerably high sensitivity. Therefore, 200 kc/s, 100 % amplitude modulation signal is applied to the sweep oscillator for this measurement. The deviation of output power is 2.5 dB over the ±15 Mc band in this case, because of the variation of modulation sensitivity of the oscillator.

ii) 200 kc Amplifier and Detector

The bandwidth of the amplifier is ±5 kc (−3 dB), and VSWR is directly read from the scale of the reactance attenuator.

iii) Microwave Detector

Its characteristics are the same as those of the IF detector.

3.1.4. Actual Characteristics

1) Temperature Characteristics of Barretter Detector

The effects of temperature on the barretter element and detector circuit become a problem especially when they are housed in the measuring equipment. Zero point adjustment becomes impossible, and difficulty in measurement is caused by drift. The temperature coefficients of the other resistances of the bridge circuit are added to the increase of barretter initial resistance with temperature rise.

Because a carbonfilm resistance has an opposite temperature coefficient to that of the barretter, the balancing condition will be worse, and temperature allowance will become more narrow. Also, the temperature coefficient of compensation capacitance of bridge is important when the substitution frequency is very high.

Effects of drift due to temperature rise are as follows:

The drift due to temperature rise of the IF detector connected to the output terminal of the repeater IF amplifier must be added to the initial drift due to the temperature rise of the equipment itself.

To decrease the long line effect, it is advisable to connect the detector directly to the IF output. However, when the barretter mount is connected directly at the output terminal of the IF amplifier, the temperature rise of the barretter is considerably large due to thermal radiation and conduction from vacuum tubes; especially, the IF amplifier output tube. Therefore, some additional cord

is required between barretter mount and IF output terminal to avoid these thermal effects.

2) Deviation of output power of sweep oscillator

The deviation of output power of the sweep oscillator depends on the characteristics of oscillator itself and the effect of tracking of repeller voltage and long line effect. Actually, the deviation of output power is 0.1~0.4 dB over ±15 Mc bandwidth.

3) APC loop Gain

The variation of APC loop gain due to the variation of microwave level depends on the detector characteristics; also it depends on the variation of klystron modulation sensitivity. An example of loop gain characteristics is shown in Fig. 17. Loop gain is adjusted to the value having a margin of more than 10 dB from the maximum value.

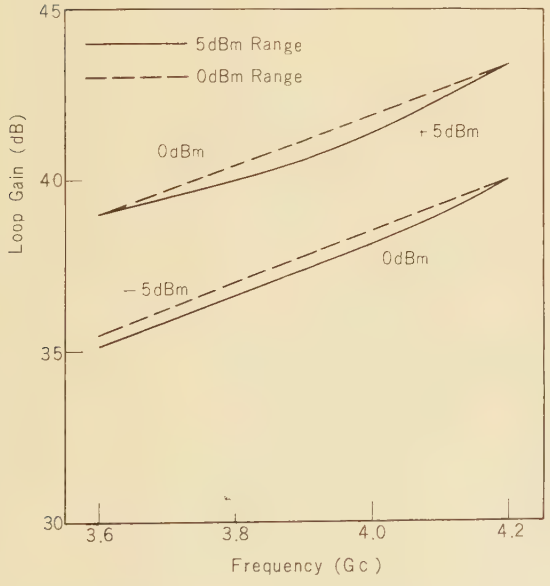

Fig. 17—Loop gain versus frequency characteristics.

4) Influence of Fluctuation of Power Supply

The variations of display of the equipment itself are less than ±0.3 dB with power supply fluctuations of ±5 %. However, the variation of repeater gain due to the fluctuation of repeater power source becomes important during measurement of repeater characteristics, Actually it is in the order of 0.05 or 0.1 dB.

5) Noise and Hum Level

Visible noise level on the cathode ray oscilloscope is suppressable by narrowing the response frequency characteristics. As described in Section 1, the self oscillating type barretter detector has a natural frequency. Noise components near the natural frequency are accentuated, and they cause increase in noise level of the display.

Therefore, it is necessary to eliminate the higher frequency region in order not to have a large peak response. Actually, the level was about 0.02 dB (*p-p*) on 1 dB scale with input level of −5 dBm. And if the measuring signal is amplitude modulated by the hum component of the repeater power supply, it also causes some error. The effect of the hum component of the measuring equipment itself is the same. At the standard condition (IF detector input of −2 dBm and gain of the vertical amplifier adjusted to 1 dB full scale), the slope caused by the hum component on the cathode ray oscilloscope is 0.5~1.0 mm with measuring equipment only and 1~2 mm through repeater.

6) Connection with Repeater

In the case the output of the measuring equipment is connected to the receiving input test terminal of the repeater, it is desirable to apply APC at that test terminal. In order to realize this condition, it is necessary to connect directiy the directional coupler including the barretter mount for APC to the waveguide input terminal of repeater.

However, because of the test terminal is of the coaxial type in some type of repeater, coaxial cords are used between the test terminal and APC circuit. This may cause long line effect, and measurement errors occur. The error due to this factor is about 0.1 dB maximum for SF-B3 system as shown in the next section.

3.1.5. Considerations about Accuracy

The accuracy of the measurements of am-

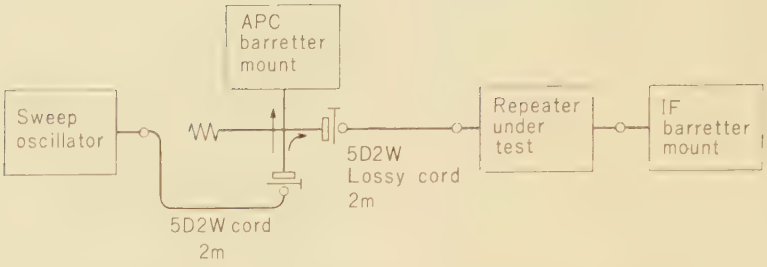

Fig. 18 (a) Connections for SF-B3 System.

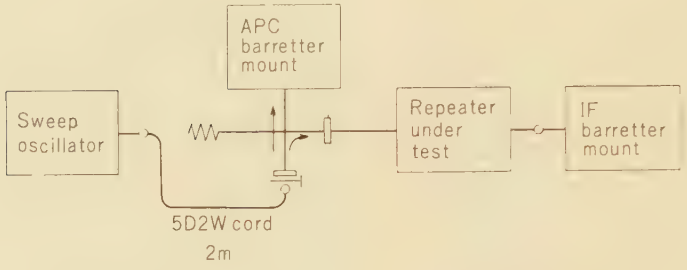

Fig. 18 (b) Connections for SF-B4 System.

Fig. 18—Connection diagram for measurements of amplitude characteristics.

plitude characteristics varies with the type of repeater. In the following, two types of repeater—the SF-B3 system and the SF-B4 system—are discussed. The SF-B3 system has a capacity of 600 CH and the SF-B4 system has a capacity of up to 960 CH.

The connection diagrams for each system are shown in Fig. 18. The following are considered as error factors:

1) residual APC output deviation,
2) characteristics of detector,
3) long line effect,
4) characteristics of waveguide circuit.

Each factor is tabulated in Table 2, (a) and (b), for SF-B3 and SF-B4.

From Table 2, it is clear that for the most typical system the SF-B3, the accuracy of measurements of μ–IF amplitude characteristics is about 0.2 dB.

The deviations of amplitude characteristics are read from the scale installed at the surface of the cathode ray oscilloscope. Calibration is achieved by 0.5 dB chopping of IF detector output. Because the chopping width is select-

Table 2

ACCURACY OF MEASUREMENT

(A) ACCURACY OF SF-B3 SYSTEM

	Error Factor	Error (dB)
Sending	Residual of APC	0.035
	APC Detector	0.01
	Directional Coupler	0.043
	Long Line Effect	0.08
	Lossy Cord	0.015
Receiving	Detector	0.01
	Calibration	0.02
	Total	0.213

(B) ACCURACY OF SF-B4 SYSTEM

	Error Factor	Error (dB)
Sending	Residual of APC	0.01
	APC Detector	0.035
	Directional Coupler	0.043
Receiving	Detector	0.01
	Calibration	0.02
	Total	0.118

ed for standard input level, −2 dBm, some errors occur with variation of detector input level. They are less than 0.02 dB over the variable range of +5 to −5 dBm.

3.2. Amplitude Characteristics Measuring Equipment for 6000 Mc Band (Type WJ-61 Measuring Equipment)

In the 6000 Mc band, wider band transmission than for 4000 Mc system has been considered. Therefore, higher accuracy measurements of amplitude characteristics are required. Because of the fact, however, that the measuring method described above seems to be the best, any essential difference is not considerable for the 6000 Mc system.

However, some improvements will be expected by considering the method of connection between the repeater and the measuring equipment, and by properly using the circuit elements or microwave components.

The different points compared with Type WJ-310 Measuring Equipment are as follows:

1) Frequency band is from 5900 to 6400 Mc.
2) Receiving detector is useful for both μ and IF signal using the individual barretter mount and simple switch. Therefore, the microwave detector provided in the adapter is removed.
3) An on-off microwave attenuator with an attenuation of 10 dB is used in order to extend the variable range of repeater input level. Resultant variable range with available APC is more than 20 dB.
4) In order to obtain high enough APC loop gain over the entire range of the APC detector input level (−5 to +5 dBm), the gain of the APC circuit is continuously adjusted by an attenuator interlocked with a microwave attenuator (reactance attenuator). In the old type WJ-310 measuring equipment, loop gain is adjusted for each 5 dB of reference detector input level. It is rather easy to maintain the loop gain of more than 40 dB without any effect from the repeater input level.

Conclusion

The objects of measurements are usual microwave circuit elements and especially multichannel microwave repeaters. The measurements of repeaters are made from microwave receiving input terminal to IF output terminal, μ–IF, or to microwave output terminal, μ–μ. Therefore, the output frequencies differ from the input frequency, and this is a dominant fact that prevents the improvement of measuring accuracy.

On the other hand, the requirements for repeater become more and more severe with the increase of transmission band width. Consequently, measuring equipment with higher accuracy is required. For example, accuracy of measurement better than 0.1 dB over a band width ±15 Mc is required for transmission of 960 channels.

In order to develope the measuring equipment having an accuracy of better than 0.1 dB, the use of a barretter as a detector was suggested, and the self balancing circuit as a detector was analyzed. Moreover, a new APC circuit using a barretter as a reference detector was suggested, and theoretical and experimental results was described. Maximum loop gain of about 70 dB was achieved for alternating current component of output deviation.

Moreover, we discussed the functions and performances of complete measuring equipments for relay stations of 4000 Mc and 6000 Mc system, and it became clear that those equipments have achieved initial goal of an accuracy of 0.1 to 0.2 dB.

References

(1) M. Ota, I. Sugiura: Microwave Amplitude Characteristics Measuring Equipment, *Electr. Commun. Labor. Techn. J. NTT, Jap.* 10, 9, 1961.

2. C. G. Montgomery: Technique of Microwave Measurements, *M.I.T. Rad. Lab. Series*, Mc Graw-Hill, for example.

3 K. Sugahara and et al: Measuring Equipment for Microwave Repeaters, *Reports of the E.C.L.*, 5, 3, p. 32, 1957.

* * * *

U.D.C. 621.318.57:519.2]:621.374.5

Binomial Probabilistic Sequential Circuit*

Makoto SUGIMORI†

This paper describes three types of recurrence circuits in which the output is given by a sequence of probability distributions to an input sequence. Such a probabilistic circuit is constructed of three circuit elements; a binomial probabilistic transform with a finite time lag, a probabilistic branch, and a distribution adder, which are introduced in this paper for the purpose of contributing to a high reliable circuit design. The author has extracted a special determinant which is the indicial function of a discrete system, and then, shows the output distribution to the input distributions sequence, the covariance between the output distributions, the additive process of the output distributions and the expression of mean and variance of these limit distributions.

Introduction

One of the most important problems in high reliability construction is to represent a given system as a probabilistic transfer system in sequence of operations. In design, the rule of transform which prescribes the system used to describe definitely but it should be represented "probabilistically" by nature.

A circuit containing delay elements such as relays in electrical circuits and neurons in the nervous system is called "a sequencial circuit" and the performance characteristic of such a circuit can be studied in terms of a truth table, logical functions with delay operator, or more intuitively, combining certain primitive logical symbols, automata or a state transition diagram.

It should be noticed that, first, in a definite transfer system an output is determined uniquely corresponding to an input sequence and the system reliability is always 1 if there is no external disturbance but this is unreal or an ideal situation. In a probabilistic transfer system an output distribution is determined uniquely corresponding to an input sequence and mean value of the output distribution is equal to the output of that definite transfer system, second, the reliability of an element in a device is a monotone decreasing function of time, but when we discuss the function of the element working in the device, the function is continued by replacement whenever that element gets out of order, therefore, the reliability of the function is not monotone and the probability of malfunctioning is given by a recurrence type Markoff process.

An object of our study is a recurrence type Markoff process. In Markoff theory, a system is described by a transition probability matrix. But we represent a given system by a probabilistic sequential circuit which consists of three circuit elements; a binomial probabilistic transform with a finite time lag, a probabilistic branch and a distribution adder, instead of the transition probability matrix. In the next section we will give the definitions of these three circuit elements and extract 7 theorems concerning the relations

* MS in Japanese received by the Electrical Communication Laboratory, on September 24, 1960. Originally published in the *Kenkyû Zituyôka Hôkoku* (*Electrical Communication Laboratory Technical Journal*), N.T.T., Vol. 10, No. 4, pp. 657-681, 1961.

† Nishibori's Research Section.

between input and output distributions of such an element. There are three fundamental circuits; a series circuit, a parallel circuit and a series-parallel circuit connecting two circuits by a delay element. Using these three fundamental circuits we will construct various binomial probabilistic sequential circuits [discrete (constant difference, nonconstant difference) system: continuous system, stationary system: quasi-stationary system: non-stationary system] and extract a special determinant, that is, a circuit operator, which is the indicial function of the discrete system, and then, using this circuit operator, we will show the output distribution in any time to an input distribution sequence, the covariance between the distributions of the output sequence, the additive process of the output distributions and the expression of mean and variance of the limit distributions.

1. Fundamental Form of Probabilistic Transform and Their Properties

In this section, we will define first the three circuit elements; a basic probabilistic transform, a probabilistic branch and a distribution adder. The basic transform is a binomial probabilistic transform. Second, we will show the properties of the fundamental circuits of the probabilistic transform in the theorems concerning the relations of input and output distributions and prepare for the construction of a probabilistic sequential circuit in Section 2, 3, and 4.

Definition 1. A binomial probabilistic transform with time lag δ is $aC_i p^i (1-p)^{a-i} (\equiv \mathrm{b}(i; a, p))$, where a is input, i is output and there is a time lag δ between a and i. In symbol, it can be represented as shown in Figure 1.

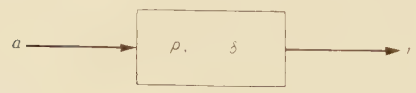

Fig. 1—A binomial probabilistic transform with parameter p, δ.

If input a is a random variable, then output i is given by a compound distribution.

Example 1. If input a is a Poisson distribution with parameter λ; $p(a)=e^{-\lambda}\lambda^a/a!$, then the output in time δ is followed;

$$p(i)=\sum_{a=0}^{\infty} p(a)\,\mathrm{b}(i; a, p),$$

$$\frac{(\lambda p)^i e^{-\lambda}}{i!}\sum_{a=i}^{\infty}\frac{\{\lambda(1-p)\}^{a-i}}{a-i},$$

$$\frac{(\lambda p)^i e^{-\lambda}}{i!}e^{\lambda(1-p)}=\frac{e^{-\lambda p}(\lambda p)^i}{i!}.$$

Consequently, the output at time δ is a Poisson distribution with parameter λp and does not exist at any other time.

Theorem 1. A series circuit of a binomial probabilistic transforms with parameter $p_i, \delta_i (i=1, 2)$ (Fig. 2 (a)), is equivalent to a binomial probabilistic circuit with parameter $\prod_{i=1}^{2} p_i, \sum_{i=1}^{2}\delta_i$ (Fig. 2 (b)).

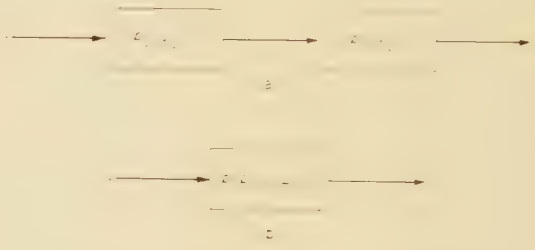

Fig. 2—A series binomial probabilistic circuit.

Proof: The proof is shown by the following:

$$\sum_{n=i}^{a}\mathrm{b}(n; a, p_1)\,\mathrm{b}(i; n, p_2)=\mathrm{b}(i; a, p_1 p_2) \qquad (1)$$

Let $n-i=m$, then the left hand of Eq. (1) is,

$$\sum_{m=0}^{a}\frac{a!}{(a-i-m)!\,m!\,i!}\left\{\frac{p_1(1-p_2)}{1-p_1}\right\}^m$$

$$\left\{\frac{p_1(1-p_2)}{1-p_1}\right\}^i \frac{(1-p_1)^a}{(1-p_2)^i} p_2{}^i$$

$$=(1-p_1)^{a-i}(p_1p_2)^i \frac{a!}{(a-i)!\,i!}$$

$$\sum_{m=0}^{a} \frac{(a-i)!}{(a-i-m)!\,m!}\left(\frac{p_1(1-p_2)}{1-p_1}\right)^m$$

$$=(1-p_1)^{a-i}(p_1p_2)^i \frac{a!}{(a-i)!\,i!}\left\{1+\frac{p_1(1-p_2)}{1-p_1}\right\}^{a-i}$$

$$=\frac{a!}{(a-i)!\,i!}(p_1p_2)^i(1-p_1p_2)^{a-i}=\mathrm{b}(i;a,p_1p_2)$$

Theorem 2. If the input of a binomial transform with parameter p, δ is a random number with mean $\bar{a}$ and variance $\bar{\bar{a}}$, then the output in time δ is a random number with mean $\bar{i}$ and variance $\bar{\bar{i}}$:

$$\bar{i}=\bar{a}p \tag{2}$$

$$\bar{\bar{i}}=\bar{a}p(1-p)+\bar{\bar{a}}p^2 \tag{3}$$

and there exists no output at any other time.

Proof: $\bar{i}=\sum_i ip(i)=\sum_a p(a)\sum_i i\,\mathrm{b}(i;a,p)$

$$=\sum_a ap(a)\cdot p=\bar{a}p$$

$$\bar{\bar{i}}=\sum_i p(i)(i-\bar{i})^2=\sum_i p(i)(i-\bar{a}p)^2$$

$$=\sum_{a,i} p(a)\,\mathrm{b}(i;a,p)(i-\bar{a}p)^2$$

$$=\sum_a p(a)\sum_i \mathrm{b}(i;a,p)\{(i-ap)^2$$

$$+2(i-ap)(ap-\bar{a}p)+(ap-\bar{a}p)^2\}$$

$$=\sum_a p(a)\{ap(1-p)+p^2(a-\bar{a})^2\}$$

$$=\bar{a}p(1-p)+\bar{\bar{a}}p^2$$

Example 2. If the input is a Poisson distribution with parameter λ, then the output in time δ is a Poisson distribution with parameter $p\lambda$ from Ex. 1, which may be shown by theorem 2: $\bar{i}=\bar{a}p$, $\bar{\bar{i}}=\bar{a}p(1-\bar{a}p)+p^2=\bar{i}$.

Example 3. If the input is a binomial distribution $\mathrm{b}(a;N,p_0)$, then the output in time δ is a binomial distribution: $\mathrm{b}(i;N,p_0p)$ from theorem 1, which may be shown by theorem 2:

$$\bar{i}=\bar{i}p=Np_0p,$$

$$\bar{\bar{i}}=\bar{a}p(1-p)+\bar{\bar{a}}p^2=Np_0p(1-p)$$

$$+Np_0(1-p_0)p^2=Np_0p(1-p_0p).$$

Theorem 3. The covariance $C(\boldsymbol{a},\boldsymbol{i})$ between input distribution $\boldsymbol{a}$ and output distribution $\boldsymbol{i}$ of a binomial transform with parameter p, δ is

$$C(\boldsymbol{a}\,\boldsymbol{i})=p\bar{\bar{a}} \tag{4}$$

Proof:

$$C(\boldsymbol{a}\,\boldsymbol{i})=\sum_{a,i} p(ai)(a-\bar{a})(i-\bar{i})$$

$$=\sum_{a,i} p(a)p_a(i)(a-\bar{a})(i-\bar{i})\,※$$

$$p_a(i)=\mathrm{b}(i;a,p)$$

$$※=\sum_a p(a)(a-\bar{a})\sum_i \mathrm{b}(i;a,p)(i-\bar{a}p)$$

$$=\sum_a p(a)(a-\bar{a})(\bar{i}_a-\bar{a}p)$$

$$\bar{i}_a=ap$$

$$\therefore\quad ※=\sum_a p(a)(a-\bar{a})(ap-\bar{a}p)$$

$$=p\sum p(a)(a-\bar{a})^2$$

$$=p\bar{\bar{a}}.$$

Theorem 4. If there is covariance $C(\boldsymbol{i}\,\boldsymbol{j})$ between input distribution $\boldsymbol{i}$, $\boldsymbol{j}$ of two binomial probabilistic transform with parameter p_1, δ; p_2, δ, then the covariance $C(\boldsymbol{i}'\,\boldsymbol{j}')$ between the outputs $\boldsymbol{i}'$, $\boldsymbol{j}'$ is

$$C(\boldsymbol{i}'\,\boldsymbol{j}')=p_1p_2\,C(\boldsymbol{i}\,\boldsymbol{j}) \tag{5}$$

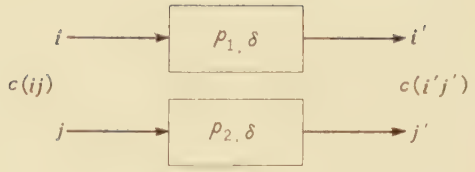

Fig. 3—A probabilistic transform of covariance.

Proof:

$$C(\boldsymbol{i}\,\boldsymbol{j}) = \sum_{i,j} p(ij)\,(i-\bar{i})\,(j-\bar{j})$$

$$C(\boldsymbol{i}'\,\boldsymbol{j}') = \sum_{i',j'} p(i'j')\,(i'-\bar{i}')\,(j'-\bar{j}')$$

$$p(i'j') = \sum_{i,j} p(i)p_i(i')p_j(j)p_j(j')$$

$$= \sum_{i,j} p_i(i')p_j(j')p(ij)$$

$$C(\boldsymbol{i}'\boldsymbol{j}') = \sum_{i,j}\sum_{i',j'} p_i(i')p_j(j')p(ij)(i'-\bar{i}')(j-\bar{j}')$$

$$\sum_{i'} p_i(i')(i'-\bar{i}') = \bar{i}'_i - \bar{i}' = p_1(i-\bar{i})$$

$$p_i(i') = b(i'; i, p_1) \qquad \bar{i}'_i = ip_1,\ \bar{i}' = \bar{i}p_1$$

$$C(\boldsymbol{i}'\boldsymbol{j}') = p_1p_2\sum_{ij} p(ij)(i-\bar{i})(j-\bar{j})$$

$$= p_1p_2\,C(\boldsymbol{i}\,\boldsymbol{j}).$$

Definition 2. A probabilistic branch transforms input for two or more directions as follows: (Fig. 4)

$$p(i_\nu) = p(a)\mathrm{b}(i_\nu; a, p_\nu),\ \nu = 1, 2, \cdots\cdots, n.$$

$$i_1 + i_2 + \cdots\cdots + i_n = a.$$

Theorem 5. If the input distribution $\boldsymbol{a}$, branches off two binomial probabilistic transforms with parameter $p_1, \delta; p_2, \delta$, then the covariance $C(\boldsymbol{i}_1, \boldsymbol{i}_2)$ between the output distributions $\boldsymbol{i}_1, \boldsymbol{i}_2$ is

$$C(\boldsymbol{i}_1, \boldsymbol{i}_2) = p_1p_2(\bar{\boldsymbol{a}} - \bar{a}) \tag{6}$$

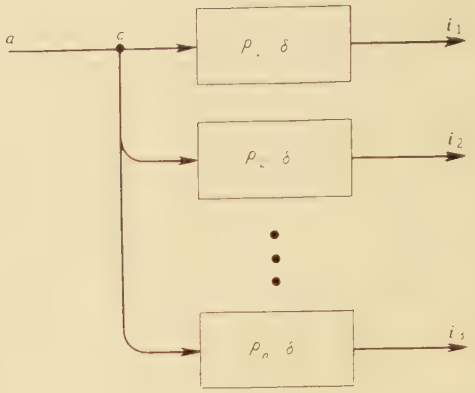

Fig. 4—A probabilistic branch c.

Proof: From the definition of probabilistic branch,

$$i_1 + i_2 = a$$

$$p_1 + p_2 = 1$$

$$G(\boldsymbol{i}_1\boldsymbol{i}_2) = \sum_a \sum_{i_1,i_2} p(a)\mathrm{b}(i_1; a, p_1)(i_1-\bar{i}_1)(i_2-\bar{i}_2)$$

$$= \sum_a \sum_{i_1} p(a)\mathrm{b}(i_1; a, p_1)(i_1-p_1\bar{a})(a-i_1-p_2\bar{a})$$

$$= \sum_a p(a) \sum_{i_1} \mathrm{b}(i_1; a, p_1)\{(i_1-ap_1)+p_1(a-\bar{a})\}$$

$$\{-(i_1-ap_1)+p_2(a-\bar{a})\} \quad ※$$

$$\sum_{i_1} \mathrm{b}(i_1; a, p_1)(i_1-ap_1)^2 = ap_1(1-p_1) = ap_1p_2$$

$$\sum_{i_1} \mathrm{b}(i_1; a, p_1)(i_1-ap_1) = 0$$

$$※ = \sum_a p(a)\{-ap_1(1-p_1)+p_1p_2(a-\bar{a})^2\}$$

$$= -\bar{a}p_1p_2 + \bar{\boldsymbol{a}}p_1p_2 = (\bar{\boldsymbol{a}}-\bar{a})p_1p_2.$$

Corollary 1. If input distribution $\boldsymbol{a}$, branches off two binomial probabilistic transforms with parameter $p_1, \delta; p_2, \delta$, then the covariance $C(\boldsymbol{a}\,\boldsymbol{i})$ between the input distribution $\boldsymbol{a}$ and output distributions $\boldsymbol{i}_1$, $\boldsymbol{i}_2$ is (Fig. 4)

$$\left.\begin{aligned} C(\boldsymbol{a}\,\boldsymbol{i}_1) &= p_1\bar{\boldsymbol{a}} \quad , \\ C(\boldsymbol{a}\,\boldsymbol{i}_2) &= p_2\bar{\boldsymbol{a}} \quad . \end{aligned}\right\} \tag{7}$$

Proof:

$$C(\boldsymbol{a}\,\boldsymbol{i}') = \sum_{a}\sum_{i'} p(ai')(i'-\bar{i}')(a-\bar{a})$$

$$= \sum_{a}\sum_{i'} p(a)\mathrm{b}(i';a,p_1)(i'-\bar{i}')(a-\bar{a})$$

$$= \sum_{a} p(a)(a-\bar{a}) \sum_{i'} \mathrm{b}(i';a,p_1)(i'-\bar{a}p_1)$$

$$= p_1 \sum_{a} p(a)(a-\bar{a})^2$$

$$= p_1\bar{\boldsymbol{a}}$$

Corollary 2. If the input distribution $\boldsymbol{a}$, branches off for two or more binomial probabilistic transforms with parameter $p_\nu, \delta_\nu, \nu = 1, 2, \cdots\cdots, n$, then the covariance $C(\boldsymbol{i}_k\,\boldsymbol{i}_l)$ between any two output distributions $\boldsymbol{i}_k, \boldsymbol{i}_l, k, l = 1, \cdots\cdots, n$ is (Fig. 4)

$$C(\boldsymbol{i}_k\,\boldsymbol{i}_l) = p_k\,p_l(\bar{\boldsymbol{a}}-\bar{a}). \tag{8}$$

Proof: From theorem 1, the circuit of Fig. 4 is equivalent to the circuit of Fig. 5 concerning to $p_1, p_2, \delta_1+\delta_2=\delta$. Therefore, from theorem 4 regarding to corollary 1, theorem 3,

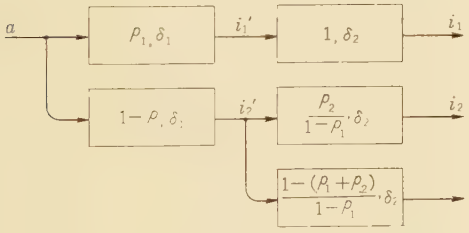

Fig. 5—An equivalent probabilistic transform with Fig. 4 concerning to i_1, i_2.

$$C(\boldsymbol{i}_1\,\boldsymbol{i}_2) = \frac{p_2}{1-p_1}\,C(\boldsymbol{i}_1'\,\boldsymbol{i}_2')$$

and from theorem 5,

$$C(\boldsymbol{i}_1'\,\boldsymbol{i}_2') = p_1(1-p_1)(\bar{\boldsymbol{a}}-\bar{a})$$

$$\therefore\quad C(\boldsymbol{i}_1\,\boldsymbol{i}_2) = p_1p_2(\bar{\boldsymbol{a}}-\bar{a})$$

Definition 3. A distribution adder is a convolutional system of which the output is the sum of the input distributions $\boldsymbol{X}, \cdots\cdots, \boldsymbol{Y}$: $\boldsymbol{X}\otimes\cdots\cdots\otimes\boldsymbol{Y}=\boldsymbol{Z}$ and there exists no time lag in add operation. In symbol, we will show this element as in Fig. 6.

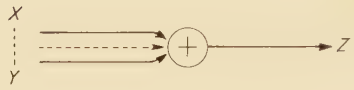

Fig. 6—A distribution adder.

Theorem 6. A parallel circuit of binomial probabilistic transforms with parameter $p_i, \delta (i=1, 2)$ (Fig. 7 (a)), is equivalent to a binomial probabilistic circuit with parameter $\prod_{i=1}^{2} p_i, \delta$ (Fig. 7 (b)).

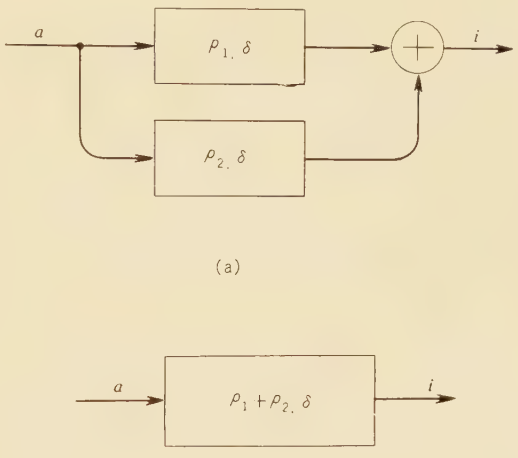

Fig. 7—A parallel binomial probabilistic circuit.

Proof: The proof is shown by the following:

$$\sum_{\nu+\mu=i} \mathrm{b}(\nu; a, p_1)\mathrm{b}\left(\mu; a-\nu, \frac{p_2}{1-p_1}\right)$$

$$=\mathrm{b}(i; a, p_1+p_2). \tag{9}$$

The left hand of Eq. (9) is,

$$\sum_{\nu+\mu=i} \mathrm{b}(\nu, \mu; a, p_1, p_2)$$

$$=\sum_{\nu+\mu=i} \frac{a!}{\nu!\,\mu!\,(a-\nu-\mu)!} p_1^{\nu} p_2^{\mu} (1-p_1-p_2)^{a-\nu-\mu},$$

substituting $\mu=i-\nu$, then

$$\sum_{\nu} \frac{a!}{\nu!(i-\nu)!\,(a-i)!} p_1^{\nu} p_2^{i-\nu} (1-p_1-p_2)^{a-i}$$

$$=\frac{a!}{(a-i)!\,i!}(1-p_1-p_2)^{a-i} \sum_{\nu} \frac{i!}{(i-\nu)!\,\nu!} p_1^{\nu} p_2^{i-\nu}$$

$$=\frac{a!}{(a-i)!\,i!}(p_1+p_2)^{i}(1-p_1-p_2)^{a-i}$$

$$=\mathrm{b}(i; a, p_1+p_2)$$

Theorem 7. If the input distribution $\boldsymbol{a}$, branches off for two binomial probabilistic circuits with parameter p_1, δ; $p_2, 2\delta$, and also, the output at time δ is transmitted to a binomial probabilistic circuit with parameter p_3, δ and the outputs ν, μ, of the two branching circuits are summarized. then the covariance $C(\boldsymbol{ij})$ between the output distribution at time δ and the output distribution at time 2δ is, (Fig. 8)

Fig. 8—A series-parallel binomial probabilistic circuit.

$$C(\boldsymbol{ij})=C(\boldsymbol{i\mu})+C(\boldsymbol{i\nu}) \tag{10}$$

Proof:

$$p(ij)=\sum_{\nu+\mu=j} p(i; \nu, \mu)$$

$$=\sum_{\nu+\mu=j} \mathrm{b}(\nu; i, p_3)\,\mathrm{b}(i, \mu; a, p_1, p_2)$$

$$\mathrm{b}(i, \mu; a, p_1, p_2)=\mathrm{b}(i; a, p_1)\,\mathrm{b}\left(\mu; a-i, \frac{p_2}{1-p_1}\right)$$

$$=\frac{a!}{i!\,\mu!\,(a-i-\mu)!} p_1^{i} p_2^{\mu} (1-p_1-p_2)^{a-i-\mu}$$

$$C(\boldsymbol{ij})=\sum_{ij} p(ij)(i-\bar{i})(j-\bar{j})$$

$$=\sum_{i\nu\mu} (i-\bar{i})(\nu+\mu-\bar{\nu}+\bar{\mu})p(i, \nu, \mu)$$

$$=\sum_{i\nu\mu} (i-\bar{i})(\nu-\bar{\nu})p(i, \nu, \mu)$$

$$+\sum_{i\nu\mu} (i-\bar{i})(\mu-\bar{\mu})p(i, \nu, \mu)$$

$$=\sum_{i\nu\mu} (i-\bar{i})(\nu-\bar{\nu})\mathrm{b}(\nu; i, p_3)\mathrm{b}(i, \mu; a, p_1, p_2)$$

$$+\sum_{i\mu} (i-\bar{i})(\mu-\bar{\mu})p(i, \mu; a, p_1, p_2)$$

$$=\sum_{i\nu} (i-\bar{i})(\nu-\bar{\nu})\mathrm{b}(\nu; i, p_3)\mathrm{b}(i; a, p_1)+C(\boldsymbol{i\mu})$$

$$=\sum_{i} (i-\bar{i})\mathrm{b}(i; a, p_1)(ip_3-\bar{i}p_3)+C(\boldsymbol{i\mu})$$

$$=p_3\sum_{i} (i-\bar{i})^2\mathrm{b}(i; a, p_1)+C(\boldsymbol{i\mu})$$

$$=p_3\bar{i}+C(\boldsymbol{i\mu})=C(\boldsymbol{i\nu})+C(\boldsymbol{i\mu})$$

2. Binomial Probabilistic Sequential Circuits. I (Constant Difference Discrete System)

In this section, first, we construct three types of discrete probabilistic sequential circuit

with a constant time difference δ: a stationary system, a quasi-stationary system and a non-stationary system, from the three circuit elements which we have defined in Section 1. It is a synchronous circuit and there exists a constant time interval δ among input distributions $\boldsymbol{a}_i, \boldsymbol{a}_{i+1}$ and output distributions $\boldsymbol{f}_i$, $\boldsymbol{f}_{i+1}, i=0, 1, \cdots\cdots$. Second, we show the properties of binomial probabilistic sequential circuit in the theorems concerning the output distributions (mean, variance, covariance, additive process and limit distribution) provided that the input distribution is a Bernoulli's sequence. We state also the output of the system is a recurrence type Markoff process and extract the transition probability matrix. Finally, we note the estimation of circuit parameter.

We will discuss the non-constant difference discrete system in Section 3 and the continuous system in Section 4.

2.1. Circuit Construction

2.1.1. Stationary System

In the stationary system, the input in time $t=0$ be a_0 and there exist no inputs, then the output distribution $\boldsymbol{f}_n$ in time $n\delta$ is given by the sum of the output distributions $\boldsymbol{f}_n{}^{*(i)}$ of the conditional probabilistic transform:

$$\boldsymbol{f}_n = \boldsymbol{f}_n{}^* \otimes \boldsymbol{f}_n{}^{**} \otimes \cdots\cdots \otimes \boldsymbol{f}_n{}^{*(n)}$$

$$\boldsymbol{f}_n{}^* = \mathrm{b}(j_1; \nu, p_1)$$

$$\boldsymbol{f}_n{}^{**} = \mathrm{b}\left(j_2; \mu, \frac{p_2}{1-F_1}\right)$$

$$\vdots$$

$$\boldsymbol{f}_n{}^{*(n)} = \mathrm{b}\left(j_n; \xi, \frac{p_n}{1-F_{n-1}}\right)$$

$$\nu + \mu + \cdots\cdots + \xi = a_0$$

$$j_1 + j_2 + \cdots\cdots + j_n = j$$

where

$$F_k = p_1 + p_2 + \cdots\cdots + p_k \qquad k=0, 1, \cdots\cdots, n.$$

The probablistic circuit can be represented as shown in Fig. 9. In this circuit every probabilistic transform has the same constant time delay. Regarding Theorem 1 and 6, we may reconstruct this circuit as shown in Fig. 10, of which all the time lags are integral multiples of a common value δ. Where $(p_1, p_2, \cdots\cdots, p_n)$ is a circuit parameter or a group of probabilistic transforms by which the system is represented.

2.1.2. Quasi-Stationary System

In the quasi-stationary system, the group of probabilistic transforms varies with the in-

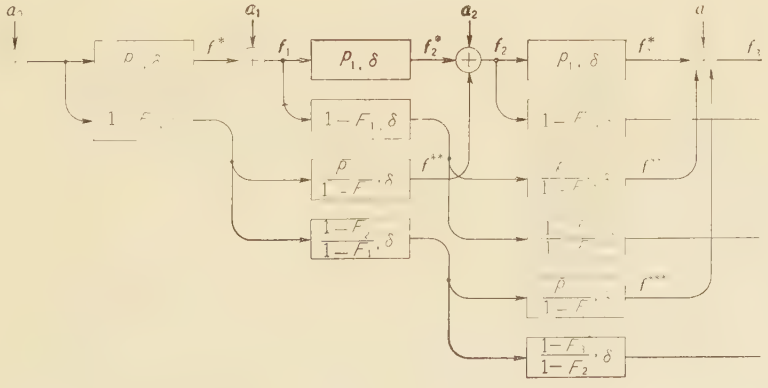

Fig. 9—Constant difference discrete binomial probabilistic circuit. Stationary system.

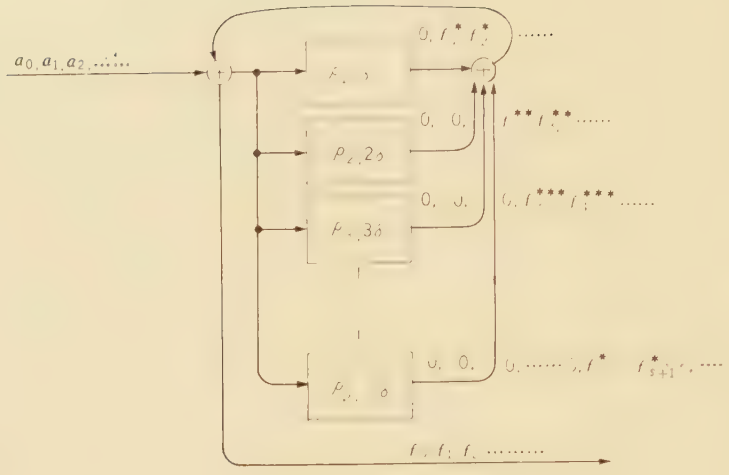

Fig. 10—Constant difference binomial probabilistic sequential circuit. Stationary system.

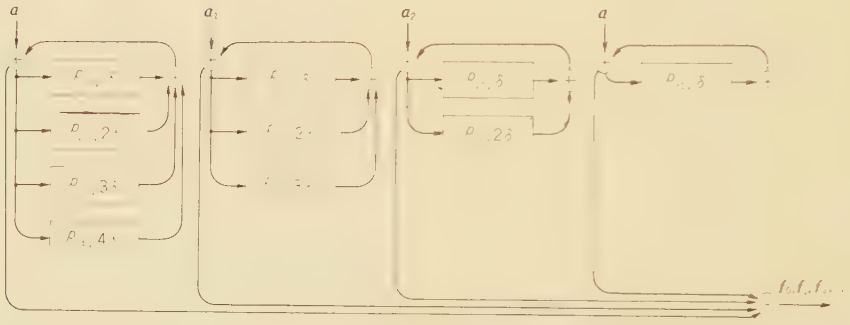

Fig. 11—Constant difference binomial probabilistic sequential circuit. Quasi-stationary system.

put a_i in time $i\delta$, $i=0, 1, \cdots\cdots$. Therefore the quasi-stationary circuit may be constructed of n stationary circuits such as shown in Fig. 11.

2.1.3. Non-Stationary System

In the non-stationary system, there exists no group of probabilistic transforms as stated above. The output distribution f_n in time $n\delta$ for input a_0 is given by the sum of the output distributions $f_n^{*(i)}$ of conditional probabilistic transform:

$$f_n = f_n^* \otimes f_n^{**} \otimes \cdots\cdots \otimes f_n^{*(n)}$$

$$f_n^* = \mathrm{b}(j_1; \nu, p_{n-1,1})$$

$$f_n^{**} = \mathrm{b}\left(j_2; \mu, \frac{p_{n-2,2}}{1-F_{n-2,2}}\right)$$

$$\vdots$$

$$f_n^{*(n)} = \mathrm{b}\left(j_n; \xi, \frac{p_{0,n}}{1-F_{0,n-1}}\right)$$

$$\nu+\mu+\cdots\cdots+\xi=a_0$$

$$j_1+j_2+\cdots\cdots+j_n=j$$

where

$$F_{l,k}=p_{l,1}+p_{l,2}+\cdots\cdots+p_{l,k},\ l, k=0, 1, \cdots\cdots, n.$$

Non-stationary systems can be represented by a probabilistic circuit as shown in Fig. 12 (a), but regarding Theorem 1 and 6, they may be reconstructed like Fig. 12 (b). Where

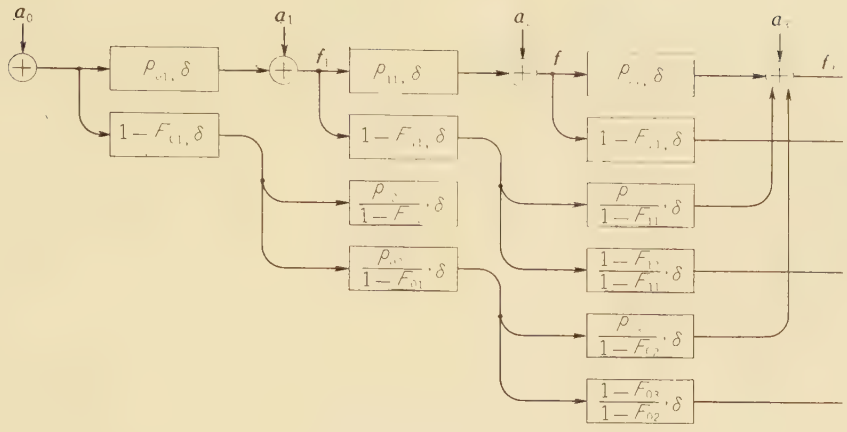

Fig. 12 (a)—Constant difference discrete binomial probabilistic circuit. Non-stationary system.

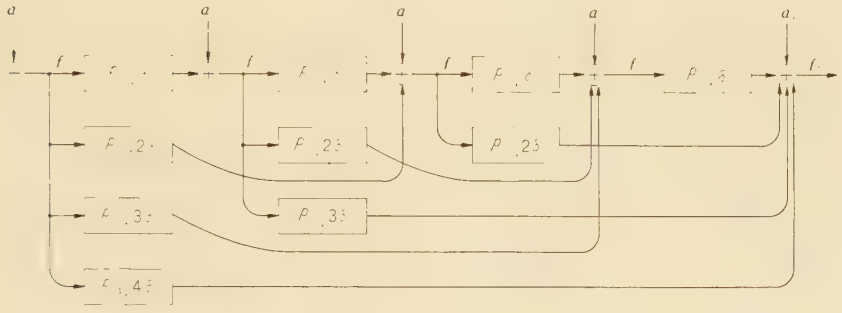

Fig. 12 (b)—Constant difference binomial probabilistic sequential circuit. Non-stationary system.

$(p_{01}, p_{02}, \cdots\cdots, p_{0n}; p_{11}, p_{12}, \cdots\cdots, p_{1,n-1}; \cdots\cdots; \cdots\cdots; p_{n-1,1})$ is a circuit parameter but there exist no group in such a parameter. There is only one difference between the stationary, the quasi-stationary and the non-stationary systems; that is a difference in connection.

2.2. Output Distribution

2.2.1. Stationary System

Theorem 8. If an input a_0 is transmitted into a discrete stationary circuit with parameter $(p_1, p_2, \cdots\cdots, p_n)$, then the output distribution $\boldsymbol{f}_n$ in time $n\delta$ is a binomial distribution:

$$\boldsymbol{f}_n = \mathrm{b}(i; a_0, D_n). \tag{11}$$

where

$$D_n = \begin{vmatrix} p_1 & p_2 & \cdots\cdots & p_n \\ -1 & p_1 & p_2 & \cdots\cdots & p_{n-1} \\ & -1 & p_1 & p_2 & \cdots\cdots & p_{n-2} \\ & & \cdots\cdots & & & \\ & & & -1 & p_1 & p_2 \\ & & & & -1 & p_1 \end{vmatrix} \tag{12}$$

which is the circuit operator.

Proof:

i $n=1$, $\boldsymbol{f}_1=\boldsymbol{f}_1^*=\mathrm{b}(j; a_0, p_1)=\mathrm{b}(j; a_0, D_1)$

ii $n=2$, $\boldsymbol{f}_2=\boldsymbol{f}_2^* \otimes \boldsymbol{f}_2^{**}$

Regarding Theorem 1, and 6,

$$\boldsymbol{f}_2=\mathrm{b}(i; a_0, p_1^2+p_2)=\mathrm{b}(i; a_0, D_2)$$

iii $n=3$, $\boldsymbol{f}_3=\boldsymbol{f}_3^* \otimes \boldsymbol{f}_3^{**} \otimes \boldsymbol{f}_3^{***}$

$$\boldsymbol{f}_3^*=\mathrm{b}(j; a_0, p_1 D_2)$$

$$\boldsymbol{f}_3^{**}=\mathrm{b}(k; a_0, p_2 D_1)$$

$$\boldsymbol{f}_3^{***}=\mathrm{b}(l; a_0, p_3)$$

$$\boldsymbol{f}_3=\sum_{i=j+k+l} \mathrm{b}(j; a_0, p_1 D_2)\cdot \mathrm{b}(k; a_0, p_1 D_1)\cdot \mathrm{b}(l; a_0, p_3)$$

From Theorem 6,

$$\boldsymbol{f}_3=\mathrm{b}(i; a_0, p_1 D_2+p_2 D_1+p_3)$$
$$=\mathrm{b}(i; a_0, D_3)$$

iv In general,

$$\boldsymbol{f}_n=\mathrm{b}(i; a_0, p_1 D_{n-1}+p_2 D_{n-2}+\cdots\cdots+p_n)$$
$$=\mathrm{b}(i; a_0, D_n).$$

For example,

$$\bar{f}_3=\bar{f}_3^*+\bar{f}_3^{**}+\bar{f}_3^{***}$$
$$=a_0(p_1 D_2+p_2 D_1+p_3)=a_0 D_3$$
$$\bar{f}_3=\bar{f}_3^*+\bar{f}_3^{**}+\bar{f}_3^{***}+2C(\boldsymbol{f}_3^*\boldsymbol{f}_3^{**})$$
$$+2C(\boldsymbol{f}_3^*\boldsymbol{f}_3^{***})+2C(\boldsymbol{f}_3^{**}\boldsymbol{f}_3^{***})$$

From Theorem 5,

$$C\boldsymbol{f}_3^*\boldsymbol{f}_3^{**})=-a_0 p_1 p_2 D_1 D_2$$

$$C(\boldsymbol{f}_3^*\boldsymbol{f}_3^{***})=-a_0 p_1 D_2 p_3$$

$$C(\boldsymbol{f}_3^{**}\boldsymbol{f}_3^{***})=-a_0 p_1 p_2 p_3$$

hence,

$$\bar{f}_3=a_0 p_1 D_2(1-p_1 D_2)+a_0 p_2 D_1(1-p_2 D_1)$$
$$+a_0 p_3(1-p_3)-a_0 2 p_1 p_2 D_1 D_2-a_0 2 p_1 D_2 p_3$$
$$-a_0 2 p_1 p_2 p_3$$
$$=a_0(p_1 D_2+p_2 D_1+p_3)(1-p_1 D_2-p_2 D_1-p_3)$$
$$=a_0 D_3(1-D_3)$$

Theorem 9. If the input distributions $(\boldsymbol{a}_0, \boldsymbol{a}_1, \boldsymbol{a}_2, \cdots\cdots, \boldsymbol{a}_n)$ of a discrete stationary circuit with parameter $(p_1, p_2, \cdots\cdots, p_n)$ is a Bernoulli's sequence, then the mean $\bar{f}_n$ and the variance $\bar{f}_n$ of the output distribution $\boldsymbol{f}_n$ in time $n\delta$ are,

$$\bar{f}_n=\sum_{i=0}^{n} \bar{a}_i D_{n-i}, \tag{13}$$

$$= \begin{matrix} \bar{a}_0 & \bar{a}_1 & \cdots\cdots\cdots & \bar{a}_n \\ -1 & p_1 & p_2 \cdots\cdots\cdots & p_n \\ & -1 & p_1 & p_2 \cdots\cdots\cdots p_{n-1} \\ & & \cdots\cdots\cdots\cdots & \\ & & & -1 \quad p_1 \quad p_2 \\ & & & \quad -1 \quad p_1 \end{matrix} \tag{14}$$

$$\bar{f}_n=\sum_{i=0}^{n} \bar{a}_i D_{n-i}(1-D_{n-1i})+\sum_{i=0}^{n} \bar{a}_i D^2_{n-i} \tag{15}$$

Proof: $\boldsymbol{a}_i$, $i=0, 1, \cdots\cdots$ are independent, so $\boldsymbol{f}_n$ is given by independent sum of $n+1$ output distributions in time $n\delta$ for input $\boldsymbol{a}_i$, $i=0, 1, \cdots\cdots$. From Theorem 8, the circuit operators in time $\delta, 2\delta, 3\delta, \cdots\cdots$ are $D_1, D_2, D_3, \cdots\cdots$, therefore, from Theorem 2, it can be formulated by Eq, (13), and Eq. (15).

2.2.2. Quasi-Stationary System

Theorem 10. If the input distributions $(\boldsymbol{a}_0, \boldsymbol{a}_1, \boldsymbol{a}_2, \cdots\cdots, \boldsymbol{a}_n)$ of a discrete quasi-stationary circuit with pararmeter $(p_{01}, p_{02}, \cdots\cdots, p_{0n}; p_{1.n-1}, p_{1.n-2}, \cdots\cdots, p_{11}; \cdots\cdots; p_{n-1.1})$ is a Bernoulli's sequence, then the mean $\bar{f}_n$ and the vari-

ance $\bar{\bar{f}}_n$ of the output distributions $\boldsymbol{f}_n$ in time $n\delta$ are,

$$\bar{f}_n = \sum_{i=0}^{n} \bar{a}_i D_{i.n-i} \tag{16}$$

$$\bar{\bar{f}}_n = \sum_{i=0}^{n} \bar{a}_i D_{i.n-i}(1-D_{i.n-i}) + \sum_{i=0}^{n} \bar{\bar{a}}_i D^2_{i.n-i} \tag{17}$$

where

$$\begin{aligned} D_{i.n-i} = {} & p_{i.1}\ p_{i.2} \cdots\cdots\cdots\cdots p_{i.n-i} \\ & -1\ p_{i.1}\ p_{i.2} \cdots\cdots\cdots\cdots p_{i.n-i-1} \\ & \quad -1\ p_{i.1}\ p_{i.2} \cdots\cdots\cdots p_{i.n-i-2} \\ & \cdots\cdots\cdots\cdots\cdots\cdots\cdots\cdots \\ & \qquad -1\ p_{i.1}\ p_{i.2} \\ & \qquad\quad -1\ p_{i.1} \end{aligned} \tag{18}$$

Proof: From Theorem 8, a component of $\boldsymbol{f}_n$ for a_i is $\mathrm{b}(i; a_i, D_{0.n-i})$, and $a_i, i=0, 1, \cdots\cdots$ are independent, so $\boldsymbol{f}_n$ is given by independent sum of $n+1$ binomial distributions, therefore, from Theorem 2, we get Theorem 10.

2.2.3. Non-Stationary System

Theorem 11. If an input a_0 is transmitted into a discrete non-stationary circuit with parameter $(p_{01}, p_{02}, \cdots\cdots, p_{0n}; p_{11}, p_{12}, \cdots\cdots, p_{1.n-1}; \cdots\cdots; \cdots\cdots; p_{n-1.1})$, then the output distribution $\boldsymbol{f}_n$ in time $n\delta$ is a binomial distributions:

$$\boldsymbol{f}_n = \mathrm{b}(i; a_0, D_{0.n}) \tag{19}$$

where

$$\begin{aligned} D_{0.n} = {} & p_{01}\ p_{02} \cdots\cdots\cdots\cdots p_{0n} \\ & -1\ p_{11}\ p_{12} \cdots\cdots\cdots\cdots p_{1.n-1} \\ & \quad -1\ p_{2.1}\ p_{2.2} \cdots\cdots\cdots p_{2.n-2} \\ & \cdots\cdots\cdots\cdots\cdots\cdots\cdots\cdots \\ & \qquad -1\ p_{n-2.1}\ p_{n-2.2} \\ & \qquad\quad -1\ p_{n-1.1} \end{aligned} \tag{20}$$

which is the circuit operator.

Proof:

i) $n=1, \quad \boldsymbol{f}_1 = \boldsymbol{f}_1{}^* = \mathrm{b}(i; a_0, p_{01}) = \mathrm{b}(i; a_0, D_{01})$

ii) $\boldsymbol{f}_n = \boldsymbol{f}_n{}^* \otimes \boldsymbol{f}_n{}^{**} \otimes \cdots\cdots \otimes \boldsymbol{f}_n{}^{*(n)}$

$\boldsymbol{f}_n{}^* = \mathrm{b}(j; a_0, p_{n-1.1} D_{0.n-1})$

$\boldsymbol{f}_n{}^{**} = \mathrm{b}(k; a_0, p_{n-2.2} D_{0.n-2})$

$\vdots$

$\boldsymbol{f}_n{}^{*(n)} = \mathrm{b}(l; a_0, p_{0n})$

$$\boldsymbol{f}_n = \sum_{i=j+k+\cdots+l} \mathrm{b}(j; a_0, p_{n-1.1} \mathrm{D}_{0.n-1})\ \mathrm{b}(k; a_0, p_{n-2.2} \mathrm{D}_{0.n-2}) \cdots\cdots \mathrm{b}(l; a_0, p_{0n})$$

From Theorem 6,

$$\boldsymbol{f}_n = \mathrm{b}(i; a_0, p_{n-1.1} \mathrm{D}_{0.n-1} + p_{n-2.2} \mathrm{D}_{0.n-2} + \cdots\cdots + p_{0.n}).$$

$$\therefore \quad \boldsymbol{f}_n = \mathrm{b}(i; a_0, \mathrm{D}_{0.n})$$

Theorem 12. If the input distributions $(\boldsymbol{a}_0, \boldsymbol{a}_1, \cdots\cdots, \boldsymbol{a}_n)$ of a discrete non-stationary circuit with parameter $(p_{01}, p_{02}, \cdots\cdots, p_{0n}; p_{11}, p_{12}, \cdots\cdots, p_{1.n-1}; \cdots\cdots; p_{n-1.1})$ is a Bernoulli's sequence, then the mean $\bar{f}_n$ and the variance $\bar{\bar{f}}_n$ of the output distribution $\boldsymbol{f}_n$ in time $n\delta$ are,

$$\bar{f}_n = \sum_{i=0}^{n} \bar{a}_i \mathrm{D}_{i.n-i} \tag{21}$$

$$\begin{aligned} = {} & \bar{a}_0\ \bar{a}_1 \cdots\cdots\cdots\cdots \bar{a}_n \\ & -1\ p_{01}\ p_{02} \cdots\cdots\cdots\cdots p_{0n} \\ & \quad -1\ p_{11}\ p_{12} \cdots\cdots\cdots p_{1.n-1} \\ & \cdots\cdots\cdots\cdots\cdots\cdots\cdots\cdots \\ & \qquad -1\ p_{n-2.1}\ p_{n-2.2} \\ & \qquad\quad -1\ p_{n-1.1} \end{aligned} \tag{21'}$$

$$\bar{\bar{f}}_n = \bar{\bar{f}}_n + \sum_{i=0}^{n} (\bar{\bar{a}}_i - \bar{a}_i) \mathrm{D}^2_{i.n-i}$$

$$\bar{f}_n = \sum_{i=0}^{n} \bar{a}_i D_{i\cdot n-i}(1 - D_{i\cdot n-i}) + \sum_{i=0}^{n} \bar{\bar{a}}_i D^2_{i\cdot n-i} \tag{22}$$

$$D_{i\cdot n-i} = \begin{vmatrix} p_{i\cdot 1} & p_{i\cdot 2} & \cdots\cdots & p_{i\cdot n-i} \\ -1 & p_{i+1\cdot 1} & p_{i+1\cdot 2} & \cdots\cdots & p_{i+1\cdot n-i-1} \\ & -1 & p_{i+2\cdot 1} & p_{i+2\cdot 2} & p_{i+1\cdot n-i-2} \\ & & \cdots\cdots & & \\ & & -1 & p_{n-2\cdot 1} & p_{n-2\cdot 2} \\ & & & -1 & p_{n-1\cdot 1} \end{vmatrix} \tag{23}$$

Proof: $\boldsymbol{a}_i$, $i=0, 1, \cdots\cdots$ are independent, so from Theorem 11, and Theorem 2, we get Theorem 12.

2.3. Examples

2.3.1. Binomial Distribution Input Sequence

If the input sequence is a binomial distribution sequence: $\boldsymbol{a}_i = b(j; U_i, \eta_i)$, $i=0, 1, 2, \cdots\cdots$, then the mean $\bar{f}_n$ and variance $\bar{\bar{f}}_n$ of the output distribution $\boldsymbol{f}_n$ are,

$$\bar{f}_n = \sum_{i=0}^{n} U_i \eta_i D_{i\cdot n-i} \tag{24}$$

$$\bar{\bar{f}}_n = \bar{f}_n - \sum_{i=0}^{n} U_i (\eta_i D_{i\cdot n-i})^2 \tag{25}$$

where $D_{i\cdot n-i}$ is Eq. (12) in a stationary system, Eq. (18) in a quasi-stationary system and Eq. (23) in a non-stationary system, will hereafter be in conformity with this notation.

2.3.2. Poisson Distributions Input Sequence

If the input sequence is a Poisson distributions sequence: $\boldsymbol{a}_i = e^{-\lambda_i} \lambda_i^j / j!$, $i=0, 1, \cdots\cdots, n$, then the mean $\bar{f}_n$ and the variance $\bar{\bar{f}}_n$ of the output distribution $\boldsymbol{f}_n$ are,

$$\bar{f}_n = \bar{\bar{f}}_n = \sum_{i=0}^{n} \lambda_i D_{i\cdot n-i} \tag{26}$$

that is a Poisson distribution with parameter $\lambda_i D_{i\cdot n-i}$.

2.3.3. Polya-Eggenberger Distributions Input Sequence

If the input sequence is a Polya-Eggenberger distributions sequence: $\boldsymbol{a}_i = \lambda_i(\lambda_i+\rho_i)(\lambda_i+2\rho_i)\cdots\cdots(\lambda_i+(j-1)\rho_i)^{-\frac{\lambda_i}{\rho_i}-j}/j!$, $\lambda_i, \rho_{i+1} > 0$, $i=0, 1, 2, \cdots\cdots, n$, then the mean $\bar{f}_n$ and the variance $\bar{\bar{f}}_n$ of the output distribution $\boldsymbol{f}_n$ are,

$$\bar{f}_n = \sum_{i=0}^{n} \lambda_i D_{i\cdot n-i} \tag{27}$$

$$\bar{\bar{f}}_n = \bar{f}_n + \sum_{i=0}^{n} \lambda_i \rho_i D^2_{i\cdot n-i} \tag{28}$$

that is a Polya-Eggenberger distribution with parameter $\lambda_n = \bar{f}_n$, $\rho_n = \frac{\sum_{i=0}^{n} \lambda_i \rho_i D^2_{i\cdot n-i}}{\bar{f}_n}$.

2.3.4. Uniform Distributions Input Sequence

If the input sequence is a uniform distributions sequence:

$$\boldsymbol{a}_i = \begin{cases} \dfrac{1}{b_i - a_i}, & a_i \le j \le b_i \\ 0, & a_i < j, \ b_i < j. \end{cases}$$

$i=0, 1, 2, \cdots\cdots, n$,

then the mean $\bar{f}_n$ and the variance $\bar{\bar{f}}_n$ of the output distribution $\boldsymbol{f}_n$ are,

$$\bar{f}_n = \sum_{i=0}^{n} \frac{a_i + b_i}{2} D_{i\cdot n-i} \tag{29}$$

$$\bar{\bar{f}}_n = \bar{f}_n + \sum_{i=0}^{n} \left\{ \frac{(b_i - a_i)^2}{12} - \frac{a_i + b_i}{2} \right\} D^2_{i\cdot n-i} \tag{30}$$

2.3.5. Geometric Distributions Input Sequence

If the input sequence is a geometric distri-

butions sequence: $a_i=p_i(1-p_i)^{j-1}$, $i=0, 1, \cdots\cdots$, n, then the mean $\bar{f}_n$ and the variance $\bar{\bar{f}}_n$ of the output distribution f_n are,

$$\bar{f}_n=\sum_{i=0}^{n}\frac{1}{p_i}\,D_{i\cdot n-i} \tag{31}$$

$$\bar{\bar{f}}_n=\bar{f}_n+\sum_{i=0}^{n}\frac{1}{p_i}\left(\frac{1}{p_i}-2\right)D^2_{i\cdot n-i} \tag{32}$$

2.3.6. Pascal Distributions Input Sequence

If the input sequence is a Pascal distributions sequence: $a_i=\binom{k-1}{k-j_i}p_i^{j_i}(1-p_i)^{k-j_i}$, $k=j_i, j_{i+1}, j_{i+2}\cdots\cdots$, $i=0, 1, \cdots\cdots$, n, then the mean $\bar{f}_n$ and the variance $\bar{\bar{f}}_n$ of the output distribution f_n are,

$$\bar{f}_n=\sum_{i=0}^{n}\frac{j_i}{p_i}\,D_{i\cdot n-i} \tag{33}$$

$$\bar{\bar{f}}_n=\bar{f}_n+\sum_{i=0}^{n}\frac{j_i}{p_i}\left(\frac{1}{p_i}-2\right)D^2_{i\cdot n-i} \tag{34}$$

2.3.7. Hypergeometric Distributions Input Sequence

If the input sequence is a hypergeometric distributions sequence: $a_i=\binom{M_i}{j}\binom{N_i-M_i}{r_i-j}\Big/\binom{N_i}{r_i}$, $0\le j<\min(r_i, M_i)$, $i=0, 1, 2, \cdots\cdots$, n, then the mean $\bar{f}_n$ and the variance $\bar{\bar{f}}_n$ of the output distribution f_n are,

$$\bar{f}_n=\sum_{i=0}^{n}r_i\frac{M_i}{N_i}\,D_{i\cdot n-i} \tag{35}$$

$$\bar{\bar{f}}_n=\bar{f}_n+\sum_{i-0}^{n}r_i\frac{M_i}{N_i}\left\{\frac{r_i-1}{N_i-1}\left(\frac{M_i}{N_i}-1\right)-\frac{M_i}{N_i}\right\}D^2_{i\cdot n-i\cdot} \tag{36}$$

2.3.8. Exponential Distributions Input Sequence

If the input sequence is a exponential distributions sequence: $a_i=\lambda_i e^{-\lambda_i j}$, $i=0, 1, \cdots\cdots$, n, then the mean $\bar{f}_n$ and the variance $\bar{\bar{f}}_n$ of the output distribution f_n are,

$$\bar{f}_n=\sum_{i=0}^{n}\frac{D_{i\cdot n-i}}{\lambda_i} \tag{37}$$

$$\bar{\bar{f}}_n=\bar{f}_n+\sum_{i=0}^{n}\frac{1}{\lambda_i}\left(\frac{1}{\lambda_i}-1\right)D^2_{i\cdot n-i} \tag{38}$$

2.3.9. Gamma Distributions Input Sequence

If the input sequence is a gamma distributions sequence: $a_i=\frac{\beta_i^{\alpha_i}}{\Gamma(\alpha_i)}j^{\alpha_i-1}e^{-\beta_i j}$, $\alpha_i, \beta_i>0$, $i=0, 1, \cdots\cdots$, n, then the mean $\bar{f}_n$ and the variance $\bar{\bar{f}}_n$ of the output distribution f_n are,

$$\bar{f}_n=\sum_{i=0}^{n}\frac{\alpha_i}{\beta_i}D_{i\cdot n-i} \tag{39}$$

$$\bar{\bar{f}}_n=\bar{f}_n+\sum_{i=0}^{n}\frac{\alpha_i}{\beta_i}\left(\frac{1}{\beta_i}-1\right)D^2_{i\cdot n-i} \tag{40}$$

2.3.10. Generalized Poisson Distributions Input Sequence

If the input sequence is a generalized Poisson distributions sequence: $a_i=\int_0^\infty e^{-\lambda_i}\frac{\lambda_i^j}{j!}dp(\lambda_i)$, $i=0, 1, \cdots\cdots$, n, then the mean $\bar{f}_n$ and the variance $\bar{\bar{f}}_n$ of the output distribution f_n are,

$$\bar{f}_n=\sum_{i=0}^{n}\int_0^\infty \lambda_i\,dp\,(\lambda_i)\,D_{i\cdot n-i} \tag{41}$$

$$\bar{\bar{f}}_n=\bar{f}_n+\sum_{i=0}^{n}\int_0^\infty(\lambda_i-m)^2\,dp\,(\lambda_i)\,D^2_{i\cdot n-i} \tag{42}$$

2.4. Representation by Markoff Process

Let $\sum_{i=1}^{s}p_i=1$, $p_i=0$ $i>s$, then there exists in stationary system s possible states: state j for the realization of the probability transform in $(j-1)$ steps before $j=1, 2, \cdots\cdots s$, and we get the transition probability matrix $P^{(n\to n+1)}$ between (n) step and $(n+1)$ step, for example in the case where $s=4$, as follows:

$$
\mathrm{P}^{(0\to 1)}=\begin{vmatrix} p_1 & 1-F_1 & 0 & 0 \\ 0 & 0 & 0 & 0 \\ 0 & 0 & 0 & 0 \\ 0 & 0 & 0 & 0 \end{vmatrix}
$$

$$
\mathrm{P}^{(1\to 2)}=\begin{vmatrix} p_1 & 1-F_1 & 0 & 0 \\ \dfrac{p_2}{1-F_1} & 0 & \dfrac{1-F_2}{1-F_1} & 0 \\ 0 & 0 & 0 & 0 \\ 0 & 0 & 0 & 0 \end{vmatrix}
$$

$$
\mathrm{P}^{(2\to 3)}=\begin{vmatrix} p_1 & 1-F_1 & 0 & 0 \\ \dfrac{p_2}{1-F_1} & 0 & \dfrac{1-F_2}{1-F_1} & 0 \\ \dfrac{p_3}{1-F_2} & 0 & 0 & \dfrac{1-F_3}{1-F_2} \\ 0 & 0 & 0 & 0 \end{vmatrix}
$$

$$
\mathrm{P}^{(3\to 4)}=\mathrm{P}^{(4\to 5)}=\mathrm{P}^{(5\to 6)}=\cdots\cdots\cdots\cdots\equiv\mathrm{P}^{(1)}
$$

$$
=\begin{vmatrix} p_1 & 1-F_1 & 0 & 0 \\ \dfrac{p_2}{1-F_1} & 0 & \dfrac{1-F_2}{1-F_1} & 0 \\ \dfrac{p_3}{1-F_2} & 0 & 0 & \dfrac{1-F_3}{1-F_2} \\ 1 & 0 & 0 & 0 \end{vmatrix} \qquad (43)
$$

where element $\mathrm{P}_{ij}^{(1)}$ is a transition probability for one step from state i to state j. Thus, the transition probability matrix $\mathrm{P}^{(1)}$ is constituted after a certain period $0\leq n<s-1$ of composition, and also the transition state diagram is formed in the order of the progress

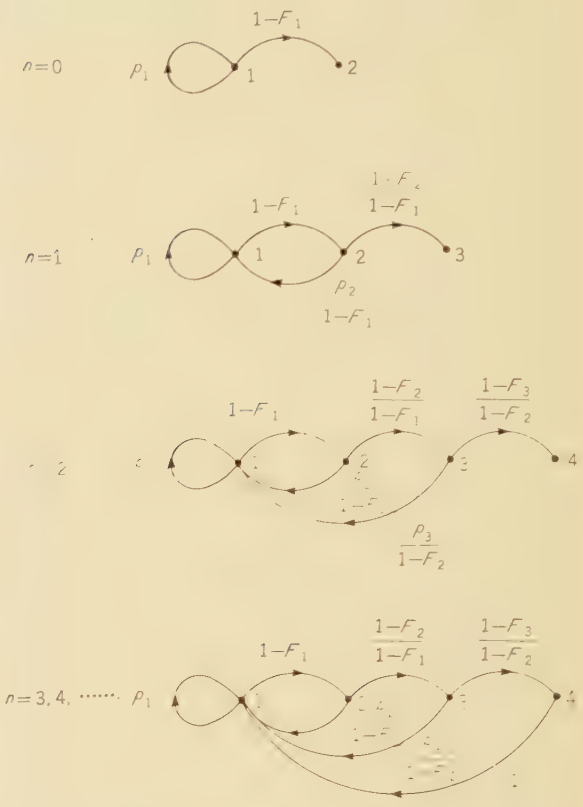

Fig. 13—Composition of transition state diagram $p^{(1)}$.

$1, 2, 3, \cdots\cdots, s$ as shown in Fig. 13, and perfected at $s-1$ th step. In this period of composition and near after, the output of stationary circuit shows transient phenomena.

If $n\geq s-1$, the transition probability $p_{ij}^{(2)}$ for 2 steps, $p_{ij}^{(k)}$ for k steps $k=2, 3, \cdots\cdots$, are given by $\mathrm{P}^{(2)}=\mathrm{P}^{(1)}\cdot\mathrm{P}^{(1)}$, $\mathrm{P}^{(k)}=\mathrm{P}^{(k-1)}\cdot\mathrm{P}^{(1)}$ as follows:

$$
\mathrm{P}^{(2)}=\begin{vmatrix} p_1 & p_2 \\ -1 & p_1 \end{vmatrix}\begin{vmatrix} (1-F_1)\ p_1 & (1-F_2) & 0 \\ (1-F_1)\ p_1(1) & 0 & (1-F_3)/1-F_1 \\ (1-F_1)\ p_2(1) & 0 & 0 \\ (1-F_1)\ p_3(1) & 0 & 0 \end{vmatrix} \qquad (44)
$$

$$
\begin{vmatrix} p_1(1) & p_1(2) \\ -1 & p_1 \end{vmatrix}
$$

$$
\begin{vmatrix} p_2(1) & p_2(2) \\ -1 & p_1 \end{vmatrix}
$$

$$
\begin{vmatrix} p_3(1) & \\ -1 & p_1 \end{vmatrix}
$$

$$P^{(3)}=\begin{vmatrix} p_1 & p_2 & p_3 & (1-F_1) & p_1 & p_2 & (1-F_2)p_1 & 1-F_3 \\ -1 & p_1 & p_2 & & -1 & p_1 & & \\ & -1 & p_1 & & & & & \\ p_1(1) & p_1(2) & p_1(3) & (1-F_1) & p_1(1) & p_1(2) & (1-F_2)p_1(1) & 0 \\ -1 & p_1 & p_2 & & -1 & p_1 & & \\ & -1 & p_1 & & & & & \\ p_2(1) & p_2(2) & & (1-F_1) & p_2(1) & p_2(2) & (1-F_2)p_2(1) & 0 \\ -1 & p_1 & p_2 & & -1 & p_1 & & \\ & -1 & p_1 & & & & & \\ p_3(1) & & & (1-F_1) & p_3(1) & & (1-F_2)p_3(1) & 0 \\ -1 & p_1 & p_2 & & -1 & p_1 & & \\ & -1 & p_1 & & & & & \end{vmatrix} \tag{45}$$

$$P^{(4)}=\begin{vmatrix} p_1 & p_2 & p_3 & p_4 & (1-F_1) & p_1 & p_2 & p_3 & (1-F_2) & p_1 & p_2 & (1-F_3)p_1 \\ -1 & p_1 & p_2 & p_3 & & -1 & p_1 & p_2 & & -1 & p_1 & \\ & -1 & p_1 & p_2 & & & -1 & p_1 & & & & \\ & & -1 & p_1 & & & & & & & & \\ p_1(1) & p_1(2) & p_1(3) & & (1-F_1) & p_1(1) & p_1(2) & p_1(3) & (1-F_2) & p_1(1) & p_1(2) & (1-F_3)p_1(1) \\ -1 & p_1 & p_2 & p_3 & & -1 & p_1 & p_2 & & -1 & p_1 & \\ & -1 & p_1 & p_2 & & & -1 & p_1 & & & & \\ & & -1 & p_1 & & & & & & & & \\ p_2(1) & p_2(2) & & & (1-F_1) & p_2(1) & p_2(2) & & (1-F_2) & p_2(1) & p_2(2) & (1-F_3)p_2(1) \\ -1 & p_1 & p_2 & p_3 & & -1 & p_1 & p_2 & & -1 & p_1 & \\ & -1 & p_1 & p_2 & & & -1 & p_1 & & & & \\ & & -1 & p_1 & & & & & & & & \\ p_3(1) & & & & (1-F_1) & p_3(1) & & & (1-F_2) & p_3(1) & & (1-F_3)p_3(1) \\ -1 & p_1 & p_2 & p_3 & & -1 & p_1 & p_2 & & -1 & p_1 & \\ & -1 & p_1 & p_2 & & & -1 & p_1 & & & & \\ & & -1 & p_1 & & & & & & & & \end{vmatrix} \tag{46}$$

where $p_i(j)\equiv\dfrac{p_{i+j}}{1-F_i}$

Let $\mathbf{D}_i(j)=$

$$\begin{vmatrix} p_i(1) & p_i(2) & \cdots\cdots & p_i(j) \\ -1 & p_1 & p_2\cdots\cdots & p_{j-1} \\ & -1 & p_1 & p_2\cdots\cdots p_{j-2} \\ & & \cdots\cdots & \\ & & -1 & p_1 \\ & & & -1 \end{vmatrix} \tag{47}$$

then we get the following theorem concerning $p_{ij}^{(n)}$.

Theorem 13. The transition probability matrix $P^{(n)}$ in a stationary system is,

$$P^{(n)}=\begin{vmatrix} \mathbf{D}_{0\cdot n} & (1-F_1)\mathbf{D}_{0\cdot n-1} & (1-F_2)\mathbf{D}_{0\cdot n-2} & (1-F_{n-1})\mathbf{D}_{0\cdot 1} \\ \mathbf{D}_{1\cdot n} & (1-F_1)\mathbf{D}_{1\cdot n-1} & (1-F_2)\mathbf{D}_{1\cdot n-2} & (1-F_{n-1})\mathbf{D}_{1\cdot 1} \\ \mathbf{D}_{2\cdot n} & (1-F_1)\mathbf{D}_{2\cdot n-1} & (1-F_2)\mathbf{D}_{2\cdot n-2} & (1-F_{n-1})\mathbf{D}_{2\cdot 1} \\ \cdots\cdots & \cdots\cdots & \cdots\cdots & \cdots\cdots \\ \mathbf{D}_{n-1\cdot n} & (1-F_1)\mathbf{D}_{n-1\cdot n-1} & (1-F_2)\mathbf{D}_{n-1\cdot n-2} & (1-F_{n-1})\mathbf{D}_{n-1\cdot 1} \end{vmatrix} \tag{48}$$

Determinant D_n: Eq. (12) and $\mathbf{D}_{i,j}$: Eq. (47) possess a next important property.

Theorem 14. D_n converges to 1/m as $n\to\infty$, where $m=\sum_i i p_i$, $\sum_i p_i=1$.

Proof: $D_n=p_1 D_{n-1}+p_2 D_{n-2}+\cdots\cdots+p_{n-1}D_1+p_n$, $\sum_i p_i=1$, so D_n is probability on which recurrent event ε occurs in time $n\delta$. Therefore if ε is not periodic, then D_n converges to 1/m, where m is the mean recurrence time.[1]

Theorem 15. $\mathbf{D}_{i,n}$ converges to 1/m as $n\to\infty$, where $m=\sum_i i p_i$, $\sum_i p_i=1$.

Proof: $\mathbf{D}_{i,n}=p_i(1)D_{n-1}+p_i(2)D_{n-2}+\cdots\cdots+p_i(n-1)D_1+p_i(n)$. From Theorem 14 $D_n\to\frac{1}{m}$, $p_i(n)\to 0$ as $n\to\infty$ and $\sum_j p_i(j)=1$, therefore $\mathbf{D}_{i,n}\to 1/m$.

From Theorem 13 and Theorem 15 we get the following theorem concerning the characteristic probability matrix P in a stationary system.

Theorem 16. $P^{(n)}$ converges to P as $n\to\infty$.

where

$$P=\begin{matrix} \frac{1}{m} & \frac{1-F_1}{m} & \frac{1-F_2}{m} & \cdots\cdots \\ \frac{1}{m} & \frac{1-F_1}{m} & \frac{1-F_2}{m} & \cdots\cdots \\ \frac{1}{m} & \frac{1-F_1}{m} & \frac{1-F_2}{m} & \cdots\cdots \\ \vdots & \vdots & \vdots & \end{matrix} \qquad (49)$$

In a non-stationary system the relation of transition is given by Markoff theory as following: $P^{(\nu\to\mu)}=P^{(\nu\to\sigma)}-P^{(\sigma\to\mu)}$, does not become stabilized and continues in a transient state forever.

2.5. Limit Distribution of Output Sequence

From Theorem 9, Theorem 10 and Theorem 14 we get the following theorems concerning the limit distribution of the output sequence provided that the input sequence is a Bernoulli's sequence.

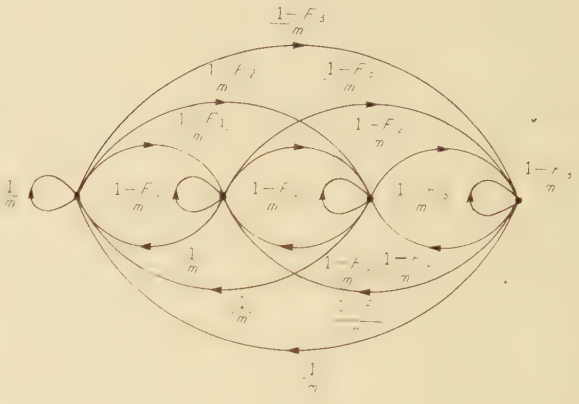

Fig. 14—Transition state diagram of P.

Theorem 17. If the input distributions of discrete stationary circuit is a Bernoulli's distributions sequence $\boldsymbol{a}_i$, $i=0,1,\cdots\cdots,\nu$, $\boldsymbol{a}_i=0$ $i>\nu$, then the mean $\bar{f}_n$ and the variance $\bar{\bar{f}}_n$ of the output distribution $\boldsymbol{f}_n$ converge to $\bar{f}$, $\bar{\bar{f}}$ as $n\to\infty$:

$$\bar{f}=\frac{1}{m}\sum_{i=0}^{\nu}\bar{a}_i \qquad (50)$$

$$\bar{\bar{f}}=\frac{1}{m}\left\{\left(1-\frac{1}{m}\right)\sum_{i=0}^{\nu}\bar{a}_i+\frac{1}{m}\sum_{i=0}^{\nu}\bar{\bar{a}}_i\right\} \qquad (51)$$

Theorem 18. If the input distributions of discrete quasi-stationary system is a Bernoulli's distributions sequence $\boldsymbol{a}_i$ $i=0,1,\cdots\cdots,\nu$, $\boldsymbol{a}_i=0$ $i>\nu$, then the mean $\bar{f}_n$ and the variance $\bar{\bar{f}}_n$ of the output distribution $\boldsymbol{f}_n$ converge to $\bar{f}$, $\bar{\bar{f}}$ as $n\to\infty$:

$$\bar{f}=\sum_{i=0}^{\nu}\frac{\bar{a}_i}{m_i} \qquad (52)$$

$$\bar{\bar{f}}=\sum_{i=0}^{\nu}\frac{1}{m_i}\left\{\left(1-\frac{1}{m_i}\right)\bar{a}_i+\frac{1}{m_i}\bar{\bar{a}}_i\right\} \qquad (53)$$

2.6. Covariance between Output Distributions

2.6.1. $C(\boldsymbol{f}_i\boldsymbol{f}_j)$

Let three systems be represented by Fig. 17 (a), Fig. 18 (a) and Fig. 19 (a) for the sake

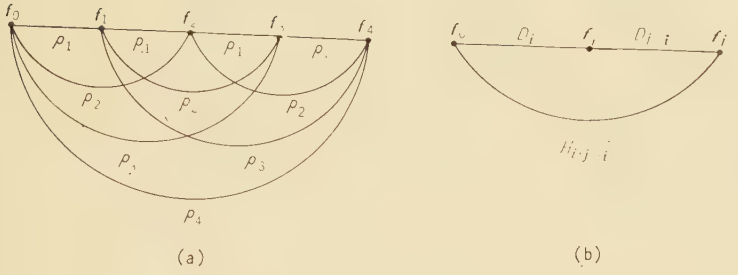

Fig. 15—Equivalent probabilistic transform regarding to f_i, f_j of stationary system.

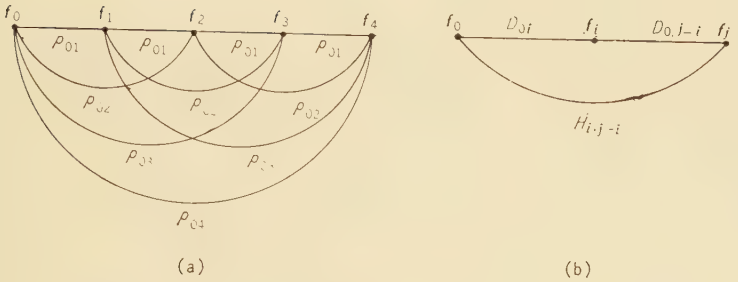

Fig. 16—Equivalent probabilistic transform regarding to f_i, f_j of quasi-stationary system.

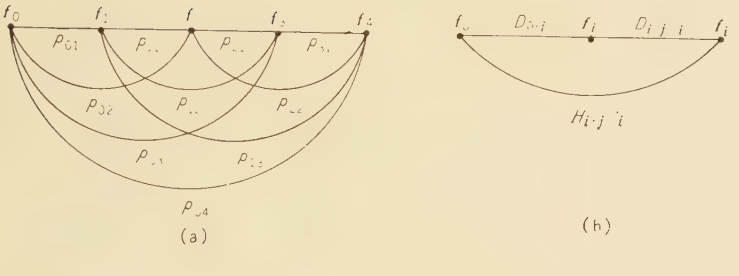

Fig. 17—Equivalent probabilistic transform regarding to f_i, f_j of non-stationary system.

of convenience, then these systems are equivalent to probabilistic circuits of Fig. 17 (b), Fig 18 (b) and Fig. 19 (b) regarding to f_i, f_j. Therefore, from Theorem 7, we get the following theorems concerning the covariance $C(f_i f_j)$ between output distributions f_i, f_j.

Theorem 19. If the input of discrete stationary circuit is only a_0 in time 0, then the covariance $C(f_i f_j)$ between the output distributions f_i, f_j is,

$$C(f_i f_j) = \bar{a}_0 D_i \{(1-D_i)D_{j-i} - H_{i\cdot j-i}\} + \bar{\bar{a}}_0 D_i (D_i D_{j-i} + H_{i\cdot j-i}) \tag{56}$$

where D_i : Eq. (12)

$$H_{i\cdot j-i} = \begin{vmatrix} p_1 & p_2 & \cdots & p_{i-1} & 0 & p_{i+1} & \cdots & p_j \\ -1 & p_1 & p_2 & \cdots & p_{i-2} & 0 & p_i & \cdots & p_{j-1} \\ & -1 & p_1 & p_2 & \cdots & p_{i-3} & 0 & p_{i-1} & \cdots & p_{j-2} \\ & & \cdots & \cdots & \cdots & \cdots & \cdots & \cdots & \cdots & \cdots \\ & & & -1 & 0 & p_2 & \cdots & \cdots & p_{j\cdot i+1} \\ & & & & -1 & 0 & 0 & \cdots & 0 \\ & & & & & -1 & p_1 & p_2 & \cdots & p_{j\cdot i-1} \\ & & & & & & \cdots & \cdots & \cdots & \cdots \\ & & & & & & & & -1 & p_1 \end{vmatrix} \tag{57}$$

$$= \sum_{k=1}^{j-1} (1-F_k) \mathrm{D}_{j-i-k} \mathbf{D}_{k\cdot i} \tag{58}$$

($\boldsymbol{D}_{ij}$: Eq. (47))

Theorem 20. If the input of discrete quasi-stationary circuit is only $\boldsymbol{a}_0$ in time 0, then the covariance $C(\boldsymbol{f}_i \boldsymbol{f}_j)$ between the output distributions $\boldsymbol{f}_i$, $\boldsymbol{f}_j$ is,

$$C(\boldsymbol{f}_i \boldsymbol{f}_j) = \bar{a}_0 \mathrm{D}_{0i} \{(1-\mathrm{D}_{0i})\mathrm{D}_{0\cdot j-i} + \mathrm{H}_{i\cdot j-i}\}$$

$$+ \bar{\bar{a}}_0 \mathrm{D}_{0i} (\mathrm{D}_{0i} \mathrm{D}_{0\cdot j-i} + \mathrm{H}_{i\cdot j-i}) \tag{59}$$

where D_{0i}: Eq. (18)

$$\mathrm{H}_{i\cdot j-i} = \begin{vmatrix} p_{01} & p_{02} \cdots\cdots p_{0\cdot i-1} & 0 & p_{0\cdot i+1} \cdots\cdots p_{0\cdot j} \\ -1 & p_{01}\ p_{02} \cdots\cdots p_{0\cdot i-2} & 0 & p_{0\cdot i} \cdots\cdots p_{0\cdot j-1} \\ & -1\ p_{01}\ p_{02} \cdots p_{0\cdot i-3} & 0 & p_{0\cdot i-1} \cdots\cdots p_{0\cdot j-2} \\ \cdots\cdots & \cdots\cdots & \cdots & \cdots\cdots \\ & -1 & 0 & p_{02} \cdots\cdots p_{0\cdot j-i+1} \\ & & -1\ 0 & 0 \cdots\cdots 0 \\ & & & -1\ p_{01}\ p_{02} \cdots p_{0\cdot j-i-1} \\ \cdots\cdots & \cdots\cdots & \cdots & \cdots\cdots \\ & & & -1\ p_{0\cdot 1} \end{vmatrix} \tag{60}$$

$$= \sum_{k=1}^{j-i} (1-F_{0k}) \mathrm{D}_{0\cdot j-i-k} \mathbf{D}_{(0)k\cdot i} \tag{61}$$

Theorem 21. If the input of discrete non-stationary circuit is only $\boldsymbol{a}_0$ in time 0, then the covariance $C(\boldsymbol{f}_i \boldsymbol{f}_j)$ between the output distributions $\boldsymbol{f}_i$, $\boldsymbol{f}_j$ is,

$$C(\boldsymbol{f}_i \boldsymbol{f}_j) = \bar{a}_0 \mathrm{D}_{0i} \{(1-\mathrm{D}_{0i})\mathrm{D}_{i\cdot j-i} + \mathrm{H}_{i\cdot j-i}\}$$

$$+ \bar{\bar{a}}_0 \mathrm{D}_{0i} (\mathrm{D}_{0i} \mathrm{D}_{i\cdot j-i} + \mathrm{H}_{i\cdot j-i}) \tag{62}$$

* see foot note.

2.6.2. Limit of $C(\boldsymbol{f}_i \boldsymbol{f}_j)$

Theorem 22. If the input of discrete stationary circuit is only $\boldsymbol{a}_0$ in time 0, then the covariance $C(\boldsymbol{f}_i \boldsymbol{f}_j)$ between the output distributions $\boldsymbol{f}_i$, $\boldsymbol{f}_j$ converges to C_{ij} as $i \to \infty$:

$$C_{ij} = \bar{a}_0 \frac{1}{m} \left(\mathrm{D}_{j-i} - \frac{1}{m} \right) + \bar{\bar{a}}_0 \frac{1}{m^2} \tag{64}$$

Proof: From Theorem 15 $\mathbf{D}_{k\cdot} \to 1/m$ as $i \to \infty$. Considering the following identity:

$$\begin{vmatrix} 1 & 1-F_1 & 1-F_2 \cdots\cdots\cdots & 1-F_n \\ -1 & p_1 & p_2 \cdots\cdots\cdots & p_n \\ & -1 & p_1 \quad p_2 \cdots\cdots & p_{n-1} \\ & \cdots\cdots & \cdots\cdots & \cdots \\ & & -1 & p_1 \end{vmatrix} = 1, \tag{65}$$

* where $\mathrm{D}_{i\cdot j}$: Eq. (20)

$$\mathrm{H}_{i\cdot j-i} = \begin{vmatrix} p_{01} & p_{02} \cdots\cdots p_{0\cdot i-1} & 0 & p_{0\cdot i+1} \cdots\cdots p_{0\cdot j} \\ -1 & p_{11} \quad p_{12} \cdots\cdots p_{1\cdot i-2} & 0 & p_{1\cdot i} \cdots\cdots p_{1\cdot j-1} \\ & -1 \quad p_{21} \quad p_{22} \cdots p_{2\cdot i-3} & 0 & p_{2\cdot i-1} \cdots\cdots p_{2\cdot j-2} \\ \cdots\cdots & \cdots\cdots & \cdots & \cdots\cdots \\ & -1 & 0 & p_{i-1\cdot 2} \cdots\cdots p_{i-1\cdot j-i+1} \\ & & -1\ 0 & 0 \cdots\cdots 0 \\ & & & -1\ p_{i+1\cdot 1}\ p_{i+1\cdot 2} \cdots p_{i+1\cdot j-i-1} \\ & & & \cdots\cdots \\ & & & -1\ p_{j-1\cdot 1} \end{vmatrix} \tag{63}$$

$$\sum_{k=1}^{j-i}(1-F_k)D_{j-i-k}=1-D_{j-i}, \tag{66}$$

therefore from Eq. (58),

$$H_{i\cdot j-i}\to\frac{1}{m}(1-D_{j-i}). \tag{67}$$

Then the probabilistic transform of Fig. 15 becomes equal to the one of Fig. 18 as $i\to\infty$, so we get Eq. (64) from Theorem 7, Theorem 3, Theorem 5 and Theorem 2.

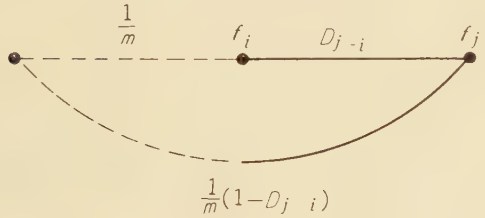

Fig. 18—Limit probabilistic transform of stationary system regarding to f_i, f_j, $i\to\infty$.

Theorem 23. If the input of discrete quasi-stationary circuit is only a_0 in time 0, then the covariance $C(f_i f_j)$ between the output distributions f_i, f_j converges to C_{ij} as $i\to\infty$:

$$C_{ij}=\bar{a}_0\frac{1}{m_0}\left(D_{0\cdot j-i}-\frac{1}{m_0}\right)+\bar{a}_0\frac{1}{m_0} \tag{68}$$

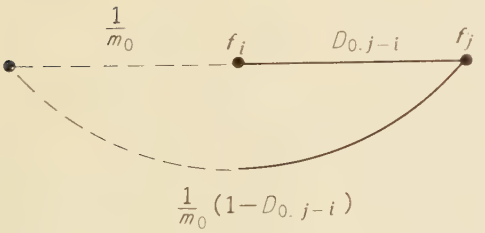

Fig. 19—Limit probabilistic transform of quasi-stationary system regarding to f_i, f_j, $i\to\infty$.

Proof: $D_{01}\to 1/m_0$, $H_{i\cdot j-i}\to\frac{1}{m_0}(1-D_{0\cdot j-i})$ as $i\to\infty$, so the circuit of Fig. 16 becomes equal to the one of Fig. 19, then we get Eq. (68).

In non-stationary system $C(f_i f_j)$ does not converge.

2.7. Additive Process of Output Distributions Sequence

2.7.1. $F_{ij}^{(0)}$

Let the additive process $F_{ij}^{(0)}$ of the output distributions f_ν, $\nu=i, i+1, \cdots\cdots, j$ for the input distribution a_0

$$F_{ij}^{(0)}=f_i\otimes f_{i+1}\otimes\cdots\cdots\otimes f_j,$$

then the mean $\bar{F}_{ij}^{(0)}$, the variance $\bar{\bar{F}}_{ij}^{(0)}$ is given by

$$\bar{F}_{ij}^{(0)}=\sum_{\nu=i}^{j}\bar{f}_\nu \tag{54}$$

$$\bar{\bar{F}}_{ij}^{(0)}=\sum_{\nu=i}^{j}\sum_{\mu=i}^{j}C(f_\nu f_\mu) \tag{55}$$

2.7.2. Limit of $F_{ij}^{(0)}$

From Theorem 22 and Theorem 23 we get the following theorems concerning the limit distribution $F^{(0)}$.

Theorem 24. If the input is only a_0 in time 0, then the mean $\bar{F}_{ij}^{(0)}$, the variance $\bar{\bar{F}}_{ij}^{(0)}$ of the additive process $F_{ij}^{(0)}$ of the output distributions f_ν, $\nu=i, i+1, \cdots\cdots, j$ in discrete stationary system converge to $\bar{F}^{(0)}$, $\bar{\bar{F}}^{(0)}$ as $i\to\infty$:

$$\bar{F}^{(0)}=\frac{1}{m}\bar{a}_0\eta \tag{69}$$

$$\bar{\bar{F}}^{(0)}=\bar{a}_0\sum_{k=-\eta}^{\eta}W(\eta\cdot k)\frac{1}{m}\left(D_k-\frac{1}{m}\right)+\bar{\bar{a}}_0\left(\frac{\eta}{m}\right)^2 \tag{70}$$

where $W(\eta\cdot k)=\eta-k,\quad k\geq 0$

$\eta+k,\quad k\leq 0$

$0\quad,\quad k>\eta,\quad k<-\eta$

$\eta=j-i$, $D_k=D_{-k}$: Eq(12), $D_0=1$

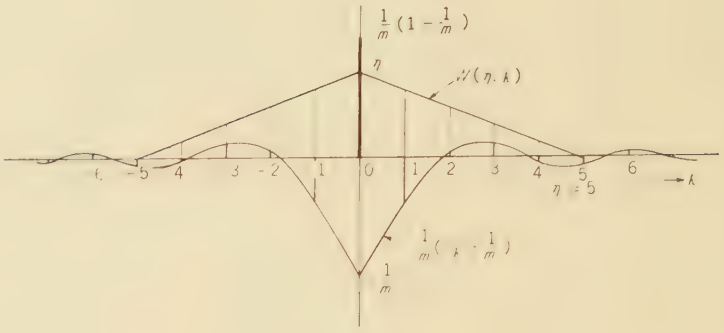

Fig. 20 $W(\eta \cdot k)$ and $\frac{1}{m}\left(D_k-\frac{1}{m}\right)$, $\eta=5$.

For example we showed $W(\eta \cdot k)$ and $\frac{1}{m}\left(D_k-\frac{1}{m}\right)$ in Fig. 20 about $\eta=5$.

Theorem 25. If the input is only $\boldsymbol{a}_0$ in time 0, then the mean $\bar{F}_{ij}^{(0)}$, the variance $\bar{\bar{F}}_{ij}^{(0)}$ of the additive process $\boldsymbol{F}_{ij}^{(0)}$ of the output distributions $\boldsymbol{f}_\nu$, $\nu=i, i+1, \cdots\cdots, j$ in a discrete quasi-stationary system converge to $\bar{F}^{(0)}$, $\bar{\bar{F}}^{(0)}$ as $i\to\infty$:

$$\bar{F}^{(0)}=\frac{1}{m_0}\bar{a}_0\eta \tag{71}$$

$$\bar{\bar{F}}^{(0)}=\bar{a}_0\sum_{k=-\eta}^{\eta} W(\eta \cdot k)\frac{1}{m_0}\left(D_{0k}-\frac{1}{m_0}\right)+\bar{\bar{a}}_0\left(\frac{\eta}{m_0}\right)^2 \tag{72}$$

where $D_{0k}=D_{0,-k}$: Eq. (18), $D_{00}=1$.

2.8. Estimation of Parameter

Let observation of variance $\bar{\bar{F}}^{(0)}$ over $\eta=1, 2, \cdots\cdots$ for input a_0 is σ_η^2, then from Theorem 24 and Theorem 25 the circuit parameters: $p_1, p_2, \cdots\cdots, p_{\eta-1}$ (or $p_{01}, p_{02}, \cdots\cdots, p_{0,\eta-1}$) are given by the following recurrence formula:

i Stationary system

$$\sigma^2{}_n-\sigma^2{}_{n-1}=a_0\left\{\sigma^2{}_1+2\sum_{i=1}^{n-1}\frac{1}{m}\left(D_i-\frac{1}{m}\right)\right\} \tag{73}$$

ii Quasi-stationary system

$$\sigma^2{}_n-\sigma^2{}_{n-1}=a_0\left\{\sigma^2{}_1+2\sum_{i=1}^{n-1}\frac{1}{m_0}\left(D_{0i}-\frac{1}{m_0}\right)\right\} \tag{74}$$

iii Non-stationary system

We can not estimate the circuit parameter of a non-stationary system in this method because the output distributions sequence does not stabilize.

3. Binomial Probabilistic Sequential Circuits (Nonconstant Difference Discrete System)

In the previous section we constructed discrete probabilistic sequential circuits with a constant time difference δ. In this section we will discuss discrete probabilistic sequential circuits with nonconstant time differences. In such asynchronous circuits the input distributions $\boldsymbol{a}_i$ are transmitted into the circuit in time $\tau_0, \tau_1, \tau_2, \cdots\cdots$, $(\tau_0<\tau_1<\tau_2<\cdots\cdots)$ and the output distributions $\boldsymbol{f}_i$ leave the circuit with the same time sequence. Using the three circuit elements discussed in Section 1, we can construct three types of nonconstant difference (or nonhomogeneous) discrete probabilistic sequential circuits as shown on Fig 21, Fig. 22 and Fig. 23, which corresponds to the stationary, the quasi-stationary and the non-stationary systems in Section 2.

The reason that we devide the discrete system into homogeneous and nonhomogeneous systems are based on control problems of output distributions sequence, that is, homogeneous discrete system for a-controll which control $\bar{f}_{n+t}$ by $\{a_i\}$ to command keeping constant time interval δ between action time

$\tau_i, \tau_{i+1}, i = 1, 2, \cdots\cdots$ and nonhomogeneous discrete system for τ–control which control $\bar{\bar{f}}_{n+t}$ by $\{\tau_i\}$ to command for any $\{a_i\}$.

In the nonconstant difference discrete system Eq. (13), (15), Eq. (16), (17) and Eq. (21), (22) are equally formulated, so we get the following theorems concerning the mean and the variance of the output distributions.

Theorem 26. If the input distributions a_0, $a_1, a_2, \cdots\cdots, a_n$ of a nonhomogeneous discrete circuit I (Fig. 21) is a Bernoulli's sequence,

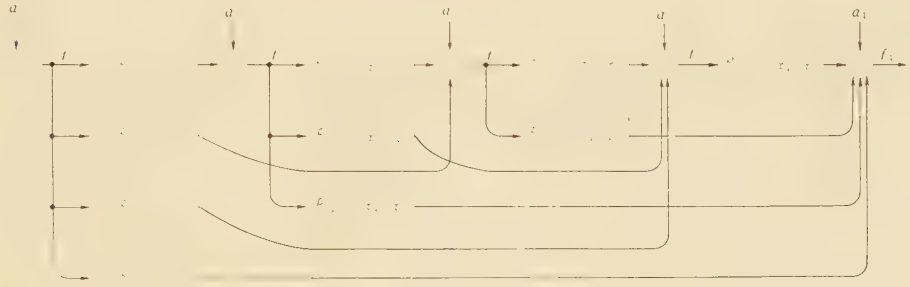

Fig. 21—Nonhomogeneous binomial probabilistic sequential circuit. 1.

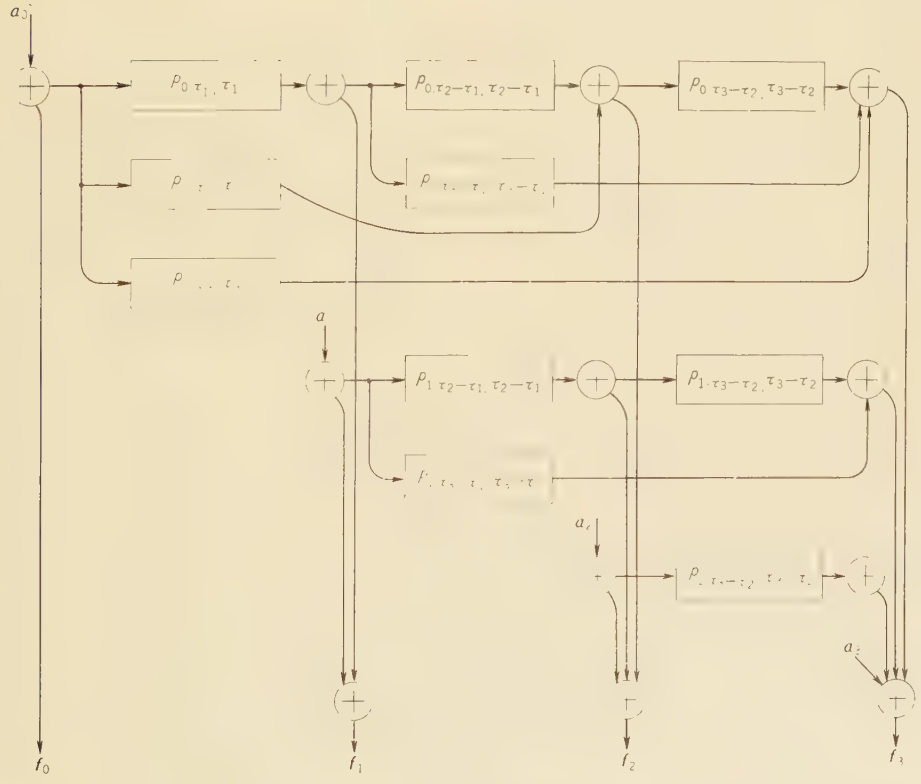

Fig. 22—Nonhomogeneous binomial probabilistic sequential circuit. 2.

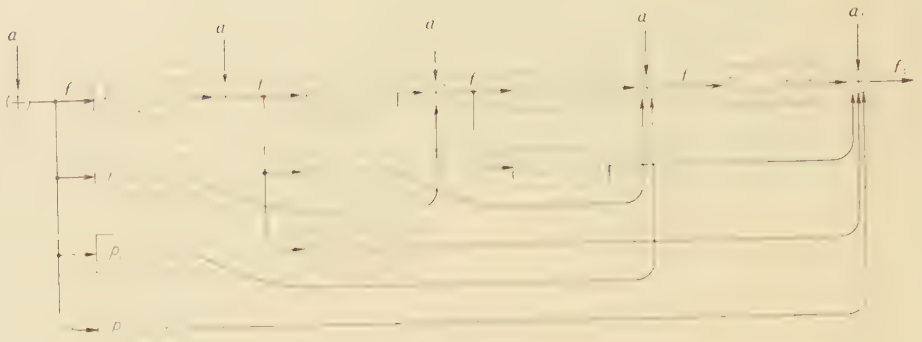

Fig. 23—Nonhomogeneous binomial probabilistic sequential circuit. 3.

then the mean $\bar{f}_n$ and the variance $\bar{\bar{f}}_n$ of the output distributions $\boldsymbol{f}_n$ in time τ_n are,

$$\bar{f}_n = \sum_{i=0}^{n} \bar{a}_i \mathrm{D}_{i\cdot n-i} \tag{75}$$

$$\begin{aligned} = \bar{a}_0 \; \bar{a}_1 \cdots\cdots \bar{a}_n \\ -1 \; p_{\tau_1-\tau_0} \, p_{\tau_2-\tau_0} \cdots\cdots p_{\tau_n-\tau_0} \\ -1 \quad p_{\tau_2-\tau_1} \, p_{\tau_3-\tau_1} \cdots\cdots p_{\tau_n-\tau_1} \\ \cdots\cdots \\ -1 \quad p_{\tau_{n-1}-\tau_{n-2}} \, p_{\tau_n-\tau_{n-2}} \\ -1 \quad p_{\tau_n-\tau_{n-1}} \end{aligned} \tag{76}$$

$$\bar{\bar{f}}_n = \sum_{i=0}^{n} \bar{a}_i \mathrm{D}_{i\cdot n-i}(1-\mathrm{D}_{i\cdot n-i}) + \sum_{i=0}^{n} \bar{\bar{a}}_i \mathrm{D}^2_{i\cdot n-i} \tag{77}$$

where

$$\begin{aligned} \mathrm{D}_{i\cdot n-i} = \; & p_{i\cdot\tau_{i+1}-\tau_i} \; p_{i\cdot\tau_{i+2}-\tau_i} \cdots\cdots p_{i\cdot\tau_n-\tau_i} \\ & -1 \quad p_{i\cdot\tau_{i+2}-\tau_{i+1}} \; p_{i\cdot\tau_{i+3}-\tau_{i+1}} \cdots\cdots p_{i\cdot\tau_n-\tau_{i+1}} \\ & -1 \quad p_{i\cdot\tau_{i+3}-\tau_{i+2}} \; p_{i\cdot\tau_{i+4}-\tau_{i+2}} \; p_{i\cdot\tau_n-\tau_{i+2}} \\ & \cdots\cdots \\ & -1 \quad p_{i\cdot\tau_n-\tau_{n-1}} \end{aligned} \tag{81}$$

$$p_{k\cdot\tau_i-\tau_j} = \int_{\tau_{i-1}-\tau_j}^{\tau_i-\tau_{i-1}} p_k(\xi)\, d\xi$$

$$\begin{aligned} \mathrm{D}_{i\cdot n-i} = \; & p_{\tau_{i+1}-\tau_i} \; p_{\tau_{i+2}-\tau_i} \cdots\cdots p_{\tau_n-\tau_i} \\ & -1 \quad p_{\tau_{i+2}-\tau_{i+1}} \; p_{\tau_{i+3}-\tau_{i+1}} \cdots\cdots p_{\tau_n-\tau_{i+1}} \\ & -1 \quad p_{\tau_{i+3}-\tau_{i+2}} \; p_{\tau_{i+4}-\tau_{i+2}} \cdots p_{\tau_n-\tau_{i+2}} \\ & \cdots\cdots \\ & -1 \quad p_{\tau_n-\tau_{n-1}} \end{aligned} \tag{78}$$

$$p_{\tau_i-\tau_j} = \int_{\tau_{i-1}-\tau_j}^{\tau_i-\tau_{i-1}} p(\xi)\, d\xi$$

Thorem 27. If the input distributions a_0, a_1, ……, a_n of a nonhomogeneous discrete circuit Π (Fig. 22) is a Bernoulli's sequence, then the mean $\bar{f}_n$ and the variance $\bar{\bar{f}}_n$ of the output distributions $\boldsymbol{f}_n$ in time τ_n are,

$$\bar{f}_n = \sum_{i=0}^{n} \bar{a}_i \mathrm{D}_{i\cdot n-i} \tag{79}$$

$$\bar{\bar{f}}_n = \sum_{i=0}^{n} \bar{a}_i \mathrm{D}_{i\cdot n-i}(1-\mathrm{D}_{i\cdot n-i}) + \sum_{i=0}^{n} \bar{\bar{a}}_i \mathrm{D}^2_{i\cdot n-i} \tag{80}$$

where

Theorem 28. If the input distributions $a_0, a_1, \cdots\cdots, a_n$ of a nonhomogeneous discrete circuit III (Fig. 23) is a Bernoulli's sequence, then the mean $\bar{f}_n$ and the variance $\bar{\bar{f}}_n$ of the output distributions $\boldsymbol{f}_n$ in time τ_n are,

$$\bar{f}_n = \sum_{i=0}^{n} \bar{a}_i \mathrm{D}_{i \cdot n-i} \tag{82}$$

$$= \begin{vmatrix} \bar{a}_0 & \bar{a}_1 \cdots\cdots\cdots\cdots & \bar{a}_n \\ -1 & p_{0\cdot\tau_1-\tau_0} \; p_{0\cdot\tau_2-\tau_0} \cdots\cdots\cdots & p_{0\cdot\tau_n-\tau_0} \\ & -1 \quad p_{1\cdot\tau_2-\tau_1} \; p_{1\cdot\tau_3-\tau_1} \cdots p_{1\cdot\tau_n-\tau_1} \\ & \cdots\cdots\cdots\cdots\cdots\cdots\cdots\cdots\cdots \\ & \qquad\qquad -1 \quad p_{n-1\cdot\tau_n-\tau_{n-1}} \end{vmatrix} \tag{83}$$

$$\bar{\bar{f}}_n = \sum_{i=0}^{n} \bar{a}_i \mathrm{D}_{i \cdot n-i}(1-\mathrm{D}_{i \cdot n-i}) + \sum_{i=0}^{n} \bar{\bar{a}}_i \mathrm{D}^2_{i \cdot n-i} \tag{84}$$

where

$$\mathrm{D}_{i \cdot n-i} = \begin{vmatrix} p_{i\cdot\tau_{i+1}-\tau_i} & p_{i\cdot\tau_{i+2}-\tau_i} \cdots\cdots\cdots\cdots\cdots\cdots & p_{i\cdot\tau_n-\tau_i} \\ -1 & p_{i+1\cdot\tau_{i+2}-\tau_{i+1}} \; p_{i+1\cdot\tau_{i+3}-\tau_{i+1}} \cdots\cdots\cdots & p_{i+1\cdot\tau_n-\tau_{i+1}} \\ & -1 \quad p_{i+2\cdot\tau_{i+3}-\tau_{i+2}} \; p_{i+2\cdot\tau_{i+4}-\tau_{i+2}} & p_{i+2\cdot\tau_n-\tau_{i+2}} \\ & \cdots\cdots\cdots\cdots\cdots\cdots\cdots\cdots\cdots\cdots\cdots\cdots\cdots \\ & \qquad\qquad -1 & p_{n=1\cdot\tau_n-\tau_{n-1}} \end{vmatrix} \tag{85}$$

$$P_{k\cdot\tau_i-\tau_j} = \int_{\tau_{i-1}-\tau_j}^{\tau_i-\tau_{i-1}} p_k(\xi)\, d\xi$$

In the nonconstant difference discrete system Eq. (56), Eq. (59) and Eq. (62) are equally formulated, so we get the following theorem concerning the covariance between output distributions.

Theorem 29. If the input distribution of a nonhomogeneous discrete circuit is only $\boldsymbol{a}_0$, then the covariance $C(\boldsymbol{f}_i \boldsymbol{f}_j)$ between output distributions $\boldsymbol{f}_i, \boldsymbol{f}_j$ is,

$$C(\boldsymbol{f}_i \boldsymbol{f}_j) = \bar{a}_0 \mathrm{D}_{0i}\{(1-\mathrm{D}_{0i})\mathrm{D}_{i\cdot j-i} - \mathrm{H}_{i\cdot j-i}\} + \bar{\bar{a}}_0 \mathrm{D}_{0i}(\mathrm{D}_{0i}\mathrm{D}_{i\cdot j-i} + \mathrm{H}_{i\cdot j-i}). \tag{86}$$

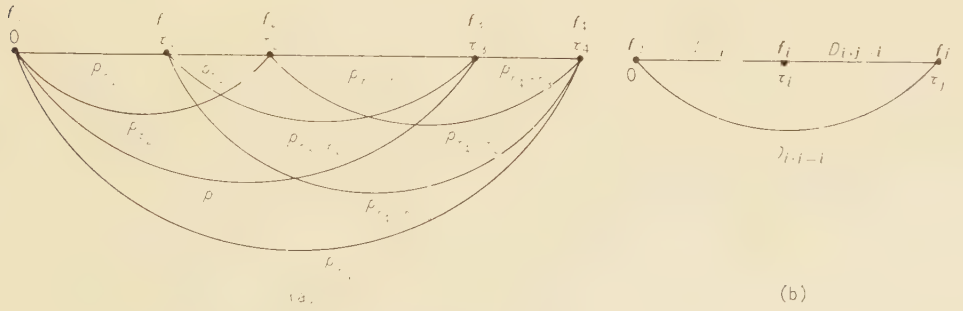

(b)

Fig. 24—Equivalent probabilistic transform regarding to $\boldsymbol{f}_i, \boldsymbol{f}_j$ of nonhomogeneous stationary system.

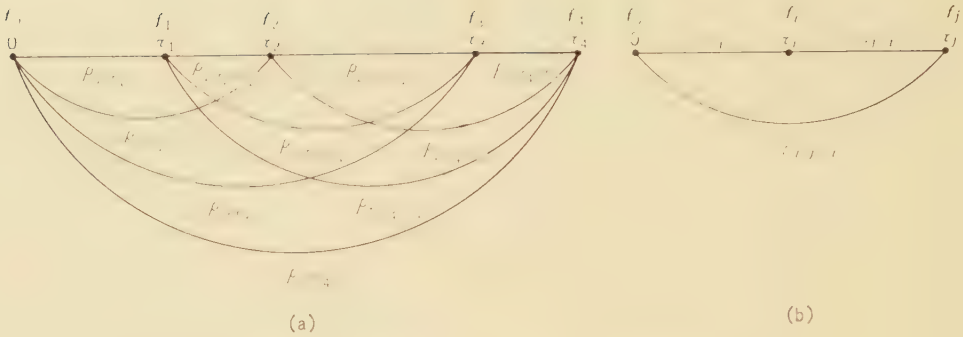

(a) (b)

Fig. 25—Equivalent probabilistic transform regarding to f_i, f_j of nonhomogeneous non-stationary system.

where

i Circuit I. (Fig. 21)

$D_{i\cdot j-i}$: Eq. (78).

$$
H_{i\cdot j-i}= \begin{matrix}
p_{\tau_1-\tau_0} & p_{\tau_2-\tau_0} & \cdots & p_{\tau_{i-1}-\tau_0} & 0 & p_{\tau_{i+1}-\tau_0} & \cdots & p_{\tau_j-\tau_0} \\
-1 & p_{\tau_2-\tau_1} & p_{\tau_3-\tau_1} & \cdots & p_{\tau_{i-1}-\tau_1} & 0 & p_{\tau_{i+1}-\tau_1} & \cdots & p_{\tau_j-\tau_1} \\
 & -1 & p_{\tau_3-\tau_2} & p_{\tau_4-\tau_2} & p_{\tau_{i-1}-\tau_2} & 0 & p_{\tau_{i+1}-\tau_2} & \cdots & p_{\tau_j-\tau_2} \\
 & & \cdots & & & & & & \\
 & & & & -1 & 0 & p_{\tau_{i+1}-\tau_{i-1}} & \cdots & p_{\tau_j-\tau_{i-1}} \\
 & & & & & -1 & 0 & \cdots & 0 \\
 & & & & & & -1 & p_{\tau_{i+2}-\tau_{i+1}} & p_{\tau_{i+3}-\tau_{i+1}} & p_{\tau_j-\tau_{i+1}} \\
 & & & & & & & \cdots & & \\
 & & & & & & & & -1 & p_{\tau_j-\tau_{j-1}}
\end{matrix}
\qquad (87)
$$

ii Circuit II. (Fig. 22)

$D_{i\cdot j-i}$: Eq. (81).

$$
H_{i\cdot j-i}= \begin{matrix}
p_{0\cdot\tau_1-\tau_0} & p_{0\cdot\tau_2-\tau_0} & \cdots & p_{0\cdot\tau_{i-1}-\tau_0} & 0 & p_{0\cdot\tau_{i+1}-\tau_0} & \cdots & p_{0\cdot\tau_j-\tau_0} \\
-1 & p_{0\cdot\tau_2-\tau_1} & p_{0\cdot\tau_3-\tau_1} & \cdots & p_{0\cdot\tau_{i-1}-\tau_1} & 0 & p_{0\cdot\tau_{i+1}-\tau_1} & \cdots & p_{0\cdot\tau_j-\tau_1} \\
 & -1 & p_{0\cdot\tau_3-\tau_2} & p_{0\cdot\tau_4-\tau_2} & p_{0\cdot\tau_{i-1}-\tau_2} & 0 & p_{0\cdot\tau_{i+1}-\tau_2} & \cdots & p_{0\cdot\tau_j-\tau_2} \\
 & & \cdots & & & & & & \\
 & & & & -1 & 0 & p_{0\cdot\tau_{i+1}-\tau_{i-1}} & \cdots & p_{0\cdot\tau_j-\tau_{i-1}} \\
 & & & & & -1 & 0 & \cdots & 0 \\
 & & & & & & -1 & p_{0\cdot\tau_{i+2}-\tau_{i+1}} & p_{0\cdot\tau_{i+3}-\tau_{i+1}} & p_{0\cdot\tau_j-\tau_{i+1}} \\
 & & & & & & & \cdots & & \\
 & & & & & & & & -1 & p_{0\cdot\tau_j-\tau_{j-1}}
\end{matrix}
\qquad (88)
$$

iii Circuit III. (Fig. 23)

$D_{i\cdot j-i}$: Eq. (85).

$$H_{i\cdot j-i}=\begin{vmatrix} p_{0\cdot\tau_1-\tau_0} & p_{0\cdot\tau_2-\tau_0}\cdots\cdots & p_{0\cdot\tau_{i-1}-\tau_0} & 0 & p_{0\cdot\tau_{i+1}-\tau_0}\cdots\cdots & p_{0\cdot\tau_j-\tau_0} \\ -1 & p_{1\cdot\tau_2-\tau_1} \; p_{1\cdot\tau_3-\tau_1}\cdots & p_{1\cdot\tau_{i-1}-\tau_1} & 0 & p_{1\cdot\tau_{i+1}-\tau_1}\cdots & p_{1\cdot\tau_j-\tau_1} \\ & -1 \quad p_{2\cdot\tau_3-\tau_2} \; p_{2\cdot\tau_4-\tau_2} & p_{2\cdot\tau_{i-1}-\tau_2} & 0 & p_{2\cdot\tau_{i+1}-\tau_2}\cdots & p_{2\cdot\tau_j-\tau_2} \\ & \cdots\cdots & & & & \\ & & -1 \quad 0 & p_{i-1,\tau_{i+1}-\tau_{i-1}}\cdots & & p_{i-1\tau_j-\tau_{i-1}} \\ & & -1 & 0 \quad 0\cdots & & 0 \\ & & & -1 \quad p_{i+1,\tau_{i+2}-\tau_{i+1}} & p_{i+1,\tau_{i+3}-\tau_{i+1}} & p_{i+1,\tau_j-\tau_{i+1}} \\ & & & \cdots\cdots & & \\ & & & & -1 & p_{j-1,\tau_j-\tau_{j-1}} \end{vmatrix} \tag{89}$$

Additive process of the output distributions sequence of the nonhomogeneous discrete system is given by Eq. (54) and Eq. (55).

There exists no limit of $C(\boldsymbol{f}_i\boldsymbol{f}_j)$ and the additive process, since action time τ_i is indefinite.

4. Binomial Probabilistic Sequential Circuits III. (Homogeneous Continuous System)

In this section, we discuss the continuous form of constant difference discrete system, which is given by $\delta\to 0$ and possesses a probability density function as a circuit parameter.

In the discrete system, the circuit is described by the difference equation:

$$D_n=\delta_n+\sum_{i=0}^{n} p_i\, D_{n-i}. \tag{90}$$

Let the continuous form of D_n be $g(t)$, then the continuous circuit is described by the following Volterra's 2-nd integral equation:

$$g(t)=\delta(t)+\int_0^t p(\xi)g(t-\xi)d\xi \tag{91}$$

where

$\delta(t)$: Dirac's delta function.

$\int_{-\infty}^{t}\delta(t)dt=E(t)$: Heaviside's unit function.

$g(t)$ is given by the solution of Eq. (91) as follows: let Laplace transform of g, p is $G(s)$, $P(s)$, then

$$G(s)=1+P(s)\cdot G(s)$$

$$\therefore\quad G(s)=\frac{1}{1-P(s)},$$

introducing $U(s)$:

$$U(s)\equiv\frac{P(s)}{1-P(s)} \tag{92}$$

then we get

$$G(s)=1+U(s)\cdot 1.$$

Therefore

$$g(t)=\delta(t)+\int_0^t u(\xi)\delta(t-\xi)d\xi=u(t), \tag{93}$$

that is, $g(t)$ is an indicial function of the circuit and the transfer function is given by $U(s)$; Eq. (92).

We get the following theorems concerning the mean and the variance of the output distributions.

Theorem 30. If the input distribution $\boldsymbol{\alpha}(t)$ of a continuous stationary circuit is a

Bernoulli's sequence, then the mean $\bar{f}(t)$ and the variance $\bar{\bar{f}}(t)$ of the output distribution $\boldsymbol{f}(t)$ in time t are,

$$\bar{f}(t)=\bar{a}(t)+\int_0^t \bar{a}(\xi)g(t-\xi)d\xi \tag{94}$$

$$\bar{\bar{f}}(t)+\bar{f}(t)+\int_0^t (\bar{\bar{a}}(\xi)-\bar{a}(\xi))g^2(t-\xi)d\xi \tag{95}$$

where

$$g(t)=\frac{1}{2\pi i}\int_{Br} e^{st}\mathrm{U}(s)\,ds$$

$$\mathrm{U}(s)=\frac{\mathrm{P}(s)}{1-\mathrm{P}(s)},\quad \mathrm{P}(s)=\int_0^\infty e^{-st}p(t)\,dt.$$

Theorem 31. If the input distribution $\boldsymbol{a}(t)$ of a continuous quasi-stationary circuit is a Bernoulli's sequence, then the mean $\bar{f}(t)$ and the variance $\bar{\bar{f}}(t)$ of the output distribution $\boldsymbol{f}(t)$ in time t are,

$$\bar{f}(t)=\bar{a}(t)+\int_0^t \bar{a}(\xi)g_\xi(t-\xi)d\xi \tag{96}$$

$$\bar{\bar{f}}(t)=\bar{f}(t)+\int_0^t (\bar{\bar{a}}(\xi)-\bar{a}(\xi))g_\xi^2(t-\xi)\,d\xi \tag{97}$$

where

$$g_\xi(t)=\frac{1}{2\pi i}\int_{Br} e^{st}\mathrm{U}_\xi(s)\,d\xi$$

$$\mathrm{U}_\xi(s)=\frac{\mathrm{P}_\xi(s)}{1-\mathrm{P}_\xi(s)},\quad \mathrm{P}_\xi(s)=\int_0^\infty e^{-st}p_\xi(t)\,dt$$

Theorem 32. If the input distribution $\boldsymbol{a}(t)$ of a continuous non-stationary circuit is a Bernoulli's sequence, then the mean $\bar{f}(t)$ and the variance $\bar{\bar{f}}(t)$ of the output distribution in time t are,

$\bar{f}(t)$: Eq. (96).
$\bar{\bar{f}}(t)$: Eq. (97).

where $g_\xi(t)$ is an indicial function of the continuous non-stationary circuit which is given by the solution of the equation:

$$g(t)=\delta(t)+\int_0^t p_\xi(t-\xi)g(\xi)d\xi. \tag{98}$$

We get the following theorems concerning the limit distribution.

Theorem 33. If the input distributions of a continuous stationary system is a Bernoulli's distributions sequence $\boldsymbol{a}(\xi), 0\leq\xi\leq\nu$, $\boldsymbol{a}(\xi)=0,\ \xi>\nu$, then the mean $\bar{f}(t)$ and the variance $\bar{\bar{f}}(t)$ of the output distribution $\boldsymbol{f}(t)$ converge to $\bar{f}$, $\bar{\bar{f}}$ as $t\to\infty$:

$$\bar{f}=\frac{1}{m}\int_0^\nu \bar{a}(\xi)\,d\xi \tag{99}$$

$$\bar{\bar{f}}=\frac{1}{m}\left(1-\frac{1}{m}\right)\int_0^\nu \bar{a}(\xi)\,d\xi+\frac{1}{m^2}\int_0^\nu \bar{\bar{a}}(\xi)\,d\xi \tag{100}$$

where $m=\int_0^\infty tp(t)dt.$

Theorem 34. If the input distributions of a continuous quasi-stationary system is a Bernoulli's distributions seqnence $\boldsymbol{a}(\xi)$ $0\leq\xi\leq\nu, \boldsymbol{a}(\xi)=0$ $\xi>\nu$, then the mean $\bar{f}(t)$ and the variance $\bar{\bar{f}}(t)$ of the output distribution converge to $\bar{f}$, $\bar{\bar{f}}$ as $t\to\infty$:

$$\bar{f}=\int_0^\nu \frac{\bar{a}(\xi)}{m_\xi}\,d\xi \tag{101}$$

$$\bar{\bar{f}}=\int_0^\nu\left\{\frac{1}{m_\xi}\left(1-\frac{1}{m_\xi}\right)\bar{a}(\xi)+\frac{1}{m_\xi^2}\right\}d\xi \tag{102}$$

where $m_\xi=\int_0^\infty tp_\xi(t)dt.$

There exists no limit distribution in a non-stationary system.

About additive process of output distributions, we get the following theorems.

Theorem 35. If the input is only $\boldsymbol{a}(0)$ in time 0, then the mean $\bar{F}^{(0)}{}_{t_1t_2}$, the variance $\bar{\bar{F}}^{(0)}{}_{t_1t_2}$ of the additive process $\boldsymbol{F}^{(0)}{}_{t_1t_2}$ of the output distributions $\boldsymbol{f}(t), t_1\leq t\leq t_2$ in a continuous stationary system converge to $\bar{F}^{(0)}$,

$\bar{F}^{(0)}$ as $t_1 \to \infty$:

$$\bar{F}^{(0)} = \frac{1}{m} T \cdot \bar{a}_{(0)} \tag{103}$$

$$\bar{\bar{F}}^{(0)} = \bar{a}_{(0)} \int_{-T}^{T} W(T \cdot t) \frac{1}{m} \left(g(t) - \frac{1}{m} \right) dt + \bar{\bar{a}}_{(0)} \left(\frac{T}{m} \right)^2 \tag{104}$$

$$W(T \cdot t) = \begin{cases} T - t & t > 0 \\ T + t & t < 0 \\ 0 & t > T,\ t < -T \end{cases}$$

$$T = t_2 - t_1,\quad g(t) = g(-t),\quad g(0) = 1$$

Theorem 36. If the input is only $\boldsymbol{a}(0)$ in time 0, then the mean $\bar{F}^{(0)}{}_{t_1 t_2}$, the variance $\bar{\bar{F}}^{(0)}{}_{t_1 t_2}$ of the additive process $\boldsymbol{F}^{(0)}{}_{t_1 t_2}$ of the output distributions $\boldsymbol{f}(t)$, $t_1 \le t \le t_2$ in a continuous quasi-stationary system converge to $\bar{F}^{(0)}$, $\bar{\bar{F}}^{(0)}$ as $t_1 \to \infty$:

$$\bar{F}^{(0)} = \frac{1}{m_0} \bar{a}_0 T \tag{105}$$

$$\bar{\bar{F}}^{(0)} = \bar{a}_0 \int_{-T}^{T} W(T \cdot t) \frac{1}{m_0} \left(g_0(t) - \frac{1}{m_0} \right) dt + \bar{\bar{a}}_0 \left(\frac{T}{m_0} \right)^2 \tag{106}$$

Example 4. Providing that the circuit parameter $p(t)$ is a gamma distribution:

$$p(t) = \frac{\beta^\alpha}{\Gamma(\alpha)} t^{\alpha-1} e^{-\beta t},\ \alpha > 0,\ \beta > 0, \tag{107}$$

the indicial function $g(t)$ of a continuous stationary circuit for integer α is given as follows:

Laplace transform of $p(t)$ is $P(s) = (\beta/s + \beta)^\alpha$, so

$$U(s) = \frac{1}{\left(\frac{s}{\beta} + 1 \right)^\alpha - 1}. \tag{108}$$

Using expansion:

$$\frac{1}{x^\alpha - 1} = \frac{1}{\alpha} \sum_{n=0}^{\alpha-1} \frac{\lambda_n}{x - \lambda_n},\ \lambda_n = e^{i \frac{2n\pi}{\alpha}} \tag{109}$$

and its inverse transform:

$$L^{-1}\left(\frac{1}{x^\alpha - 1} \right) = \frac{1}{\alpha} \sum_{n=0}^{\alpha-1} e^{\gamma_n t} \cos(\omega_n t + \theta \cdot n) \tag{110}$$

the indicial function $g(t)$ (inverse transform of $U(s)$) is given by

$$g(t) = \frac{1}{m} \left\{ 1 + \sum_{n=1}^{\alpha-1} e^{-(1-\gamma_n)\beta t} \cos(\omega_n \beta t + \theta \cdot n) \right\} \tag{111}$$

where $m = \alpha/\beta$

$\gamma_n = \cos \theta \cdot n$

$\omega_n = \sin \theta \cdot n$

$\theta = 2\pi/\alpha$

For $\alpha = 1, 2, 3, 4$, $g(t)$ is as follows:

$$\alpha = 1:\quad g(t) = \frac{1}{m} \tag{112}$$

$$\alpha = 2:\quad g(t) = \frac{1}{m} (1 - e^{-2\beta t}) \tag{113}$$

$$\alpha = 3:\quad g(t) = \frac{1}{m} \left\{ 1 - 2e^{-3/2\beta t} \cos\left(\frac{\sqrt{3}}{2} \beta t + \frac{2}{3} \pi \right) \right\} \tag{114}$$

$$\alpha = 4:\quad g(t) = \frac{1}{m} (1 - 2e^{-\beta t} \sin \beta t - e^{-2\beta t}) \tag{115}$$

Conclusion

In order to represent a system by a probabilistic circuit, we have defined three circuit elements: a binomial probabilistic transform, a probabilistic branch and a distribution adder, and constructed a binomial probabilistic sequential circuit of these circuit elements, which is a sort of probabilistic filter.

We extracted a special determinant which is an indicial function, and showed the relation between the transfer function and the mean, the variance of the output distribution about the binomial system.

There exists no transient period in Poisson process since the transition probability is fixed in starting point. In this paper, we discussed a system of which the transition probability varies with time or conforms after a certain transient period. In this stabilizing period, the output distribution of the circuit is revealed in such a transient phenomena that is the same with a transient in an electrical circuit as far as mean. We showed the mean and variance of distributive solution in a transient period of this circuit.

If we substitute three circuit elements: binomial probabilistic transform with parameter p, δ, probabilistic branch and distributive adder for multiplier with multiple p, time lag δ, a branch that transfers the same value to many directions and adder, respectively, then we get a definite electrical transfer circuit and may be visualized as the output (mean value) of the probabilistic sequential circuit.

The control process should be studied further in which the reliability of the output is improved. The author wants to express his thanks to E. Nishibori and N. Ikeno at the ECL laboratory to whose stimulous important discussion in 1959.

References

(1) W. Feller: "Probability theorey and its applications", John Wiley and Sons, Inc., New York; N. Y., Vol. 1; 1950.

* * * *

Papers Contributed to Scientific and Technical Journals by the Members of the Laboratory

Papers Published in Other Publications of the Electrical Communication Laboratory

U.D.C. 534.863 : 621.395.6.001.2 : 621.391

Betriebsdäpfung as the Design Criterion of Electroacoustic Transducers
Toshio HAYASAKA, Ryozo ARAKI
Kenkyû Zituyôka Hôkoku (Electr. Comm. Labor. Techn. Jour.), NTT, **10,** 7, pp 1431–1438, July, 1961

This paper describes the method of designing electroacoustic transducers using "Betriebsdämpfung" as the design criterion. Betriebsdämpfung is consider to be more suitable for the appraisal of high quality transducer than efficiency.

U.D.C. 546.28 : 548.55 : 620.197.2 : 539.232

An Investigation of Surface Treatments for Single-Crystal Silicon (Chemical Methods for Surface Stabilization)
Kazumasa ONO, Katsuhisa FURUSYO
Kenkyû Zituyôka Hôkoku (Electr. Comm. Labor. Techn. Journ.), NTT, **10**, 8, pp. 1745–1752, July, 1961

A surface treatment method for Si to stabilize the characteristics of Si diodes and transistors is proposed, and the results of experiments are described.

U.D.C. 546.82 : 541.138 : 539.232

Studies on the Electrochemical Properties of Titanium
Hiroshi CHIBA
Kenkyû Zituyôka Hôkoku (Electr. Comm. Labor. Techn. Journ.), NTT, **10,** 8, pp. 1653–1683, Aug., 1961

Electrochemical behavior of titanium in various electrolytic solutions, mechanism of formation of anodic films and the electrochemical properties of the film were studied.

U.D.C. 621.311.6.025.1 : 621.311.025.3 : 621.311–962

On the Parallel Operation of AC Non-break Set
Denji SUGIYAMA, Masao TANAKA, and *Shoji HARAGUTI*
Kenkyû Zituyôka Hôkoku (Electr. Comm. Labor. Techn. Journ.), NTT, **10**, 7, pp. 1369–1389, July, 1961

Experimental study of the synchronized change over system of an interruption-free AC power supply set is described.

Translations of many of these papers will appear in a future addition of the Review of Electrical Communication Laboratory.

Please address requests for copies of these papers, which are in Japanese, directly to the authors to whom credited at: The Electrical Communication Laboratory, 1551 Kitizyôzi, Musasino-si, Tokyo.

U.D.C. 621.318.371.001.2 : 621.385.62.032.264.3

Design Considerations for a Solenoid Magnet
Kazuhiro MIYAUCHI
Kenkyû Zituyôka Hôkoku (Electr. Comm. Labor. Techn. Journ.), NTT, **10**, 7, pp. 1337–1367, July, 1961

A design method for a solenoid magnetic of high flux density, low power consumption, and small size is discussed.

U.D.C. 621.318.56.012.001.2

Inquiry into the performance of Electromagnetic Relays.
Yasuo TOMITA
Kenkyû Zituyôka Hôkoku (Electr. Comm. Labor. Techn. Journ.), NTT, **10**, 7, pp. 1415–1429, July, 1961

A theoretical inquiry of the important performance coefficients of electromagnetic relays is described. A design method is also briefly explained.

U.D.C. 621.318.562.3.012.001.2

Analysis of the Fundamental Performance of Balanced Type Polarized Relays
Yasuo TOMITA
Kenkyû Zituyôka Hôkoku (Electr. Comm. Labor. Techn. Journ.), NTT, **10**, 7, pp. 1391–1413, July, 1961

The fundamental performance of balanced type polarized relays is analysed and comparison between theoretical values and experimental values is made.

U.D.C. 621.374.3 : 621.382.2 : 621.318.57

Diode Gate Matrix Access Arrangement for Memory Devices.
Junji YAMATO, Kikunobu KUSUNOKI
Kenkyû Zituyôka Hôkoku (Electr. Comm. Labor. Techn. Journ.), NTT, **10**, 8, pp. 1719–1740, Aug., 1961

Junction diode gates arranged in a matrix can supply ac power to memory devices with high efficiency, high S/N, and high speed.

U.D.C. 621.394.11-185.4 : 621.371.029.64 : 621.391.833

High Speed Data Transmission on Radio Relay Link Telephone Line
Toshiaki KISHIGAMI, Nozomi EGASHIRA, Tunehisa SUGAI, Toshi MINAMI, Hiroshi SUNAGAWA, and *Shunitu HAMAO*
Kenkyû Zituyôka Hôkoku (Electr. Comm. Labor. Techn. Journ.), NTT, **10**, 8, pp. 1685–1717, Aug., 1961

Results of error rate and distortion characteristics for various modulation methods over radio relay link telephone lines are presented.

U.D.C. 621.395.6.012.8.001.2 : 534.6

Researches on the Equivalent Circuits used in the Design of Acoustic Transducers
Suzue ISHII
Kenkyû Zituyôka Hôkoku (Electr. Comm. Labor. Techn. Journ.), NTT, **10**, 8, pp. 1441–1576, Aug., 1961

Derivations of equivalent circuits from the construction of acoustic transducers and method of design with considerations for the non-uniformity of manufactured parts are given.

U.D.C. 621.436-234.001.2 : 621.313.12

Development of Barrel-Type Crankless Combustion Engine
Minoru TAKE
Kenkyû Zituyôka Hôkoku (Electr. Comm. Labor. Techn. Jour.), NTT, **10,** 7, pp. 1243–1336, Aug., 1961

Development of barrel-type crankless combustion engine and results of its life test described.

U.D.C. 681.142.001.2 : 518.5 : 621.374.3

High Speed Arithemetic System
Noriyoshi KUROYANAGI
Kenkyû Zituyôka Hôkoku (Electr. Comm. Labor. Techn. Journ.), NTT, **10**, 8, pp. 1577–1651, 1961

Study of dynamic characteristics of a high speed adder shifter and detector is made based upon new idea. Consideration of arithmetic apparatus composed of these elements is also made.

Papers Published in Publication of Scientific and Technical Societies

U.D.C. 534.75 : 621.391.822

The Masking Effects of Band Noise
Shuzo SAITO, Shingo WATANABE
Jour. Inst. Electr. Commun. Eng., Japan. **44,** 7, pp. 1085–1091, 1961

The masking effects of band noise are measured and thereafter normalized representation of masking effects are induced. These results are useful for the prediction of articulation scores of speech sounds.

U.D.C. 534.863 : 621.391.883

Normalized Representation of Noise Band Masking and its Application to the Prediction of Speech Intelligibility
Shuzo SAITO, Shingo WATANABE
J. Acoust. Soc. Amer. **33,** 8, pp. 1013–1021, 1961

The normalized representation of band noise masking is deduced and applied to the prediction of speech intelligibility.

U.D.C. 541.64 : 541.25 : 678.012

The Studies of Molecular Weight Distribution and Properties of Dilute Solutions
III The Studies of Molecular Weight Dependence on the Hydrodynamic Properties in Polymer Solutions
Nobuo YAMADA, *Hideomi MATSUDA*, and *Haruo NAKAMURA*
Chem. High Polymers, **18,** 195, pp. 452–455, 1961

The relationships between parameters which represent molecular weight dependence upon sedimentation constant, diffusion constant, and intrinsic viscosity are derived; and the validity of parameters obtained from experiments is considered.

U.D.C. 546.711′62′56 : 538.2

On the New Magnetic Phase in the Manganese-Aluminium-Copper System
TSUBOYA Ichiro
J. Phys. Soc. Japan, **16,** 10, pp. 1875, 1961

It was observed that there exists a new ferromagnetic phase in copper Mn-Al-Cu alloys in the composition range of 25 to 45 % Mn, 37.5 to 50 % Al, and 12.5 to 25 % Cu. The magnetic natures and the crystal structure were investigated.

U.D.C. 546.826′431 : 548.55

Discussion on the Crystal Growth of Barium Titanate Single Crystals in Flux Fusion.
Shigeru WAKU
J. Chem. Soc. Jap. **64,** 8, pp. 1378–1387, 1961

Cause of the rapid growth of butterfly twin and [110] dendrites of barium titanate is discussed.

U.D.C. 546.826′431 : 548.55

Influence of Impurities in Barium Titanate Single Crystals
Shigeru WAKU
J. Chem. Soc. Jap. **64,** 8, pp. 1387–1390, 1961

Relation between the initial resistivity of barium titanate single crystals grown by the KF flux method and the impurities in the raw materials is discussed.

U.D.C. 546.826′431 : 548.55 : 537.311.3

Single crystals of semiconductive barium titanate
Shigeru WAKU
J. Chem. Soc. Jap. **64,** 7. pp. 1176–1178, 1961

Resistivity versus temperature curves of semiconductive barium titanate single crystals containing small amounts of La_2O_3 or Ta_2O_5 are measured.

U.D.C. 621.372.54.029.63/.64

Transmission Characteristics and Methods of Designing Branching Filters for Microwave Radio Relay Systems.
Sukemoto KAWAZU, *Hidehiko SUGAHARA*, and *Hideo ISHII*
Jour. Inst. Electr. Commun. Eng. Japan. **44,** 8, pp. 1207–1216, Aug. 1961

A design method for obtaining branching filters with good transmission characteristics for broad-band radio relay systems is established and experimentally confirmed.

U.D.C. 621.382.2 : 539.125.5

Effect of Neutron Irradiation on Characteristics of Esaki-Diodes
Yoshitaka FURUKAWA
Jour. Inst. Electr. Commun. Eng. Japan. **44,** 8, pp. 1185–1190, Aug. 1961

Excess current in Esaki-diodes is increased by neutron irradiation. The expression for excess current deduced from band to deep level tunneling and recombination processes can account for the experimental results.

U.D.C. 621.382.2 : 621.373.431.1

Analysis of a Stable Multivibrator with Esaki-Diode
Eiji IWAHASHI
Jour. Inst. Electr. Commun. Eng. Japan. **44,** 7, pp. 1085–1091, July 1961

An analysis of the mechanism of relaxation oscillation in a stable multivibrator with an Esaki-diode is presented and experimental results are given.

U.D.C. 621.395.625.3

Reproduction of Magnetically Recorded Digital Data
Masaaki NISHIKAWA
Jour. Inst. Electr. Commun. Eng, Japan. **44,** 8, pp. 1216–1223, Aug. 1961

This paper investigates the relation between the reproduced signal and the design parameters for the case of saturation-type magnetic recording.

U.D.C. 621.9.01 : 534.321.9

A Study of Ultrasonic Machining (Contact angle, Machining load. Penetration depth)
Masahiro OHIRA, *Harumichi KAGEYAMA*, and *Osamu AKUTU*
J. Soc. Precision Mech. Jap. **27,** 7, pp. 480–493, July 1961

Experimental results and their comparison with a theoretical analysis of contact angle between tool and work surface of impulsive loads in machining and depth of penetration of abrasive particles into the work surface are described.

U.D.C. 678.012 : 541.64

The Studies of Molecular Weight Distribution and Properties of Dilute Solutions
IV Discussions on the Measured Molecular Weight Distribution
Nobuo YAMADA, *Hideomi MATSUDA*, and *Haruo NAKAMURA*
Chem. High Polymers, **18**, 195, pp. 455–459, 1961

The average molecular weights Msv and Mov were derived to confirm molecular weight distribution obtained from sedimentation and diffusion. Different observed average molecular weights are compared with those calculated from distribution.

U.D.C. 678.012 : 541.64

A Study of Molecular Weight Distribution and Properties of Dilute Solutions. (V) The Determination of Molecular Weight Distribution from Sedimentation and Diffusion Measurements.
Nobuo YAMADA, *Hideomi MATSUDA*, *Haruo NAKAMURA*, and *Yuji YAMASHITA*
Chem. High Polymers, **18**, 195, pp. 459–465, 1961

The molecular weight distribution curve can be determined for the polystyrene-MEK system using the weight distribution curves of sedimentation and diffusion constants.

* * * *

CONTENTS